Electronic Supplementary Information for

Supramolecular Enantiomeric and Structural Differentiation of Amino Acid Derivatives with Achiral Pillar[5]arene Homologs

Jiecheng Ji[#,a] Yizhou Li[#,a] Chao Xiao,[a] Guo Cheng,[a] Kui Luo,[a] Qiyong Gong,[a] Dayang Zhou,[b] Jason J. Chruma,[a] Wanhua Wu*,[a] Cheng Yang*[a]

[a] *Huaxi MR Research Center (HMRRC), Department of Radiology, West China Hospital, Key Laboratory of Green Chemistry &Technology, College of Chemistry, and Healthy Food Evaluation Research Center, Sichuan University, 29 Wangjiang Road, Chengdu, 610064, China.*

[b] *Comprehensive Analysis Center, ISIR, Osaka University (Japan).*

Contents

Experimental Procedures

1 General

Chemicals and instruments:
All of the chemicals used for synthesis were analytically pure and were used as received. Solvents were dried and distilled before use for synthesis. ^{1}H NMR and ^{13}C NMR spectra were recorded at room temperature on a Bruker AMX–400 (operating at 400 MHz for ^{1}H NMR and 101 MHz for ^{13}C NMR) in $CDCl_3$ and/or CD_3OD with TMS as internal standard. HRMS were measured with a Waters–Q–TOF Premiers (ESI). UV-vis spectra and binding constants with UV–vis titration were obtained on JASCO V–650. CD spectra were acquired using J-1500 CD spectrometer. Fluorescence spectra were acquired using Fluoromax-4 spectrofluorometer. ITC data were acquired using VP-ITC.
The single crystal structure of the complexes **H4**@HAN, **H5**@HAN, **H6**@HAN, **H7**@HAN can be found at the Cambridge Crystallographic Data Centre, CCDC numbers: 1880191, 1880195, 1880192, 1880193.
All the chemicals were obtained from suppliers, used without further purification in case of analysis investigation. Solvents were distilled before used for analysis.

2 Synthesis and structure characterization data of the host and guest

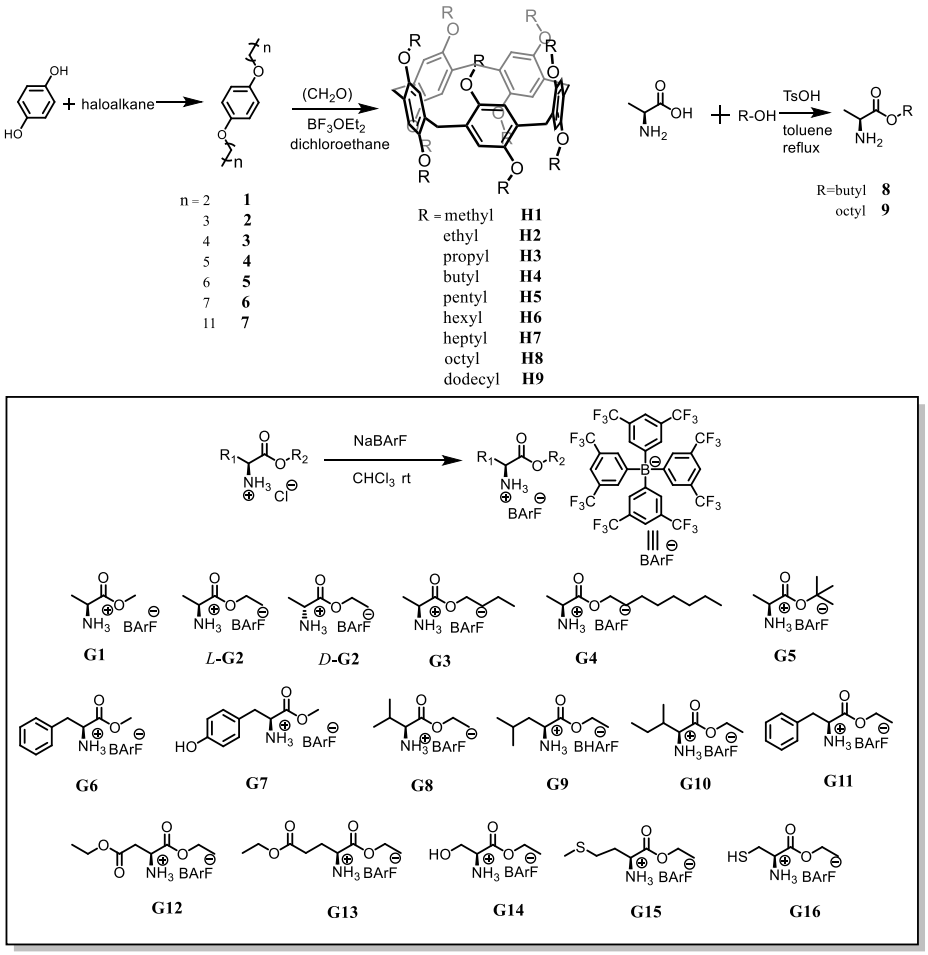

Scheme S1. Synthesis route of pillar[5]arene derivatives and ammonium guests.

Synthesis of **1**

A stirred ethanolic (106.0 mL) solution containing hydroquinone (11.7 g, 106.9 mmol) and KOH (14.66 g, 261.7 mmol) was heated to reflux under a N_2 atmosphere for 20 min. 1-Propyl bromide (17.9 g, 145.5 mmol) then was added dropwise over 30 min, and the heated reaction mixture was stirred under reflux for an additional 2 h. The solvent was removed under reduced pressure, and the residue was dissolved in CH_2Cl_2 and washed with water for 3 times. The organic phase was dried over Na_2SO_4 and the solvent was removed under reduced pressure. The crude product was purified by passing through a silica gel column with petroleum ether as the eluent to afford **1** as a white solid (11.7 g, yield: 67.2 %). ^{1}H NMR (400 MHz, $CDCl_3$): δ 6.82 (s, 4H), 3.88 (t, *J* = 6.6 Hz and *J* = 6.6 Hz, 4 H), 1.80 – 1.75 (m, 4 H), 1.02 (t, *J* = 7.4 Hz and *J* = 7.4 Hz, 6 H). ^{13}C NMR (101 MHz, $CDCl_3$): δ 153.28, 115.43, 70.15, 22.81, 10.57.

Synthesis of **2**

A stirred ethanolic (50 mL) solution containing hydroquinone (13.0 g, 106.0 mmol) and KOH (13.0 g, 261.0 mmol) was heated to reflux under a N_2 atmosphere for 20 min. *n*-Butyl bromide (32.0 g, 234.0 mmol) was then added dropwise over 30 min, and the heated reaction mixture was stirred at reflux for an additional 2 h. The solvent was removed under reduced pressure, and the residue was dissolved in CH_2Cl_2 and washed with water for 3 times. The organic phase was dried over Na_2SO_4 and the solvent was removed under reduced pressure. The crude product was purified by passing through a silica gel column with petroleum ether as the eluent to give **2** as a white solid (15.8 g, yield: 61.5 %). ^{1}H NMR (400 MHz, $CDCl_3$): δ 6.82 (s, 4H), 3.91 (t, *J* = 6.5 Hz and *J* = 6.5 Hz, 4 H), 1.77 – 1.70 (m, 4 H), 1.52 – 1.43 (m, 4 H), 0.96 (t, *J* = 7.4 Hz and *J* = 7.4 Hz, 6 H). ^{13}C NMR (101 MHz, $CDCl_3$): δ 153.27, 115.40, 68.32, 31.53, 19.31, 13.90.

Synthesis of **3**

A mixture of hydroquinone (4.0 g, 36.3 mmol) and KCO_3 (30.0 g, 254.0 mmol) in *N*,*N*-dimethylformamide (50.0 mL) was stirred under a N_2 atmosphere for 20 min. 1-Bromopentane (13.6 g, 89.7 mmol) was then added dropwise over 30 min, and the reaction mixture was heated at 60 °C for an additional 23 h. The solvent was removed under reduced pressure, and the residue was dissolved in CH_2Cl_2 and washed with water for 3 times. The organic phase was dried over Na_2SO_4 and the solvent was removed under reduced pressure. The crude product was purified by passing through a silica gel column with petroleum ether as the eluent to give **3** as a white solid (5.1 g, yield: 56.1 %). ^{1}H NMR (400 MHz, $CDCl_3$): δ 6.82 (s, 4 H), 3.91 (t, *J* = 6.6 Hz and *J* = 6.6 Hz, 4 H), 1.79 – 1.72 (m, 4 H), 1.47 – 1.33 (m, 4 H), 0.96 (t, *J* = 7.1 Hz and *J* = 7.0 Hz, 6 H). ^{13}C NMR (101 MHz, $CDCl_3$): δ 153.26, 115.40, 68.63, 29.16, 28.28, 22.54, 14.06.

Synthesis of **4**

A mixture of hydroquinone (3.0 g, 27.3 mmol) and KOH (6.6 g, 115.0 mmol) in *N*,*N*-dimethylformamide (23.0 mL) was stirred under a N_2 atmosphere for 20 min. 1-Bromohexane (10.0 g, 61.4 mmol) was then added dropwise over 30 min, and the reaction mixture was stirred at 25 °C for additional 23 h. The solvent was removed under reduced pressure, and the residue was dissolved in $CHCl_3$ and washed with water for 3 times. The organic phase was dried over Na_2SO_4 and the solvent was removed under reduced pressure. The crude product was purified by passing through a silica gel column with petroleum ether as the eluent to give **4** as a white solid (2.6 g, yield: 34.3 %). ^{1}H NMR (400 MHz, $CDCl_3$): δ 6.82 (s, 4 H), 3.90 (t, *J* = 6.6 Hz and *J* = 6.6 Hz, 4 H), 1.78 – 1.71 (m, 4 H), 1.48 – 1.41 (m, 4 H), 1.34 – 1.31 (m, 4 H), 0.90 (t, *J* = 6.9 Hz and *J* = 6.8 Hz, 6 H). ^{13}C NMR (101 MHz, $CDCl_3$): δ 153.18, 115.42, 68.37, 33.87, 32.73, 29.24, 27.97, 25.34.

Synthesis of **5**

A dimethyl sulfoxide (177.0 mL) solution containing hydroquinone (3.0 g, 27.3 mmol) and KOH (11.6 g, 207.0 mmol) was stirred under a N_2 atmosphere for 20 min. 1-Bromoheptane (10.0 g, 55.9 mmol) was then added dropwise over 30 min, and the reaction mixture was stirred at 25 °C for an additional 12 h. The solvent was removed under reduced pressure, and the residue was dissolved in $CHCl_3$ and washed with water for 3 times. The organic phase was dried over Na_2SO_4 and the solvent was removed under reduced pressure. The crude product was purified by passing through a silica gel column with petroleum ether as the eluent to give **5** as a white solid (3.7 g, yield: 37.7 %). ^{1}H NMR (400 MHz, $CDCl_3$): δ 6.84 (s, 4 H), 3.92 (t, *J* = 6.6 Hz and *J* = 6.6 Hz, 4 H), 1.81 – 1.74 (m, 4 H), 1.49 – 1.44 (m, 4 H), 1.39 – 1.32 (m, 12 H), 0.91 (t, *J* = 6.8 Hz and *J* = 7.1 Hz, 6 H). ^{13}C NMR (101 MHz, $CDCl_3$): δ 153.25, 115.39, 68.65, 31.86, 29.47, 29.15, 26.09, 22.66, 14.12.

Synthesis of **6**

A mixture of hydroquinone (4.0 g, 36.3 mmol) and K_2CO_3 (25.0 g, 219.0 mmol) in *N*,*N*-dimethylformamide (72.0 mL) was stirred under a N_2 atmosphere for 20 min. 1-Chloroctane (15.7 g, 106.0 mmol) was then added dropwise over 30 min, and the reaction mixture was stirred at 60 °C for an additional 23 h. The solvent was removed under reduced pressure, and the residue was dissolved in $CHCl_3$ and washed with water for 3 times. The organic phase was dried over Na_2SO_4 and the solvent was removed under reduced pressure. The crude product was purified by passing through a silica gel column with petroleum ether as the eluent to give **6** as a white solid (7.7 g, yield: 76.4 %). ^{1}H NMR (400 MHz, $CDCl_3$): δ 6.82 (s, 4 H), 3.89 (t, *J* = 6.6 Hz and *J* = 6.6 Hz, 4 H), 1.78 – 1.71 (m, 4 H), 1.47 – 1.40 (m, 4 H), 1.33 – 1.25 (m, 16 H), 0.88 (t, *J* = 6.9 Hz and *J* = 6.9 Hz, 6 H). ^{13}C NMR (101 MHz, $CDCl_3$): δ 153.21, 115.38, 68.64, 31.85, 29.43, 29.42, 29.28, 26.09, 22.68, 14.11.

Synthesis of **7**

A mixture of containing hydroquinone (3.0 g, 27.2 mmol) and K_2CO_3 (18.8 g, 164.4 mmol) in *N*,*N*-dimethylformamide (54.0 mL) was stirred under a N_2 atmosphere for 20 min. 1-Chlordodecane (13.8 g, 55.0 mmol) was then added dropwise over 30 min, and the reaction mixture was stirred at 80 °C for an additional 35 h. The solvent was removed under reduced pressure, and the residue was dissolved in $CHCl_3$ and washed with water for 3 times. The organic phase was dried over Na_2SO_4 and the solvent was removed under reduced pressure. The crude product was purified by passing through a silica gel column with dichloromethane as the eluent to give **7** as a white solid (1.3 g, yield: 10.7 %). ^{1}H NMR (400 MHz, $CDCl_3$): δ 6.81 (s, 4 H), 3.89 (t, *J* = 6.6 Hz and *J* = 6.6 Hz, 4 H), 1.78 – 1.71 (m, 4 H), 1.47-1.40 (s, 4 H), 1.26 (s, 32 H), 0.88 (t, *J* = 6.6 Hz and *J* = 7.0 Hz, 6 H). ^{13}C NMR (101 MHz, $CDCl_3$): δ 153.20, 115.56, 68.65, 31.94, 29.68, 29.65, 29.62, 29.61, 29.44, 29.42, 29.37, 26.08, 22.71, 14.13.

General method for synthesis of Pillar[5]arenes

A 1,2-dichloroethane solution containing monomer (1 equiv) and polyoxymethylene (3 equiv) was stirred for 10 min at room temperature. Boron fluoride diethyl ether (1 equiv) was then added, and the reaction mixture was stirred at 25 °C for an additional 20 min. The solvent was removed under reduced pressure, and the residue was dissolved in $CHCl_3$ and washed with water for 3 times. The organic phase was dried over Na_2SO_4 and the solvent was removed under reduced pressure. The crude product was purified by passing through a silica gel column with dichloromethane as the eluent to provide the corresponding pillar[5]arene as a colorless solid.[1]

Compound **H1**: Colorless solid (3.6 g, 59.2 %). ^{1}H NMR (400 MHz, $CDCl_3$): δ 6.77 (s, 10 H), 3.78 (s, 10 H), 3.66 (s, 30H). ^{13}C NMR (101 MHz, $CDCl_3$): δ 150.72, 128.30, 113.93, 55.76, 29.56. EI -HRMS: m/z calcd for $C_{45}H_{50}O_{10}Na$ $[M+Na]^+$: 773.3296, found 773.3307.

Compound **H2**: Colorless solid (3.6 g, 50.3 %). ^{1}H NMR (400 MHz, $CDCl_3$): δ 6.76 (s, 10 H), 3.88 – 3.83 (m, 20 H), 3.76 (s, 10 H), 1.30 (t, *J* = 6.4 Hz and *J* = 6.8 Hz, 30 H). ^{13}C NMR (101 MHz, $CDCl_3$): δ 150.03, 128.54, 115.06, 63.78, 29.83, 15.14. EI-HRMS: m/z calcd for $C_{55}H_{70}O_{10}Na$ $[M+Na]^+$: 913.4861, found 913.4927.

Compound **H3**: Colorless solid (1.1 g, 34.4 %). ^{1}H NMR (400 MHz, $CDCl_3$): δ 6.81 (s, 10H), 3.81 – 3.77 (m, 30H), 1.79 – 1.71(m, 20H), 1.01(t, *J* = 7.3 Hz and *J* = 7.4 Hz, 30H). ^{13}C NMR (101 MHz, $CDCl_3$): δ 149.80, 128.28, 114.90, 69.88, 29.55, 23.04, 10.80. EI-HRMS: m/z calcd for $C_{65}H_{90}O_{10}Na$ $[M+Na]^+$: 1053.6426, found 1053.6235.

Compound **H4**: Colorless solid (0.68 g, 41.3 %). ^{1}H NMR (400 MHz, $CDCl_3$): δ 6.89 (s, 10H), 3.88 – 3.86 (m, 20H), 3.75 (s, 10H), 1.83 – 1.80 (m, 20H), 1.60 – 1.51 (m, 20H), 1.00 (t, *J* = 7.3 Hz and *J* = 7.4 Hz, 30H). ^{13}C NMR (101 MHz, $CDCl_3$): δ 149.43, 127.98, 113.77, 67.58, 32.13, 29.13, 19.55, 14.10. EI-HRMS: m/z calcd for $C_{75}H_{110}O_{10}Na$ $[M+Na]^+$: 1193.7991, found 1193.7527.

Compound **H5**: Colorless solid (1.4 g, 44.5 %). ^{1}H NMR (400 MHz, $CDCl_3$): δ 6.86 (s, 10H), 3.85(t, *J* = 6.4 Hz and *J* = 6.4 Hz, 20H), 3.76 (s, 10H), 1.86 – 1.79 (m, 20H), 1.54 – 1.47 (m, 20H), 1.45 – 1.36 (m, 20H), 0.94 (t, *J* = 7.2 Hz and *J* = 7.2 Hz, 30H). ^{13}C NMR (101 MHz, $CDCl_3$): δ 149.65, 128.11, 114.29, 68.14, 30.93, 29.69, 28.55, 22.69, 14.10. MALDI-HRMS: m/z calcd for $C_{85}H_{130}O_{10}$ $[M]^+$: 1310.9664, found 1310.9749; $C_{85}H_{130}O_{10}Na$ $[M+Na]^+$: 1333.9556, found 1333.9075.

Compound **H6**: Colorless solid (0.8 g, 47.9 %). ^{1}H NMR (400 MHz, $CDCl_3$): δ 6.86 (s, 10H), 3.85 (t, *J* = 5.9 Hz and *J* = 6.0 Hz, 20H), 3.75 (s, 10H), 1.85 – 1.82 (m, 20H), 1.54 – 1.52 (m, 20H), 1.36 – 1.34 (m, 40H), 0.91 (t, *J* = 6.4 Hz and *J* = 6.8 Hz, 30H). ^{13}C NMR (101 MHz, $CDCl_3$): δ 149.59, 128.11, 114.05, 68.08, 31.90, 30.00, 29.21, 26.07, 22.70, 14.11. MALDI-HRMS: m/z calcd for $C_{95}H_{150}O_{10}Na$, $[M+Na]^+$: 1475.1155, found 1474.9368; $C_{95}H_{150}O_{10}K$, $[M+K]^+$: 1491.0894, found 1490.9090.

Compound **H7**: Colorless solid (0.8 g, 48.6 %). ^{1}HNMR (400 MHz, $CDCl_3$): δ 6.89 (s, 10H), 3.86 (s, 20H), 3.75 (s, 10H), 1.83 (s, 20H), 1.55 – 1.51 (m, 20H), 1.38 – 1.32 (m, 60H), 0.90 (t, *J* = 6.1 Hz and *J* = 6.8 Hz, 30H). ^{13}C NMR (101 MHz, $CDCl_3$): δ 149.41, 127.97, 113.66, 67.86, 31.95, 30.09, 29.47, 26.41, 22.77, 14.15. MALDI-HRMS: m/z calcd for $C_{105}H_{170}O_{10}$, $[M]^+$: 1592.2828, found 1592.1582; $C_{105}H_{170}O_{10}Na$, $[M+Na]^+$: 1615.2720, found 1615.1225. Melting points: 131.8 °C. Elemental analyses: C, 74.0 %; H, 9.8%.

Compound **H8**: Colorless solid (2.4 g, 46.4 %). ^{1}H NMR (400 MHz, $CDCl_3$): δ 6.85 (s, 10H), 3.85 (s, 20H), 3.75 (s, 10H), 1.81 (s, 20H), 1.54 – 1.48 (m, 20H), 1.35 – 1.22 (m, 80H), 0.85 (t, *J* = 6.1 Hz and *J* = 7.1 Hz, 30H). ^{13}C NMR (101 MHz, $CDCl_3$): δ 149.64, 128.06, 114.37, 68.12, 31.84, 29.97, 29.65, 29.32, 26.41, 22.66, 14.10. MALDI-HRMS: m/z calcd for $C_{115}H_{190}O_{10}Na$, $[M+Na]^+$: 1755.4285, found 1755.2834; $C_{115}H_{190}O_{10}K$, $[M+K]^+$: 1771.4024, found 1771.2631.

Compound **H9**: Colorless solid (0.2 g, 38.8 %). ^{1}H NMR (400 MHz, $CDCl_3$): δ 6.79 (s, 10H), 3.91 – 3.74 (m, 30 H), 1.81 (s, 20 H), 1.48 (s, 20 H), 1.31 (s, 20 H), 1.25 – 1.10 (m, 140 H), 0.78 (t, *J* = 7.1 Hz and *J* = 7.3 Hz, 30H). ^{13}C NMR (101 MHz, $CDCl_3$): δ 148.59, 126.99, 113.20, 66.90, 30.94, 28.92, 28.83, 28.77, 28.65, 28.45, 28.37, 28.19, 25.25, 21.70, 13.12. MALDI-HRMS: m/z calcd for $C_{155}H_{270}O_{10}$, $[M]^+$: 2293.0653, found 2293.0012; $C_{155}H_{270}O_{10}Na$, $[M+Na]^+$: 2316.0545, found 2315.9330.

Synthesis of **8**

A stirred toluene (50 mL) solution containing L-alanine (1 g, 11.2 mmol), *p*-toluenesulfonic acid (1.9 g, 11 mmol), and butyl alcohol (10 mL) was heated to reflux for 24 h. The solvent was removed under reduced pressure, and the residue was dissolved in $CHCl_3$ and washed with water for 3 times. The organic phase was dried over Na_2SO_4 and the solvent was removed under reduced pressure. The crude product was purified by passing through a silica gel column with EA: MeOH: NH_4OH = 40: 1: 0.6 as the eluent to give **8** as a yellow oil (527.8 mg, yield: 32.5 %). ^{1}H NMR (400 MHz, $CDCl_3$): δ 4.16 – 4.05 (m, 2H), 3.57 – 3.52 (m, 1H), 1.66 – 1.57 (m, 2H), 1.43 – 1.31 (m, 5H), 0.93 (t, *J* = 7.4 Hz and *J* = 7.4 Hz, 3H). ^{13}C NMR (101 MHz, $CDCl_3$): δ 176.63, 64.70, 50.01, 30.60, 20.65, 19.02, 13.61.

Synthesis of **9**

A stirred toluene (50 mL) solution containing L-alanine (1 g, 11.2 mmol), *p*-toluenesulfonic acid (1.9 g, 11 mmol) and octanol (2 mL) was refluxed for 24 h. The solvent was removed under reduced pressure, and the residue was dissolved in $CHCl_3$ and washed with water for 3 times. The organic phase was dried over Na_2SO_4 and the solvent was removed under reduced pressure. The crude product was purified by passing through a silica gel column with EA: MeOH: NH_4OH = 40: 1: 0.6 as the eluent to give **9** as a yellow oil (594 mg, yield: 43.5 %). ^{1}H NMR (400 MHz, $CDCl_3$): δ 4.11 – 4.06 (m, 2H), 3.54 – 3.49 (m, 1H), 1.65 – 1.59 (m, 2H), 1.32 – 1.25 (m, 10H), 0.86 (t, *J* = 6.9 Hz and *J* = 6.7 Hz, 3H). ^{13}C NMR (101 MHz, $CDCl_3$): δ 176.63, 64.70, 50.01, 30.60, 20.65, 19.02, 13.61.

General method for synthesis of guests

A chloroform (30 mL) solution containing the -amino ester hydrochloride salt (1 equiv, 0.36 mM; Before this experiment, **8** and **9** need to be acidified) and sodium tetrakis [3, 5-bis(trifluoromethyl)phenyl] borate (BArFNa) (1 equiv, 0.36 mM) was stirred for 24 h at 35 °C. The resulting precipitate was removed by filtration, and the solvent of filtrate was removed under reduced pressure to obtained the desired ammonium BArF salt.

Compound **G1**: Colorless solid (219.9 mg, 63.2 %). ^{1}H NMR (400 MHz, $CDCl_3$): δ 7.70 (s, 8H), 7.55 (s, 4H), 6.98 (s, 3H), 3.90 (s, 1H), 3.82 (s, 3H), 1.50 (d, *J* = 7.3 Hz, 3H). ^{13}C NMR (101 MHz, $CDCl_3$): δ 169.20, 162.42, 161.92, 161.43, 160.93, 134.74,129.46, 129.21, 128.86, 128.55, 125.85, 123.14, 120.43, 117.66, 54.68, 50.41, 15.80.

Compound *L*-**G2**: Colorless solid (208.0 mg, 58.8 %). ^{1}H NMR (400 MHz, $CDCl_3$): δ 7.71 (s, 8H), 7.55 (s, 4H), 6.65 (s, 3H), 4.30 – 4.25 (m, 2H), 3.90 – 3.89 (m 1H), 1.50 (d, *J* = 7.3 Hz, 3H), 1.27 (t, *J* = 7.2 Hz and *J* = 7.2 Hz, 3H). ^{13}C NMR (101 MHz, $CDCl_3$): δ 169.10, 162.41, 161.91, 161.42, 160.92, 134.75, 129.15, 128.89, 128.81, 128.57, 125.86, 123.15, 120.44, 117.67, 117.64, 117.60, 64.63, 50.24, 15.86, 13.63.

Compound *D*-**G2**: Colorless solid (247.7 mg, 71.2 %). ^{1}H NMR (400 MHz, $CDCl_3$): δ 7.70 (s, 8H), 7.55 (s, 4H), 6.82 (s, 3H), 4.29 – 4.23 (m, 2H), 3.90 (s, 1H), 1.50 (d, *J* = 6.9 Hz, 3H), 1.25 (t, *J* = 7.1 Hz and *J* = 7.1 Hz, 3H). ^{13}C NMR (101 MHz, $CDCl_3$): δ 168.63, 162.41, 161.91, 161.42, 160.92, 134.74, 128.82, 125.87, 123.16, 120.45, 117.65, 64.94, 50.60, 15.82, 13.58.

Compound **G3**: Colorless solid (258.7 mg, 71.2 %). ^{1}H NMR (400 MHz, $CDCl_3$): δ 7.71 (s, 2H), 7.56 (s, 4H), 6.46 (s, 3H), 4.27 – 4.20 (m, 2H), 3.91 (s, 1H), 1.66 – 1.60 (m, 2H), 1.50 (d, *J* = 7.2 Hz, 3H), 1.36 – 1.27 (m, 2H), 0.90 (t, *J* = 7.4 Hz and *J* = 7.4 Hz, 3H). ^{13}C NMR (101 MHz, $CDCl_3$): δ 169.78, 162.40, 161.91, 161.41, 160.92, 134.76, 129.61, 129.14, 128.80, 128.57, 125.87, 123.16, 120.45, 117.60, 68.12, 49.97, 30.04, 18.74, 15.94, 13.32.

Compound **G4**: Colorless oil (267.2 mg, 69.7 %). ^{1}H NMR (400 MHz, $CDCl_3$): δ 7.70 (s, 8H), 7.55 (s, 4H), 6.99 (s, 3H), 4.28 – 4.17 (m, 2H), 3.91 (m, 1H), 1.68 – 1.62 (m, 2H), 1.51 (d, *J* = 7.0 Hz, 3H), 1.28 – 1.26 (m, 10H), 0.88 (t, *J* = 6.6 Hz and *J* = 7.0 Hz, 3H). ^{13}C NMR (101 MHz, $CDCl_3$): δ 169.81, 162.40, 161.91, 161.41, 160.92, 134.78, 129.62, 129.10, 128.82, 128.59, 125.88, 123.17, 120.46, 117.59, 115.86, 68.38, 49.93, 31.66, 29.03, 28.99, 28.13, 25.55, 22.55, 15.99, 13.98.

Compound **G5**: Colorless solid (214.3 mg, 59.0 %). ^{1}H NMR (400 MHz, $CDCl_3$): δ 7.71 (s, 8H), 7.56 (s, 4H), 6.55 (s, 3H), 3.80 (s, 1H), 1.47 (s, 12H). ^{13}C NMR (101 MHz, $CDCl_3$): δ 167.86, 162.44, 161.94, 161.44, 160.95, 134.72, 129.49, 129.20, 128.92, 128.54, 125.83, 123.13, 120.42, 117.68, 88.06, 50.98, 27.51, 16.04.

Compound **G6**: Colorless solid (258.7 mg, 68.9 %). ^{1}H NMR (400 MHz, $CDCl_3$): δ 7.70 (s, 8H), 7.53 (s, 4H), 7.37 (t, *J* = 2.5 Hz and *J* = 3.4 Hz, 3H), 7.06 (m, 2H), 6.44 (s, 3H), 4.16 – 4.07 (m, 1H), 3.84 (s, 3H), 3.43 – 3.38 (m, 1H), 3.08 – 3.02 (m, 1H). ^{13}C NMR (101 MHz, $CDCl_3$): δ 168.49, 162.40, 161.90, 161.41, 160.92, 134.77, 131.03, 130.32, 129.62, 129.53, 129.10, 128.83, 128.59, 125.88, 123.17, 120.46, 117.61, 55.33, 54.62, 35.76.

Compound **G7**: Colorless solid (47.7 mg, 12.3 %). ^{1}H NMR (400 MHz, $CDCl_3$): δ 7.70 (s, 8H), 7.54 (s, 4H), 6.92 (d, *J* = 8.5 Hz, 2H), 6.80 (d, *J* = 8.5 Hz, 2H), 6.65 (s, 3H), 4.07 – 4.05 (m, 1H), 3.88 (s, 3H), 3.32 – 3.27 (m, 1H), 3.02 – 2.96 (m, 1H). ^{13}C NMR (101 MHz, $CDCl_3$) δ 167.99, 162.40, 161.90, 161.41, 160.91, 156.49, 134.77, 130.22, 129.10, 128.82, 128.60, 125.89, 123.18, 122.65, 120.47, 117.61, 117.13, 55.37, 54.62, 34.99.

Compound **G8**: Colorless solid (264.4 mg, 72.3 %). ^{1}H NMR (400 MHz, $CDCl_3$): δ 7.70 (s, 8H), 7.55 (s, 4H), 6.57 (s, 3H), 4.40 – 4.20 (m, 2H), 3.87 – 3.74 (m, 1H), 2.40 – 2.32 (m, 1H), 1.28 (t, *J* = 7.2 Hz and *J* = 7.2 Hz, 3H), 0.98 – 0.89 (m, 6H). ^{13}C NMR (101 MHz, $CDCl_3$): δ 167.77, 162.40, 161.91, 161.41, 160.92, 134.77, 129.44, 129.41, 129.38, 129.15, 129.13, 129.10, 129.07, 128.84, 128.81, 128.78, 128.76, 128.60, 128.50, 128.47, 128.45, 125.90, 123.19, 120.48, 117.68, 117.64, 117.60, 64.96, 59.94, 29.21, 17.65, 16.28, 13.71.

Compound **G9**: Colorless solid (222.8 mg, 60.5 %). ^{1}H NMR (400 MHz, $CDCl_3$): δ 7.70 (s, 8H), 7.55 (s, 4H), 7.39 (s, 3H), 4.33 – 4.16 (m, 2H), 3.90 (s, 1H), 1.95 – 1.76 (m, 1H), 1.68 – 1.58 (m, 2H), 1.25 (t, *J* = 7.1 Hz and *J* = 7.1 Hz, 3H), 0.95 – 0.87 (m, 6H). ^{13}C NMR (101 MHz, $CDCl_3$): δ 169.29, 162.40, 161.90, 161.41, 160.91, 134.78, 129.42, 129.39, 129.37, 129.34, 129.10, 129.08, 129.05, 129.02, 128.79, 128.77, 128.74, 128.71, 128.62, 128.48, 128.45, 128.42, 128.40, 125.91, 123.20, 120.49, 117.61, 117.57, 117.54, 117.50, 64.34, 52.63, 39.25, 24.62, 21.90, 21.89, 21.11, 13.63.

Compound **G10**: Colorless solid (232.7 mg, 63.2 %). ^{1}H NMR (400 MHz, $CDCl_3$): δ 7.70 (s, 8H), 7.54 (s, 4H), 7.03 (s, 3H), 4.40 – 4.20 (m, 2H), 3.85 (m, 1H), 1.46 – 1.33 (m, 1H), 1.28 – 1.31 (m, 3H), 1.27 – 1.16 (m, 2H), 0.98 – 0.89 (m, 6H). ^{13}C NMR (101 MHz, $CDCl_3$): δ 171.95, 162.39, 161.90, 161.41, 160.91, 134.78, 129.48, 129.10, 128.81, 128.78, 128.75, 128.60, 125.89, 123.18, 121.29, 120.46, 120.01, 117.68, 117.64, 117.60, 117.55, 117.52, 64.42, 36.27, 24.74, 14.57, 13.81, 11.31.

Compound **G11**: Colorless solid (310.5 mg, 81.6 %). ^{1}H NMR (400 MHz, $CDCl_3$): δ 7.70 (s, 8H), 7.54 (s, 4H), 7.40 (s, 3H), 7.11 – 7.10 (m, 2H), 6.61 (s, 3H), 4.33 (m, 2H), 4.11 (s, 1H), 3.42 (m, 1H), 3.06 (m, 1H), 1.34 (t, *J* = 7.1 Hz and *J* = 7.1 Hz, 3H). ^{13}C NMR (101 MHz, $CDCl_3$): δ 167.87, 162.40, 161.90, 161.41, 160.92, 134.78, 131.66, 130.13, 129.32, 129.12, 129.09, 129.06, 129.03, 128.94, 128.80, 128.78, 128.75, 128.72, 128.61, 128.49, 128.46, 128.43, 128.40, 125.90, 123.19, 120.48, 117.61, 117.58, 117.54, 64.59, 55.22, 35.94, 13.74.

Compound **G12**: Colorless solid (285.4 mg, 75.3 %). ^{1}H NMR (400 MHz, $CDCl_3$): δ 7.70 (s, 8H), 7.55 (s, 4H), 7.42 (s, 3H), 4.32 – 4.25 (m, 2H), 4.16 – 4.13 (m, 2H), 4.10-4.07 (m, 1H), 3.03 – 2.88 (m, 2H), 1.29 – 1.18 (m, 6H). ^{13}C NMR (101 MHz, $CDCl_3$): δ 171.53, 166.51, 166.47, 162.45, 161.95, 161.45, 160.96, 134.83, 129.67, 129.46, 129.43, 129.40, 129.38, 129.14, 129.12, 129.09, 129.06, 128.83, 128.80, 128.78, 128.75, 128.66, 128.52, 128.49, 128.46, 128.44, 125.95, 123.24, 120.54, 117.66, 117.62, 117.58, 65.23, 63.77, 50.99, 31.72, 31.69, 13.51, 13.50.

Compound **G13**: Colorless solid (297.7 mg, 77.5 %). ^{1}H NMR (400 MHz, $CDCl_3$): δ 7.71 (s, 8H), 7.61 (s, 3H), 7.55 (s, 4H), 4.35 – 4.26 (m, 2H), 4.16 – 4.08 (m, 2H), 3.87 – 3.79 (m, 1H), 2.73 – 2.54 (m, 2H), 2.25 – 2.12 (m, 2H), 1.30-1.21 (m, 6H). ^{13}C NMR (101 MHz, $CDCl_3$): δ 177.38, 167.70, 162.40, 161.90, 161.41, 160.91, 134.76,

129.18, 129.13, 129.10, 128.87, 128.85, 128.79, 128.55, 125.84, 123.13, 117.64, 117.61, 117.57, 65.22, 63.97, 53.96, 31.56, 24.43, 13.72, 13.54.

Compound **G14**: Colorless solid (214.6 mg, 59.8 %). ^{1}H NMR (400 MHz, $CDCl_3$): δ 7.70 (s, 8H), 7.56 (s, 4H), 6.79 (s, 3H), 4.35 – 4.29 (m, 2H), 4.03 – 3.99 (m, 1H), 3.96 – 3.87 (m, 2H), 1.28 (t, *J* = 7.1 Hz and *J* = 7.2 Hz, 3H). ^{13}C NMR (101 MHz, $CDCl_3$): δ 165.96, 162.38, 161.89, 161.39, 160.90, 134.74, 129.19, 129.16, 129.13, 129.10, 128.87, 128.84, 128.81, 128.79, 125.85, 123.15, 120.43, 117.68, 117.64, 117.61, 117.56, 65.14, 58.69, 55.16, 13.66.

Compound **G15**: Colorless solid (221.5 mg, 59.1 %). ^{1}H NMR (400 MHz, $CDCl_3$): δ 7.70 (s, 8H), 7.55 (s, 4H), 7.34 (s, 3H), 4.37 – 4.22 (m, 2H), 4.07 (s, 1H), 2.76 – 2.68 (m, 2H), 2.40 – 2.28 (m, 1H), 2.13 – 2.10 (m, 1H), 2.06 (s, 3H), 1.26 (t, *J* = 7.2 Hz and *J* = 7.3 Hz, 3H). ^{13}C NMR (101 MHz, $CDCl_3$): δ 167.54, 162.39, 161.90, 161.40, 160.91, 134.77, 129.44, 129.41, 129.38, 129.36, 129.13, 129.10, 129.07, 129.04, 128.81, 128.79, 128.76, 128.73, 128.60, 128.47, 128.44, 128.42, 128.40, 125.89, 123.19, 120.48, 65.24, 56.18, 30.65, 25.78, 14.74, 13.65.

Compound **G16**: Colorless solid (254.5 mg, 69.8 %). ^{1}H NMR (400 MHz, $CDCl_3$): δ 7.71 (s, 8H), 7.56 (s, 4H), 6.84 (s, 3H), 4.32 – 4.25 (m, 2H), 4.00 (s, 1H), 3.11 – 3.07 (m, 1H), 2.99 – 2.92 (m, 1H), 1.46 – 1.42 (m, 1H), 1.28 (t, *J* = 7.1 Hz and *J* = 7.2 Hz, 3H). ^{13}C NMR (101 MHz, $CDCl_3$): δ 165.97, 162.41, 161.91, 161.41, 160.92, 134.77, 134.24, 129.61, 129.20, 129.18, 129.15, 129.12, 128.89, 128.86, 128.83, 128.81, 128.57, 125.86, 123.15, 117.71, 117.67, 117.63, 65.59, 55.11, 24.34, 13.70.

3 NMR and HRMS spectra

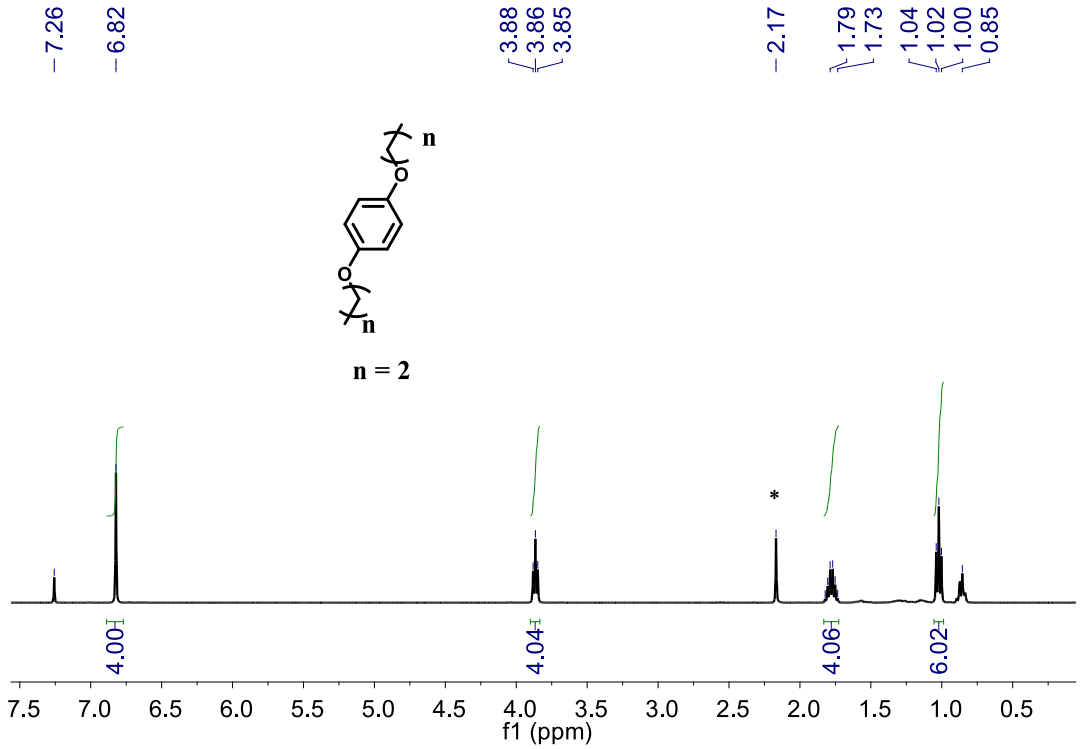

Figure S1. ^{1}H NMR spectrum (400 MHz, chloroform–*d,* room temperature) of **1**. *Acetone was used as an internal standard.

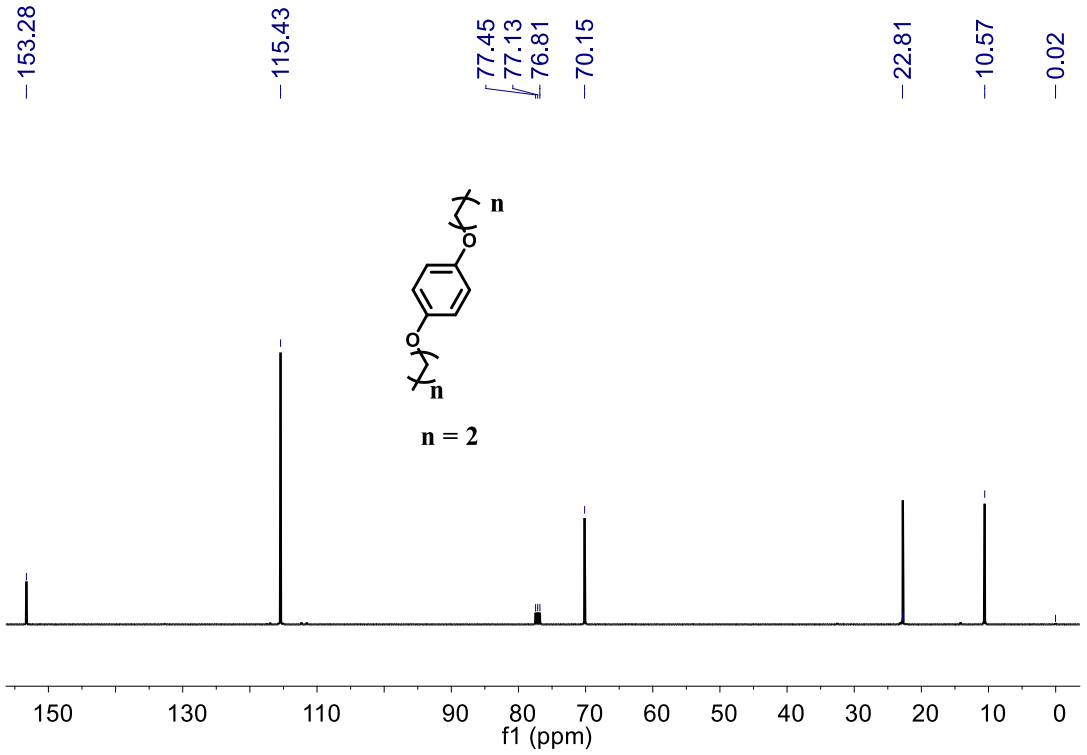

Figure S2. ^{13}C NMR spectrum (101 MHz, chloroform–*d,* room temperature) of **1**.

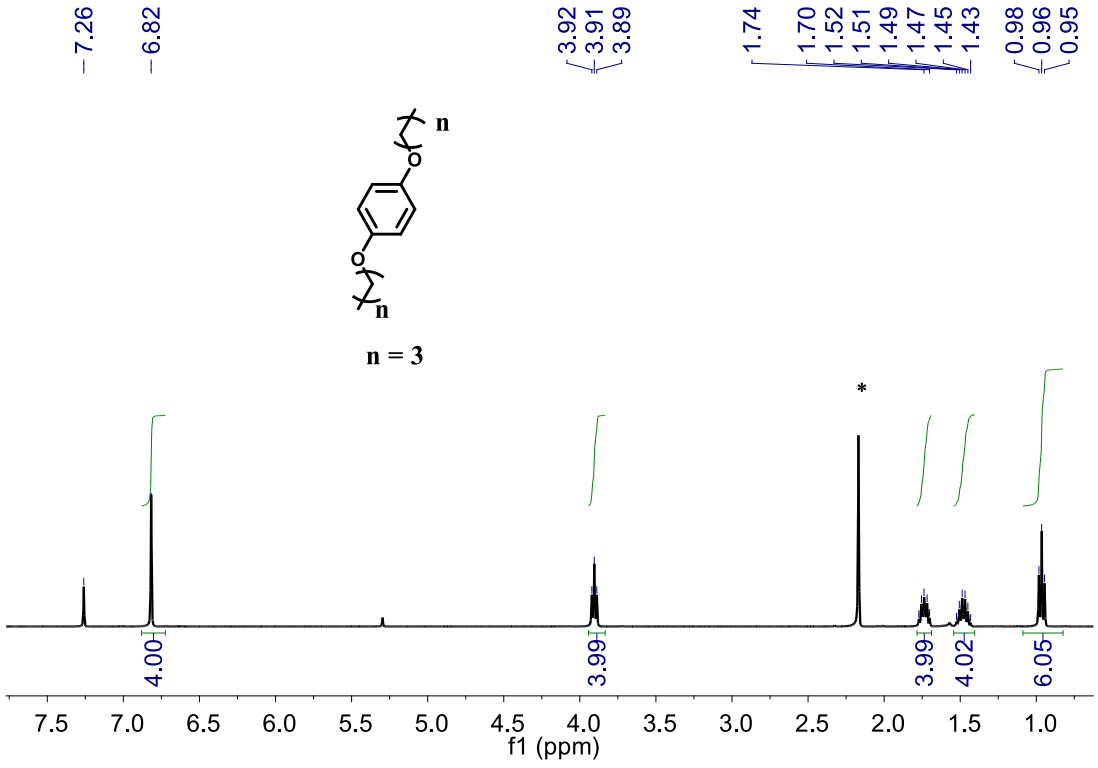

Figure S3. ^{1}H NMR spectrum (400 MHz, chloroform–*d,* room temperature) of **2**. *Acetone was used as an internal standard.

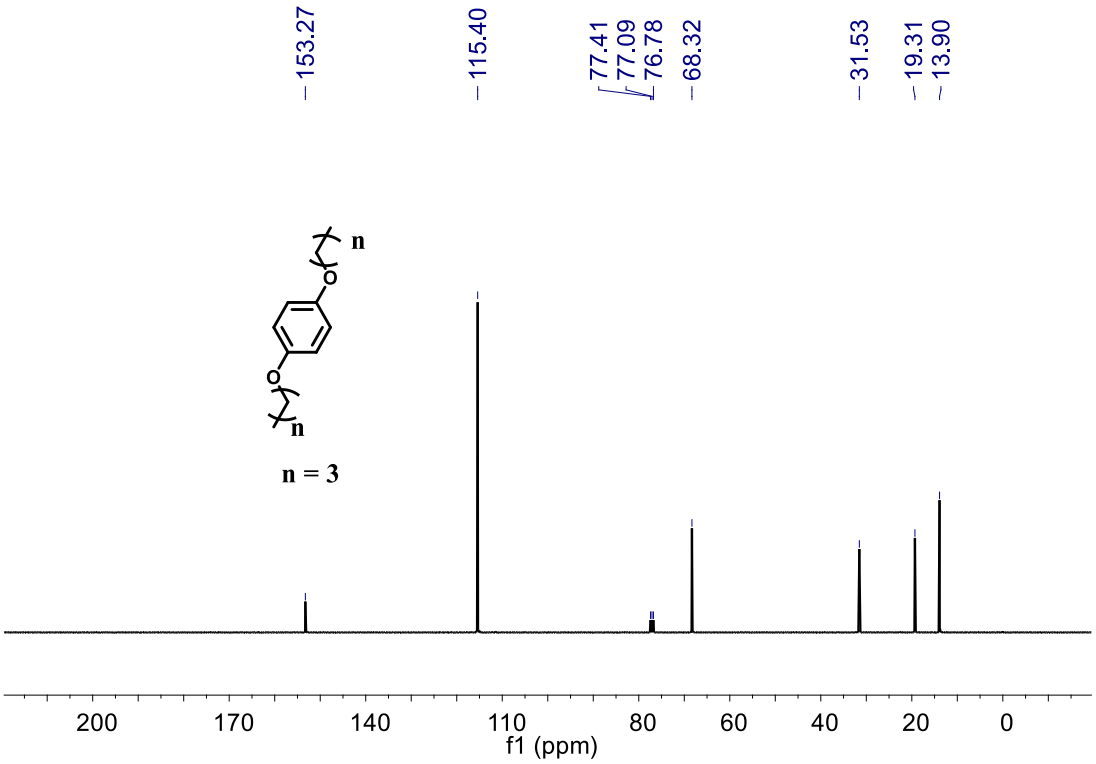

Figure S4. ^{13}C NMR spectrum (101 MHz, chloroform–*d,* room temperature) of **2.**

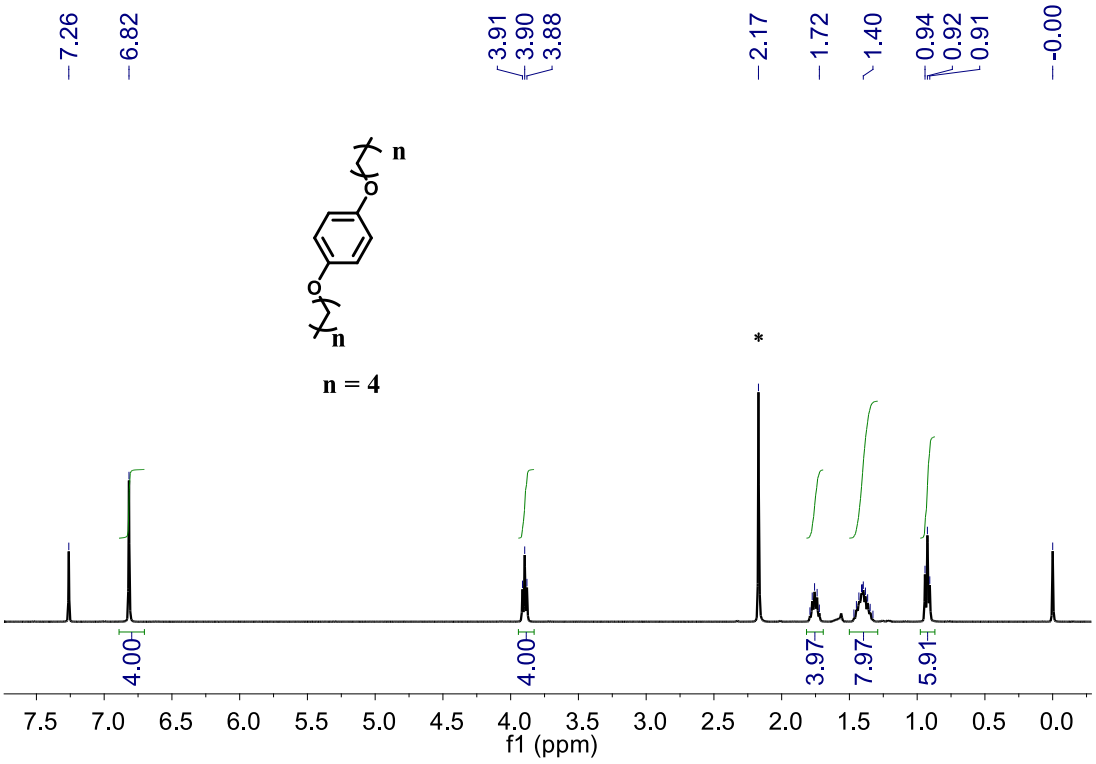

Figure S5. ^{1}H NMR spectrum (400 MHz, chloroform–*d,* room temperature) of **3**. *Acetone was used as an internal standard.

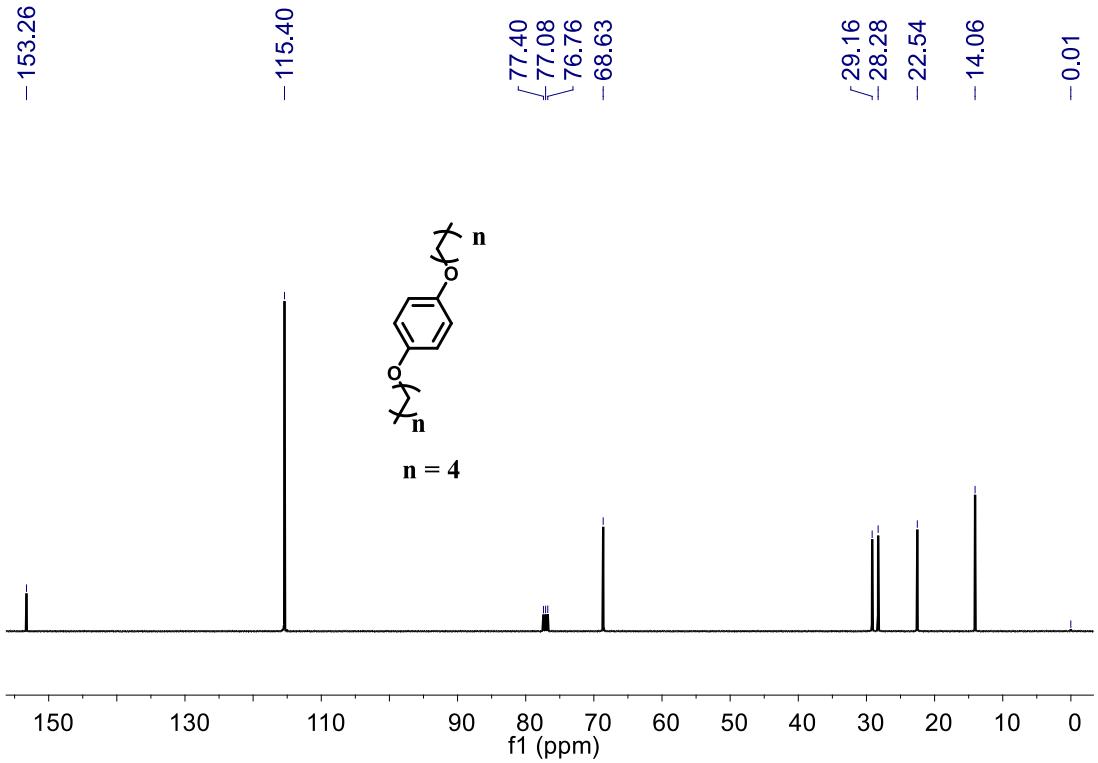

Figure S6. ^{13}C NMR spectrum (101 MHz, chloroform–*d,* room temperature) of **3**.

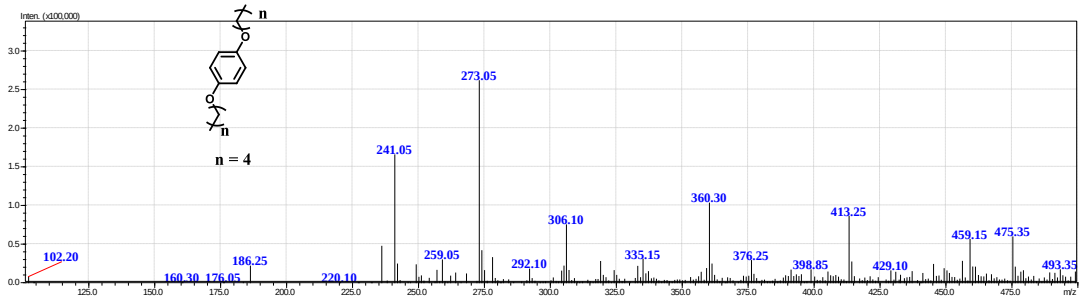

Figure S7. Mass spectrum of **3**. Assignment of main peaks: *m/z* $[M+Na]^+$, 273.1825, found: 273.05.

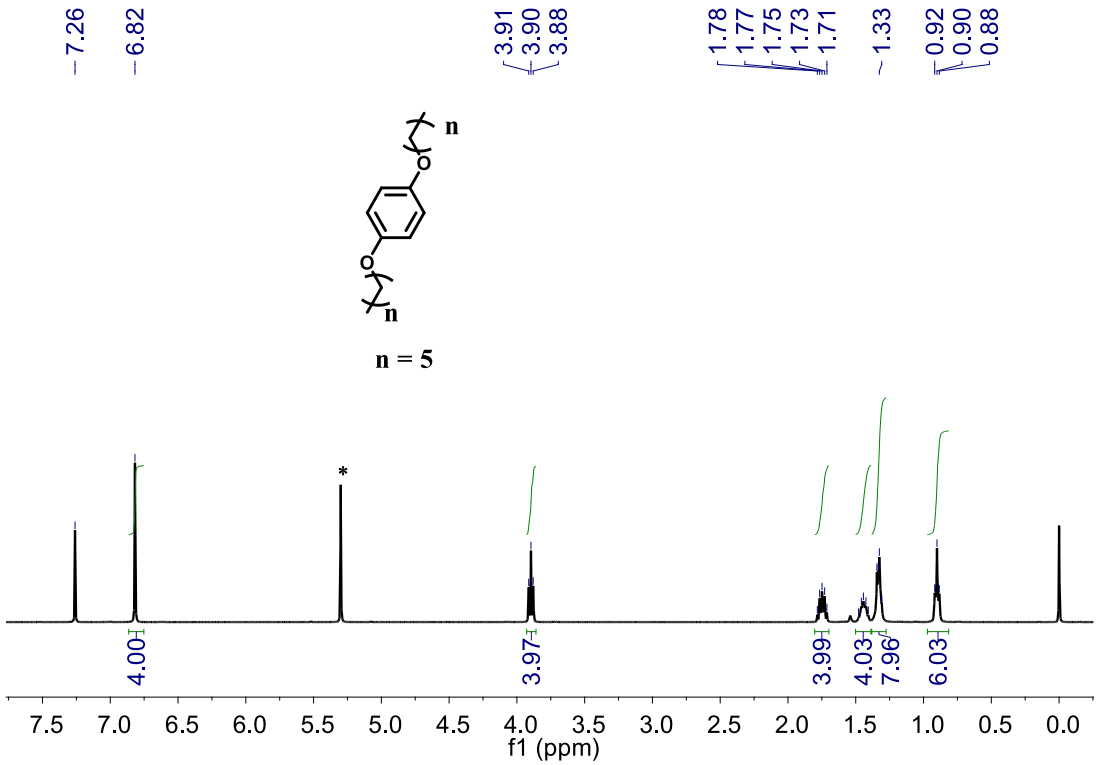

Figure S8. ^{1}H NMR spectrum (400 MHz, chloroform–*d,* room temperature) of **4**. *CH_2Cl_2.

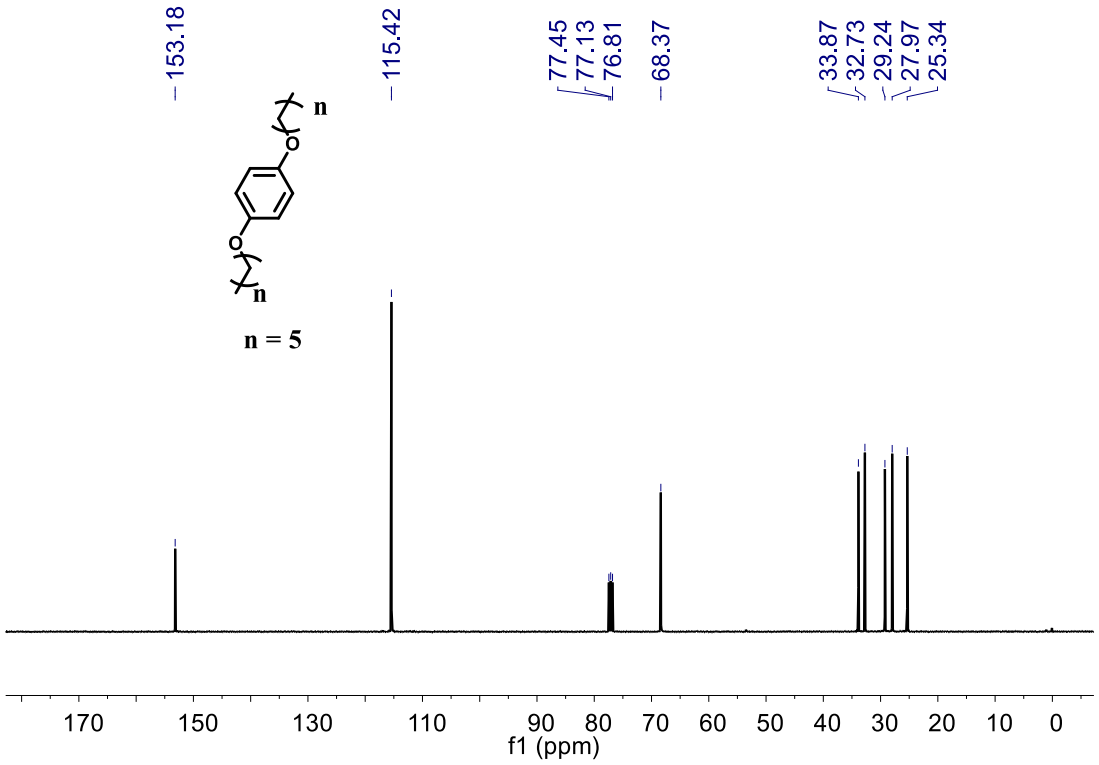

Figure S9. ^{13}C NMR spectrum (101 MHz, chloroform–*d,* room temperature) of **4**.

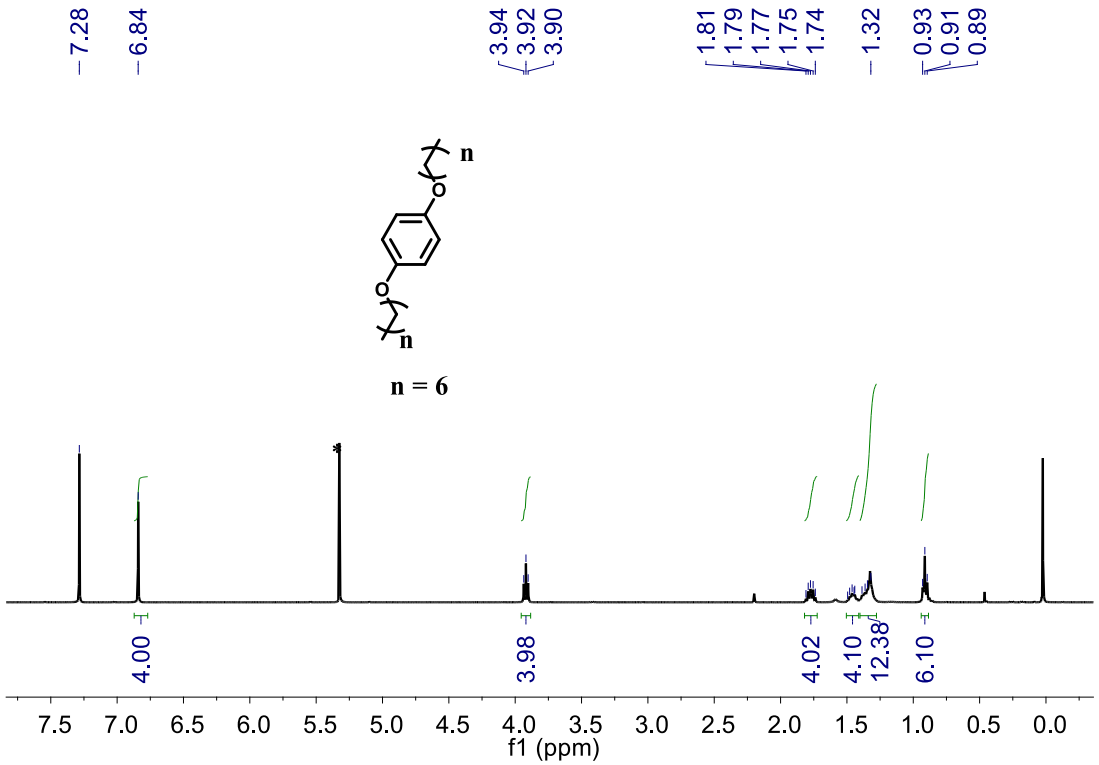

Figure S10. ^{1}H NMR spectrum (400 MHz, chloroform–*d*, room temperature) of **5**. *CH_2Cl_2.

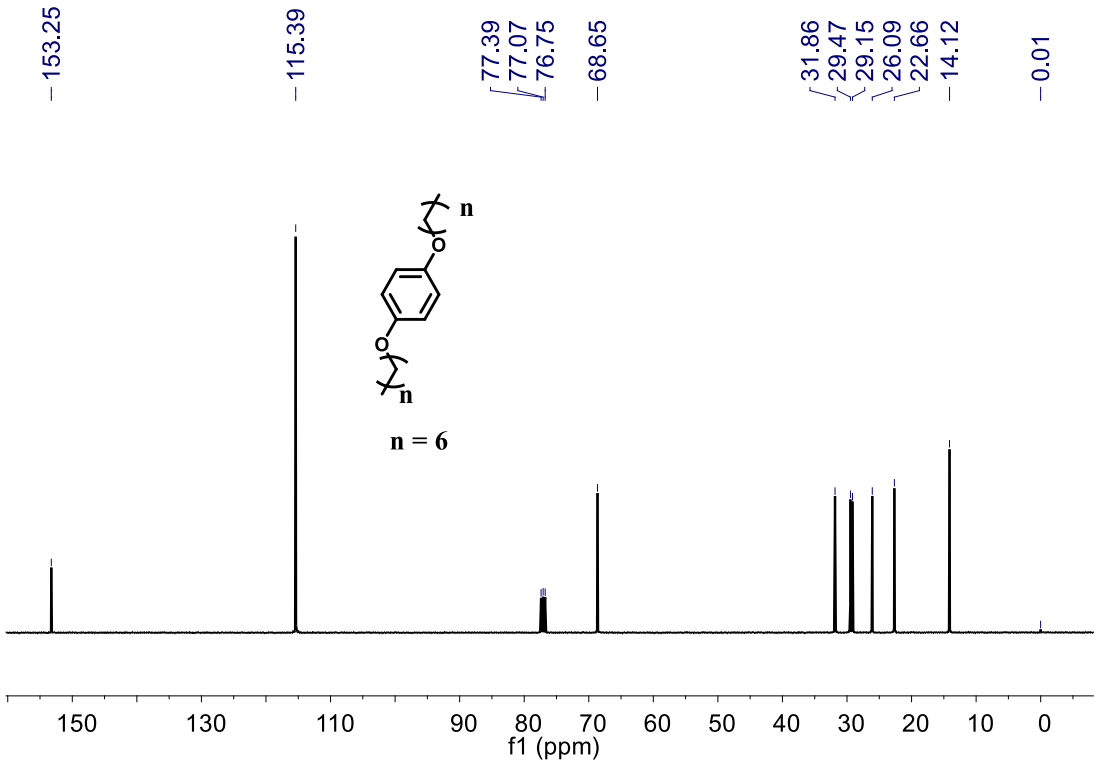

Figure S11. ^{13}C NMR spectrum (101 MHz, chloroform–*d*, room temperature) of **5**.

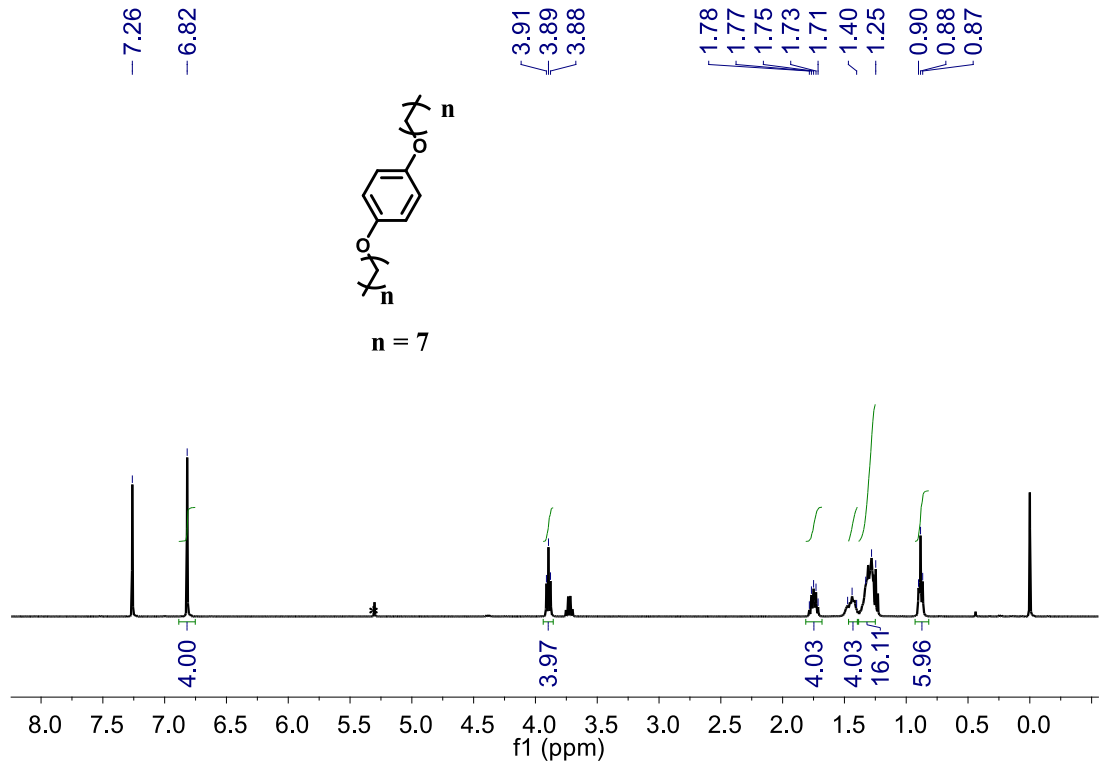

Figure S12. ^{1}H NMR spectrum (400 MHz, chloroform–*d*, room temperature) of **6**. *CH_2Cl_2.

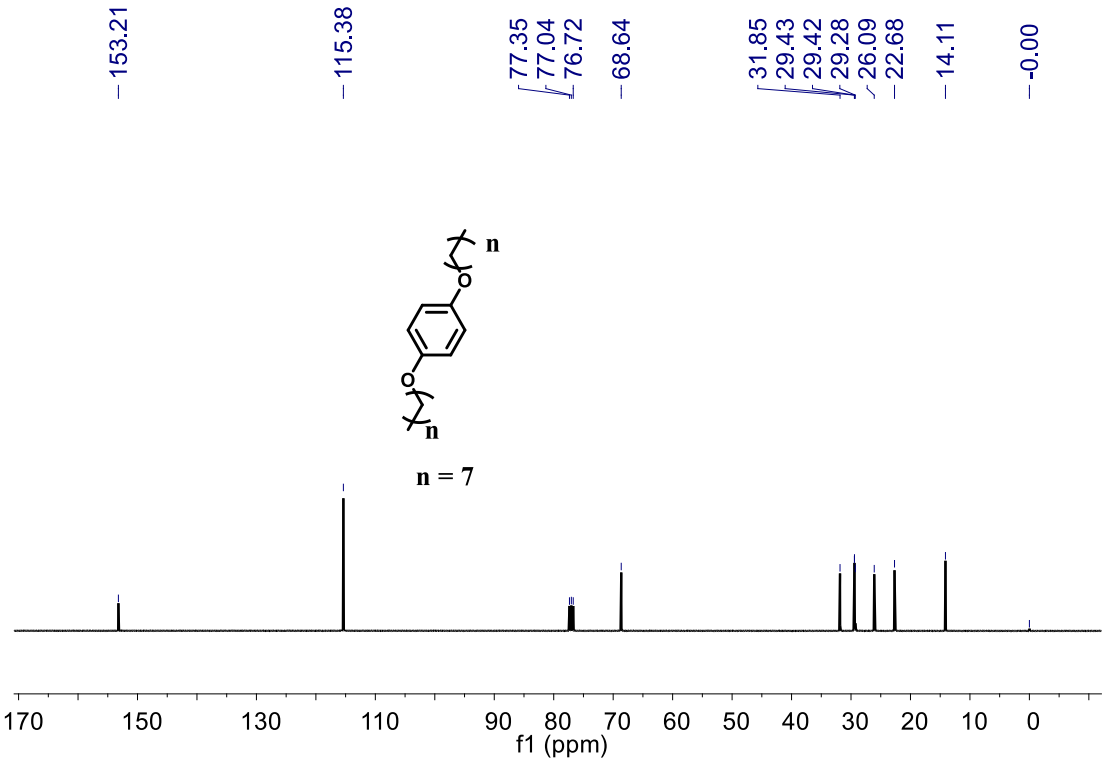

Figure S13. ^{13}C NMR spectrum (101 MHz, chloroform–*d*, room temperature) of **6**.

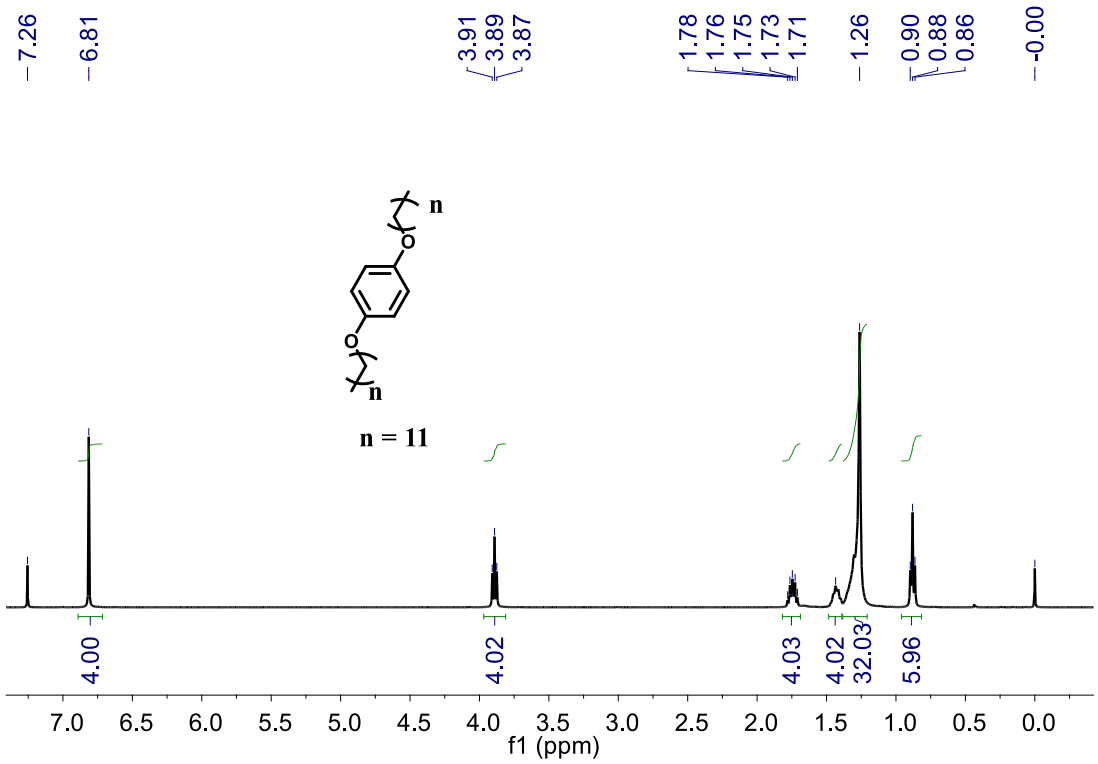

Figure S14. ^{1}H NMR spectrum (400 MHz, chloroform–*d*, room temperature) of **7**.

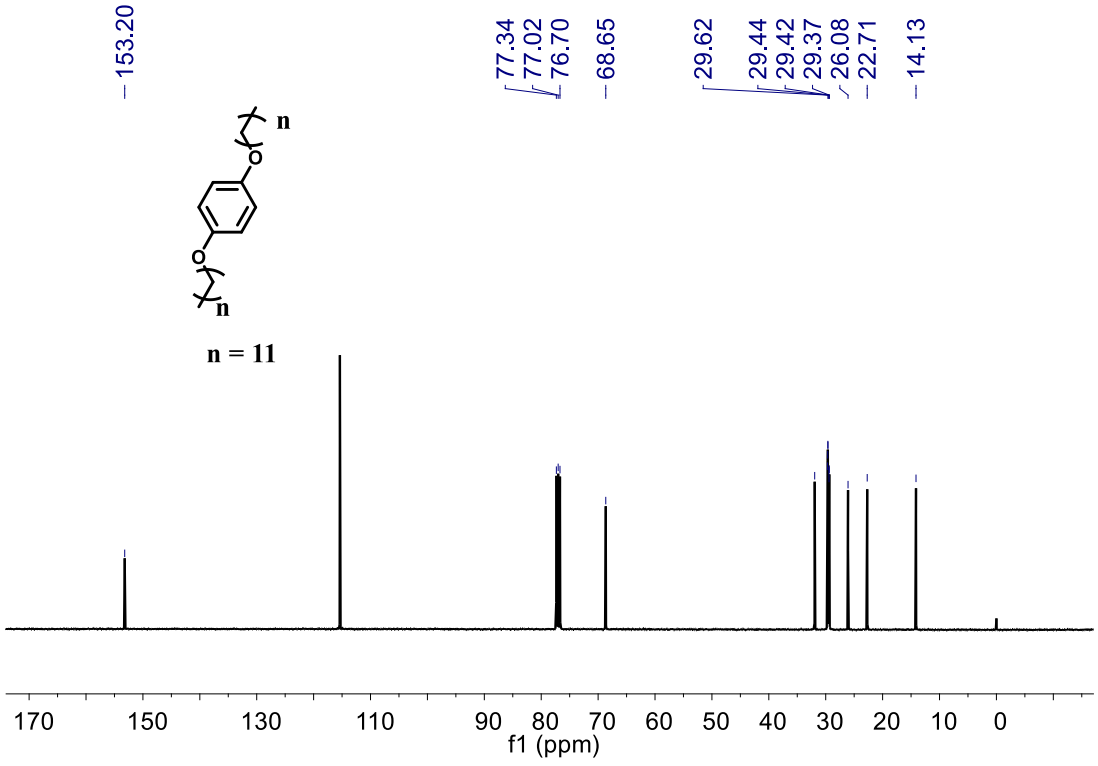

Figure S15. ^{13}C NMR spectrum (101 MHz, chloroform–*d*, room temperature) of **7**.

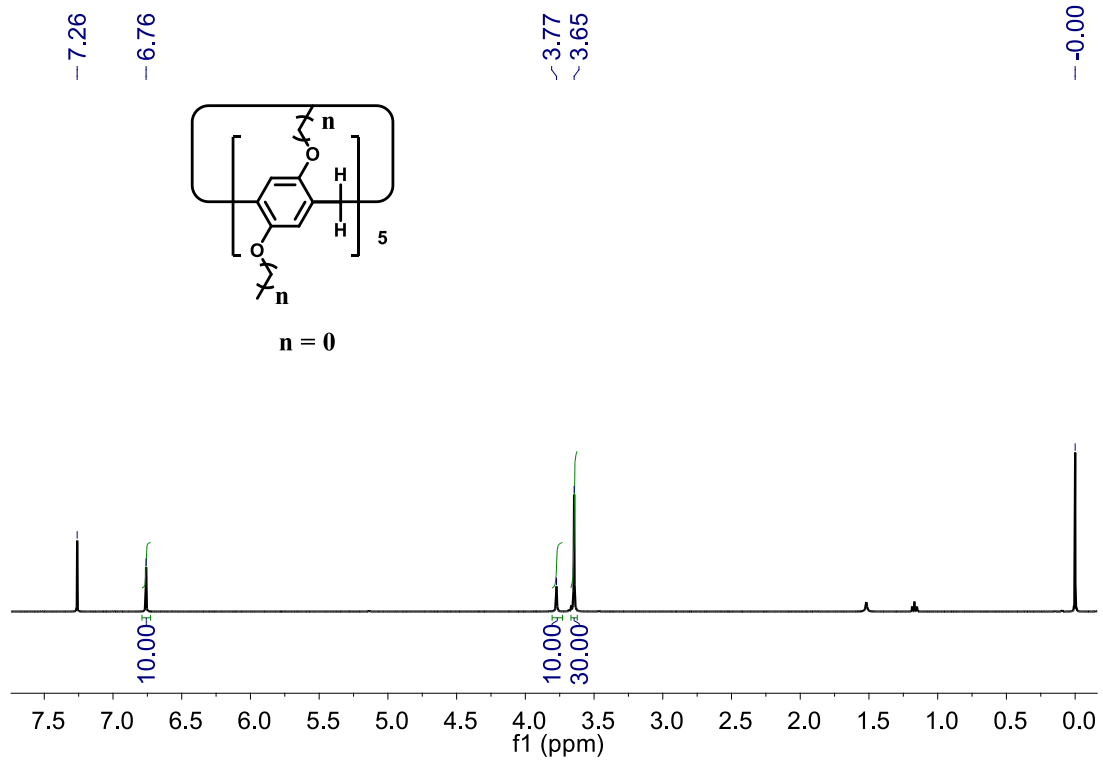

Figure S16. ^{1}H NMR spectrum (400 MHz, chloroform–*d*, room temperature) of **H1**.

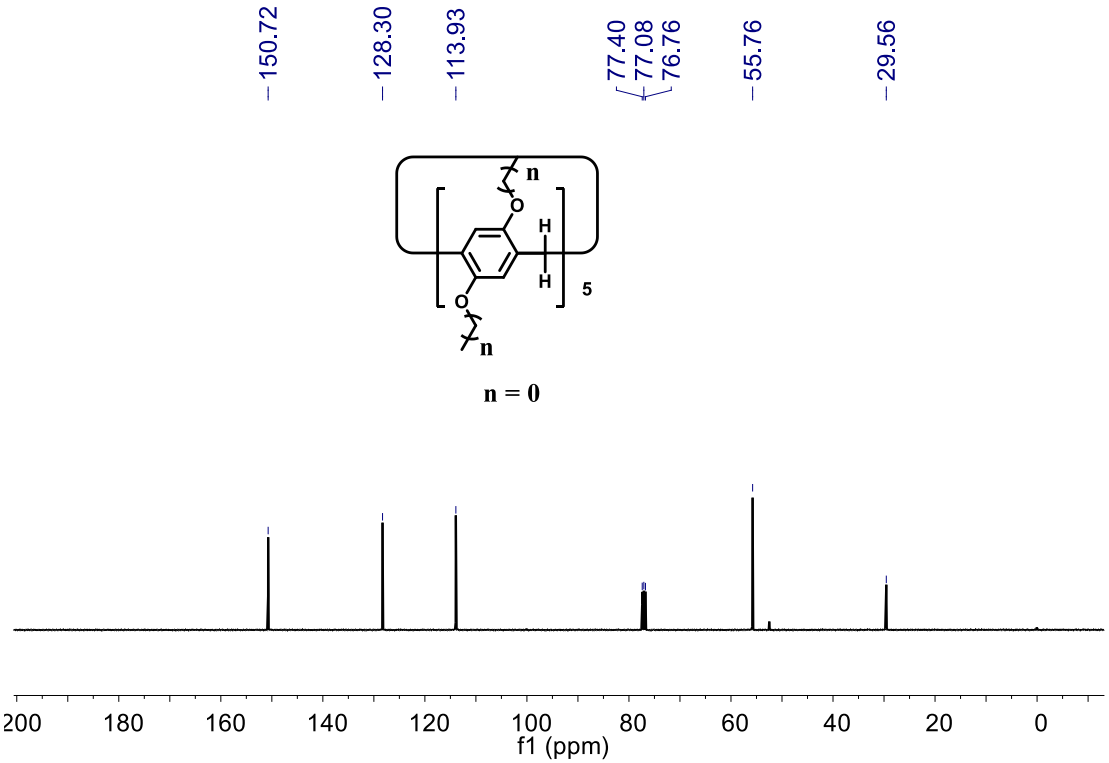

Figure S17. ^{13}C NMR spectrum (101 MHz, chloroform–*d*, room temperature) of **H1**.

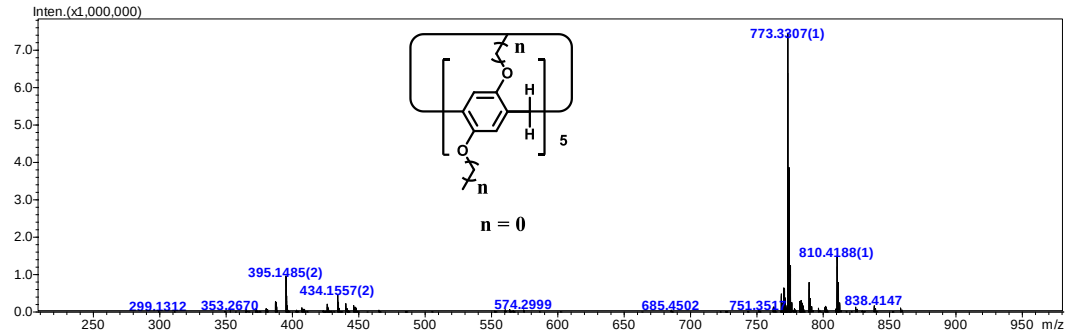

Figure S18. Electrospray ionization mass spectrum of **H1**. Assignment of main peaks: *m/z* $[C_{45}H_{50}NaO_{10}]^+$, $[M+Na]^+$: 773.3296, found: 773.3307.

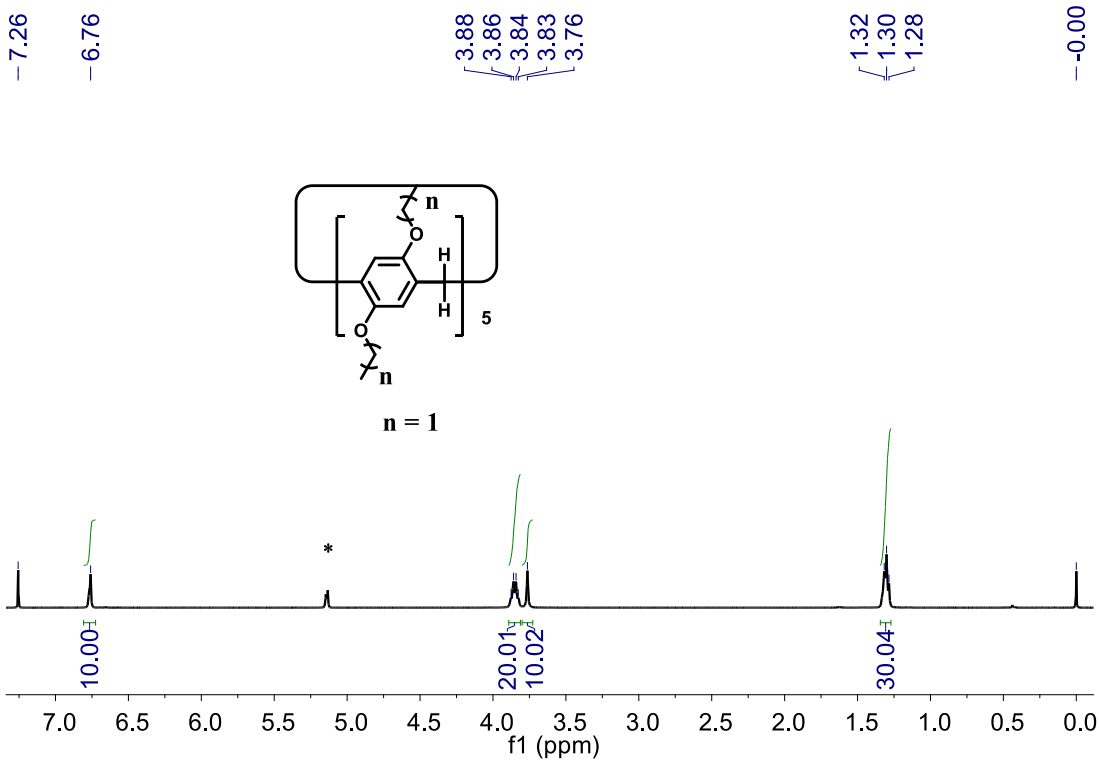

Figure S19. ^{1}H NMR spectrum (400 MHz, chloroform–*d*, room temperature) of **H2**. * CH_2Cl_2.

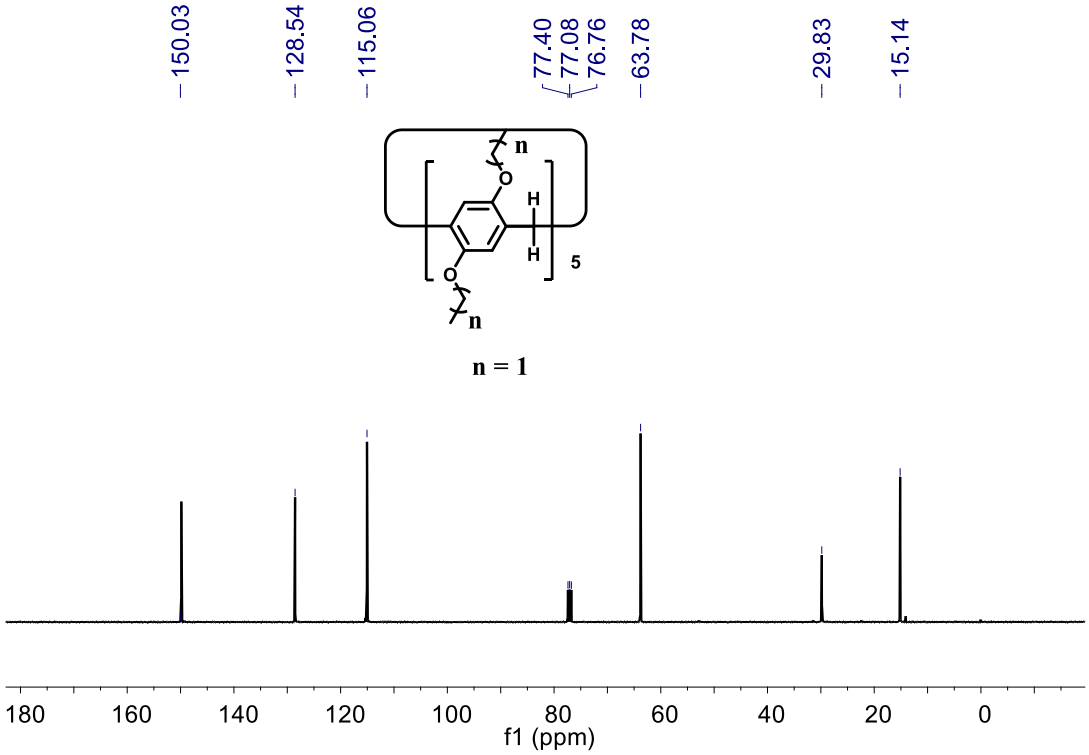

Figure S20. ^{13}C NMR spectrum (101 MHz, chloroform–*d,* room temperature) of **H2**.

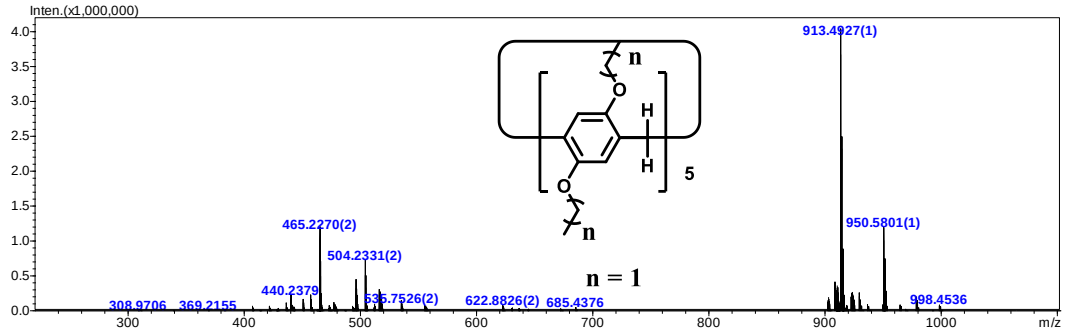

Figure S21. Electrospray ionization mass spectrum of **H2**. Assignment of main peaks: *m/z* $[C_{55}H_{70}NaO_{10}]^+$, $[M+Na]^+$: 913.4861, found: 913.4927.

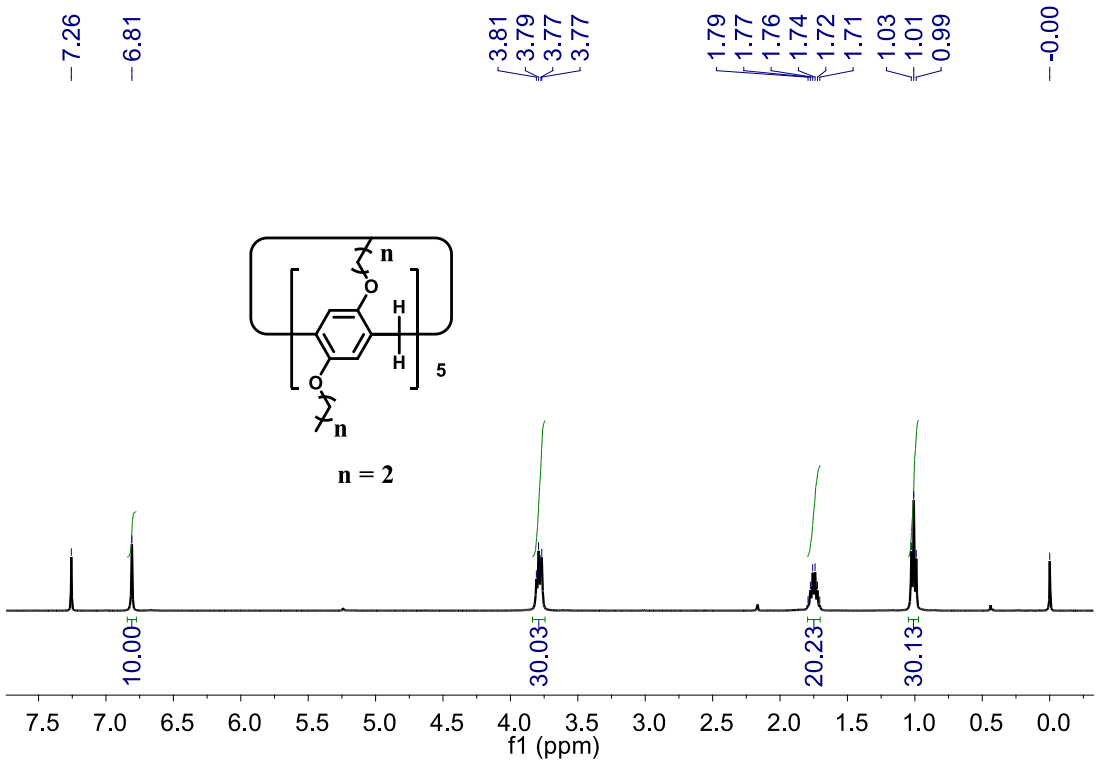

Figure S22. ^{1}H NMR spectrum (400 MHz, chloroform–*d*, room temperature) of **H3**.

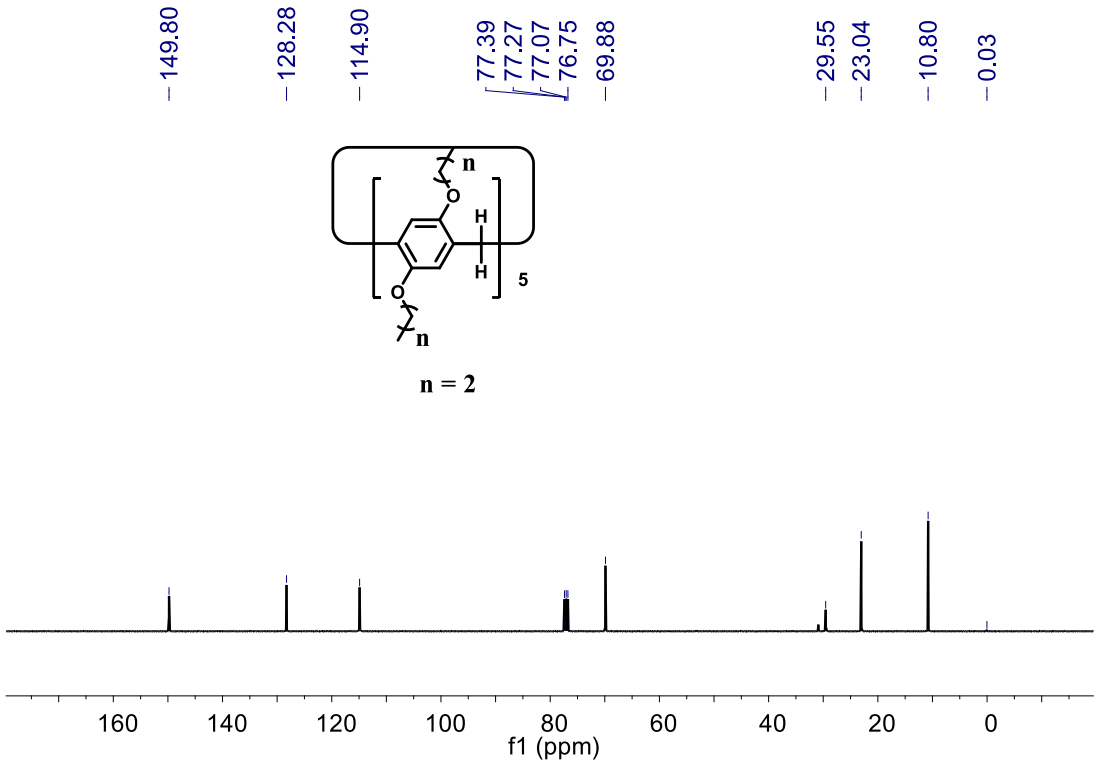

Figure S23. ^{13}C NMR spectrum (101 MHz, chloroform–*d*, room temperature) of **H3**.

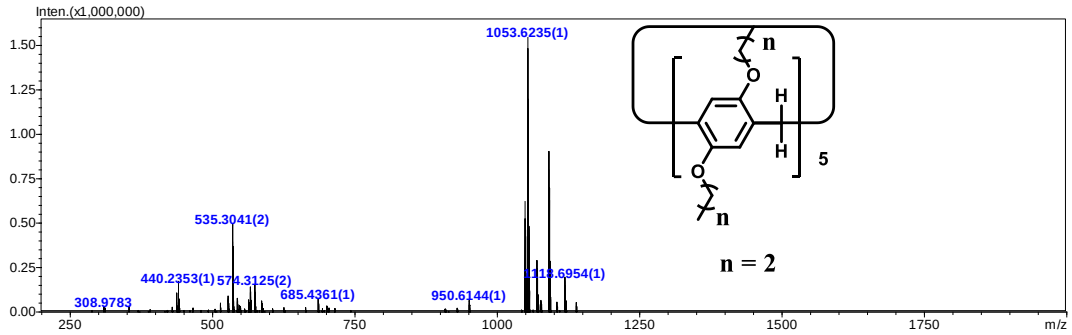

Figure S24. Electrospray ionization mass spectrum of **H3**. Assignment of main peaks: *m/z* $[C_{65}H_{90}NaO_{10}]^+$, $[M+Na]^+$: 1053.6426, found: 1053.6235.

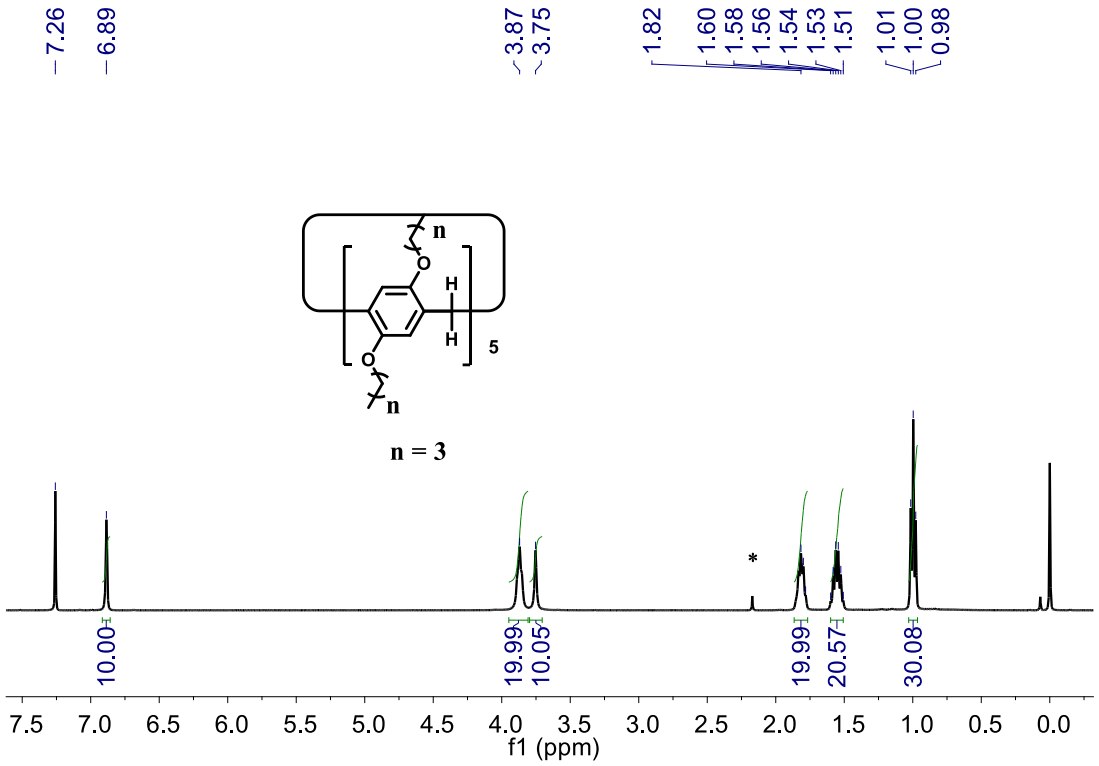

Figure S25. ^{1}H NMR spectrum (400 MHz, chloroform–*d*, room temperature) of **H4**. *Acetone was used as an internal standard.

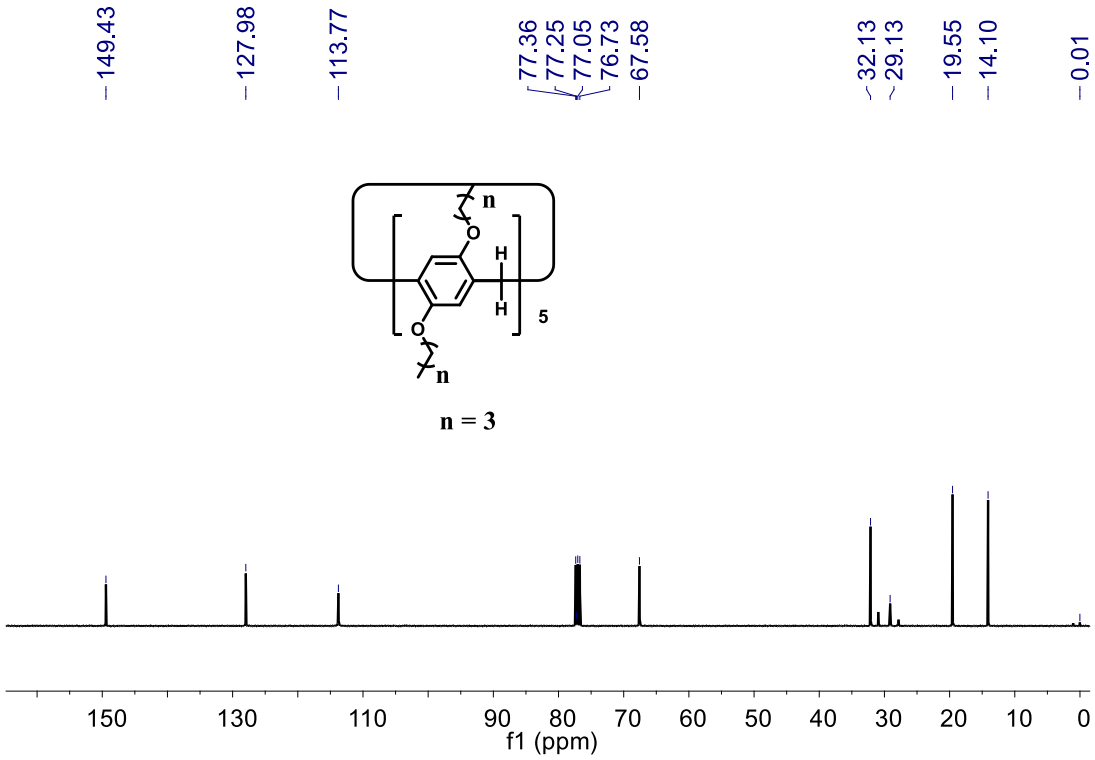

Figure S26. ^{13}C NMR spectrum (101 MHz, chloroform–*d,* room temperature) of **H4**.

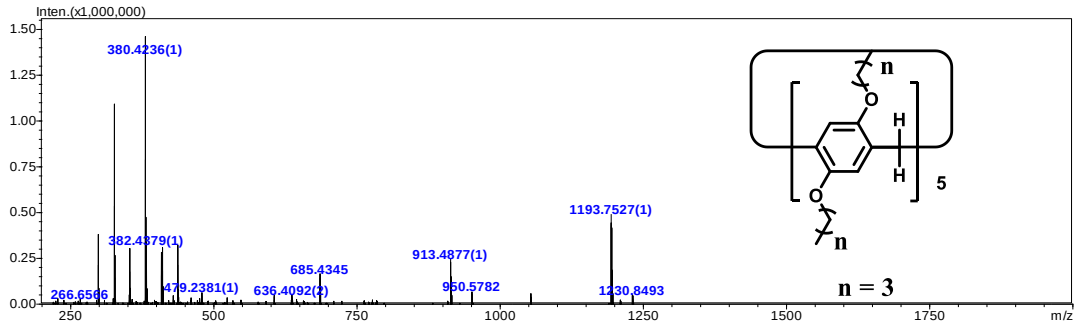

Figure S27. Electrospray ionization mass spectrum of **H4**. Assignment of main peaks: *m/z* $[C_{75}H_{110}NaO_{10}]^+$, $[M+Na]^+$: 1193.7991, found: 1193.7527.

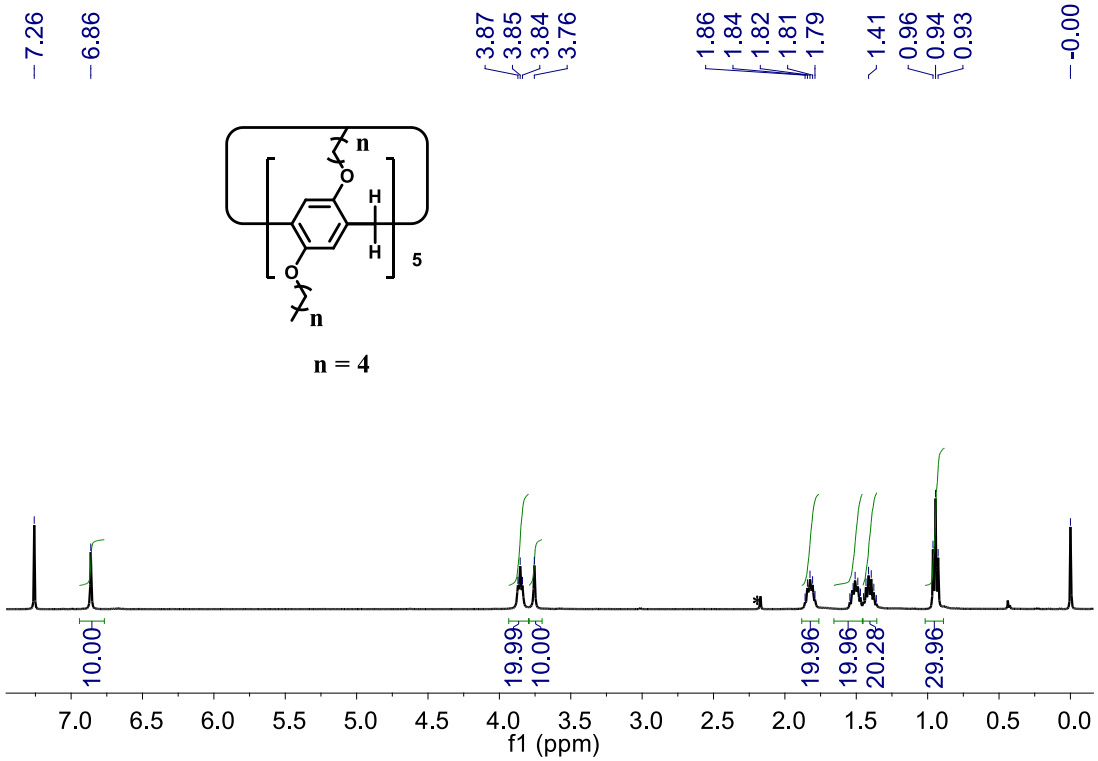

Figure S28. ^{1}H NMR spectrum (400 MHz, chloroform–*d*, room temperature) of **H5**. *Acetone was used as an internal standard.

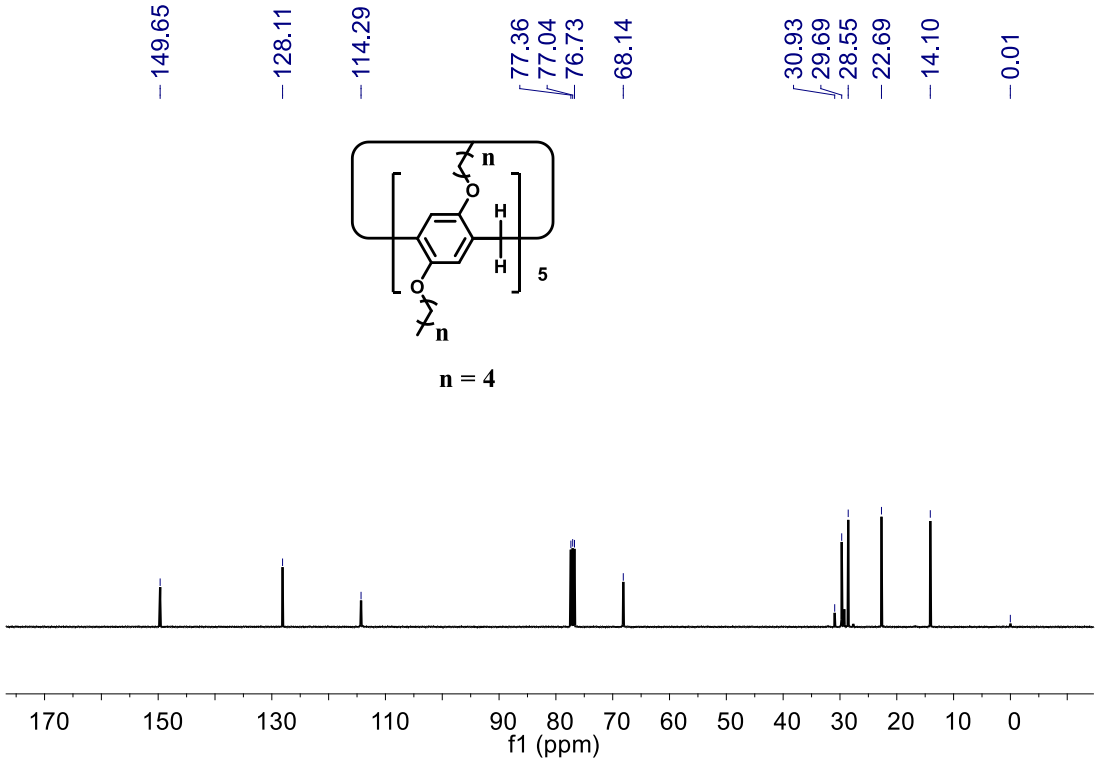

Figure S29. ^{13}C NMR spectrum (101 MHz, chloroform–*d*, room temperature) of **H5**.

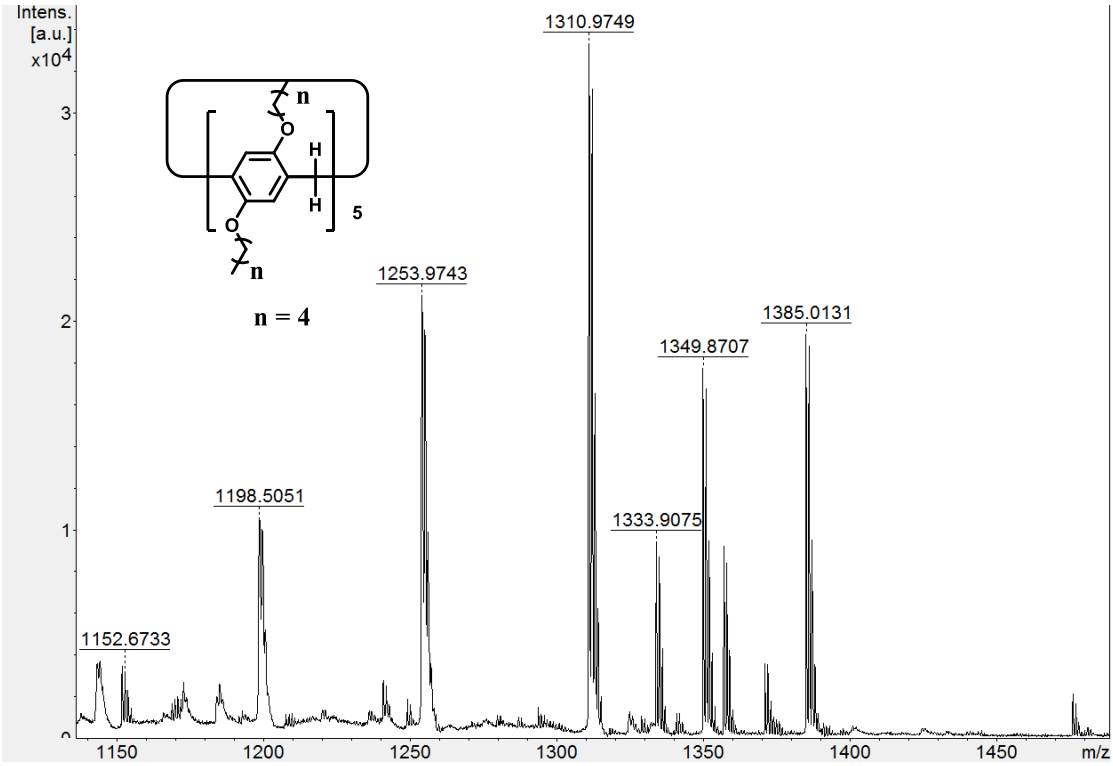

Figure S30. MALDI-HRMS of **H5.**

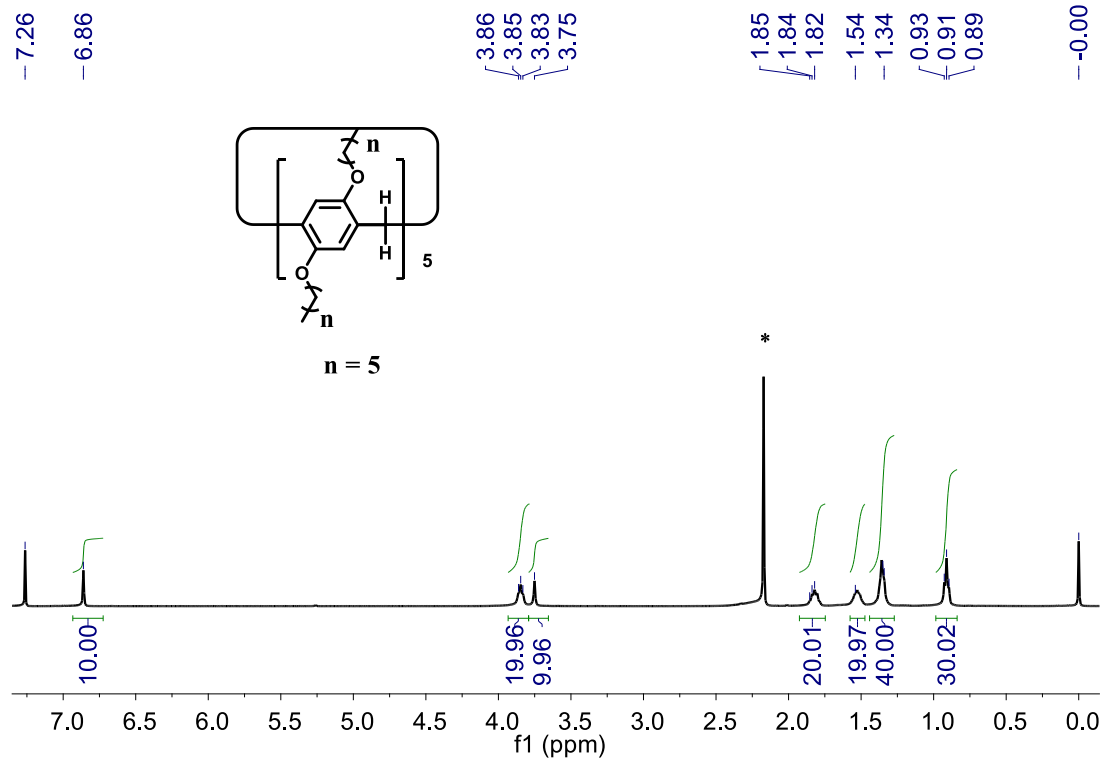

Figure S31. ^{1}H NMR spectrum (400 MHz, chloroform–*d,* room temperature) of **H6**. *Acetone was used as an internal standard.

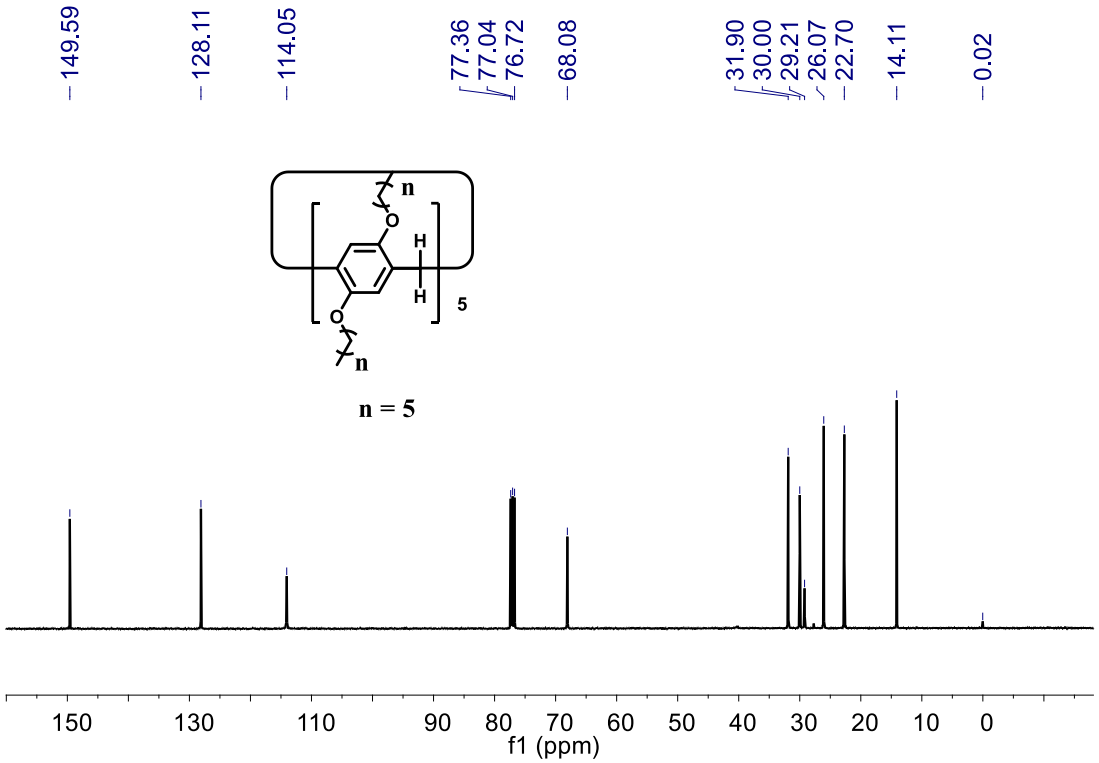

Figure S32. ^{13}C NMR spectrum (101 MHz, chloroform–*d,* room temperature) of **H6**

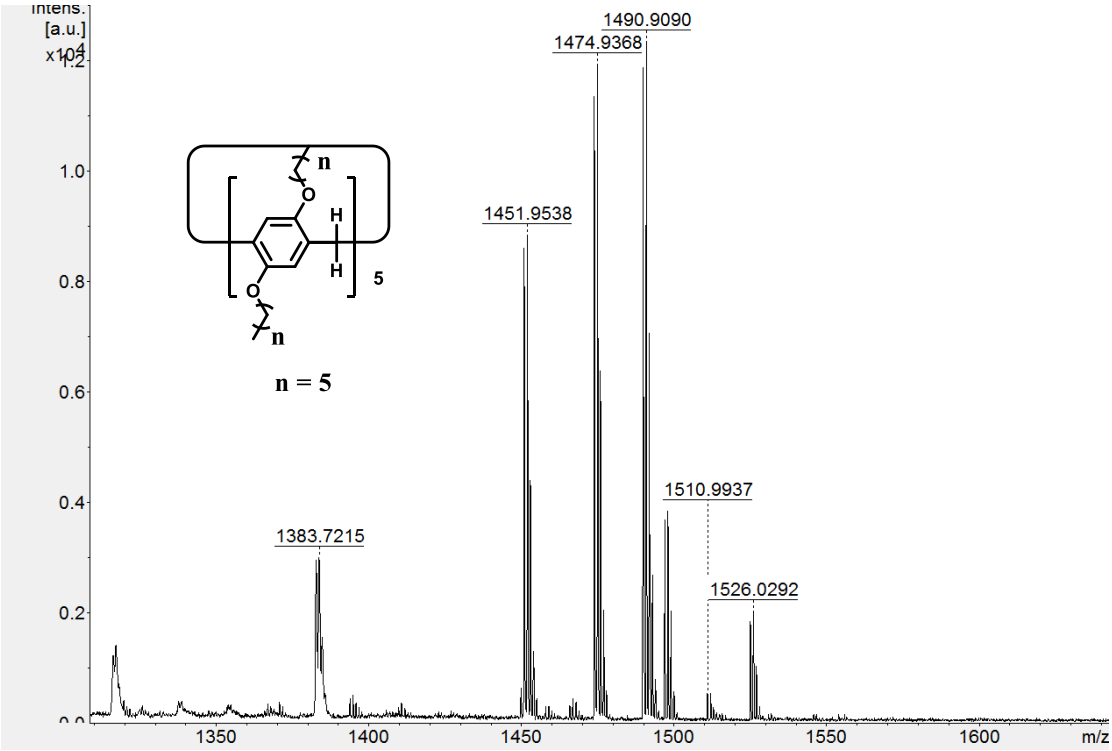

Figure S33. MALDI-HRMS of **H6.**

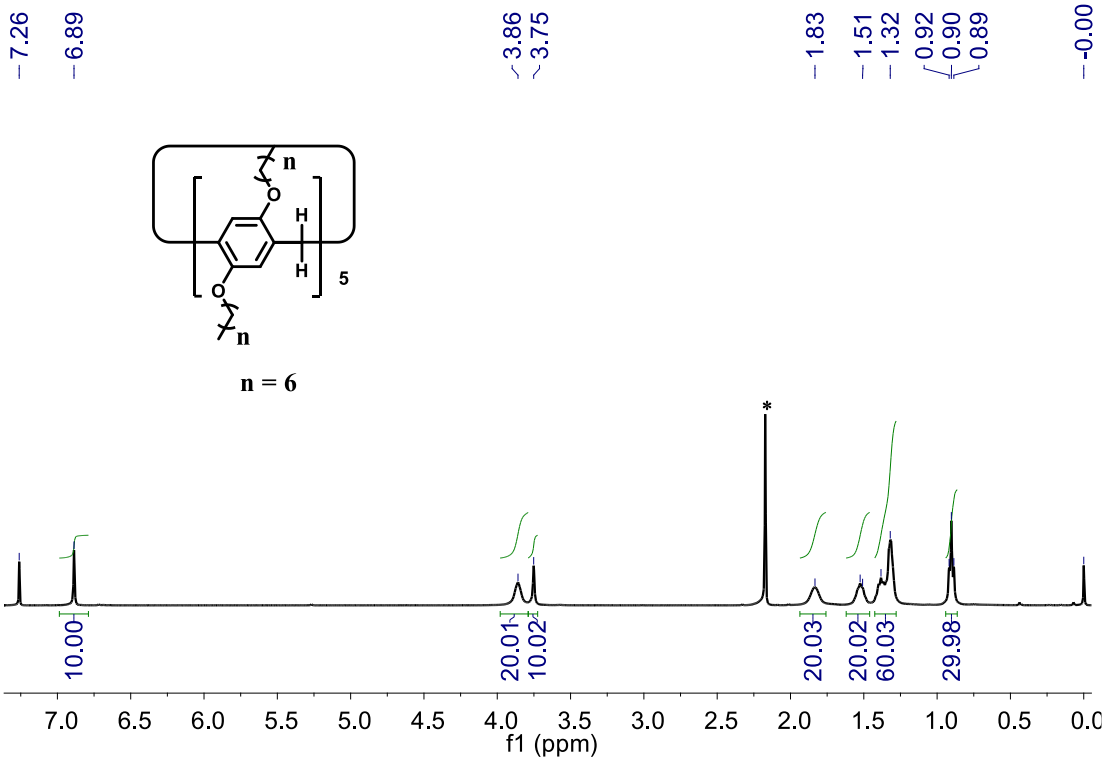

Figure S34. ^{1}H NMR spectrum (400 MHz, chloroform–*d,* room temperature) of **H7**. *Acetone was used as an internal standard.

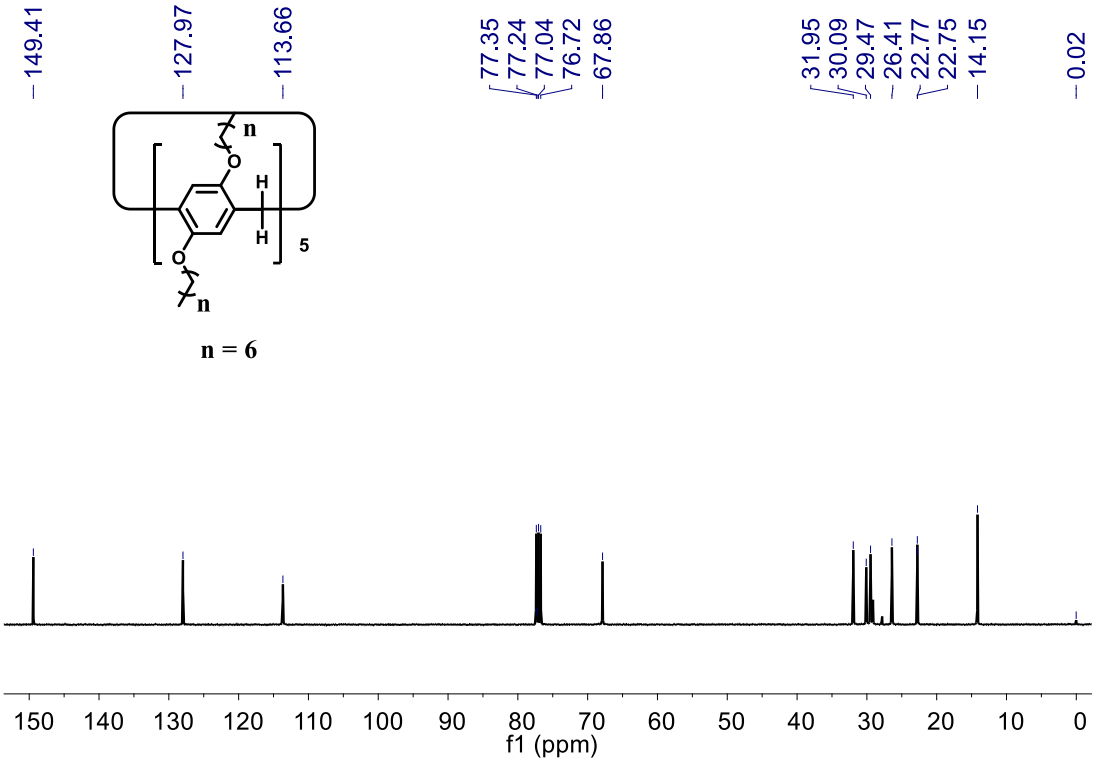

Figure S35. ^{13}C NMR spectrum (101 MHz, chloroform–*d,* room temperature) of **H7**.

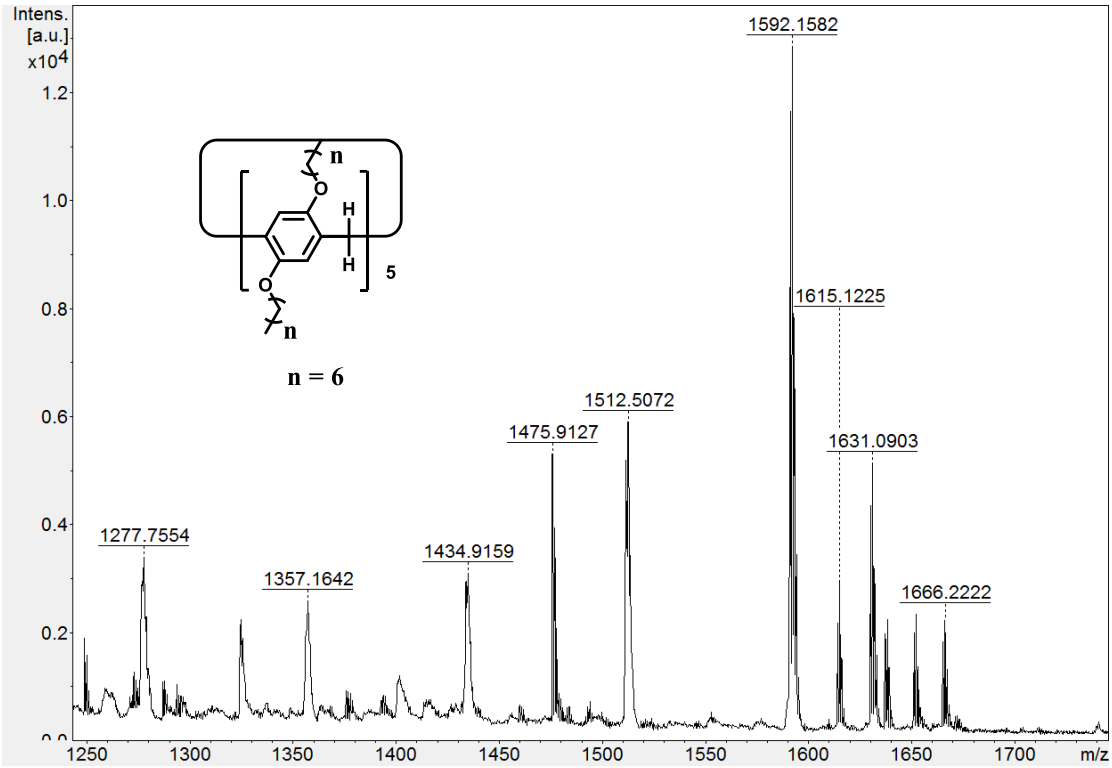

Figure S36. MALDI-HRMS of **H7**.

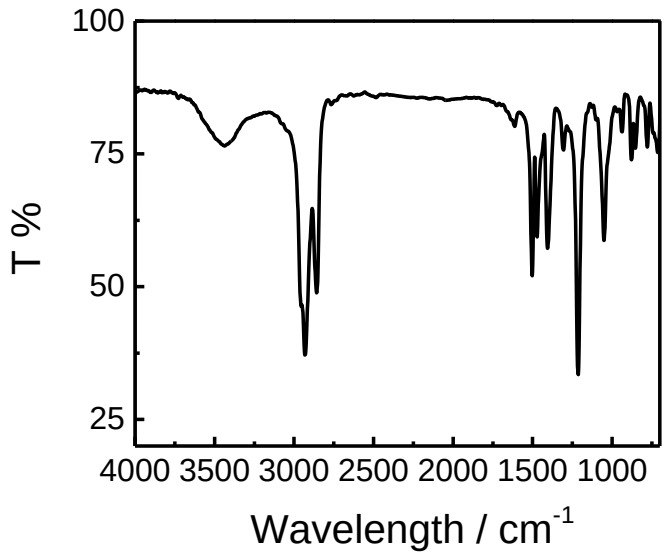

Figure S37. Infrared spectroscopy of **H7**.

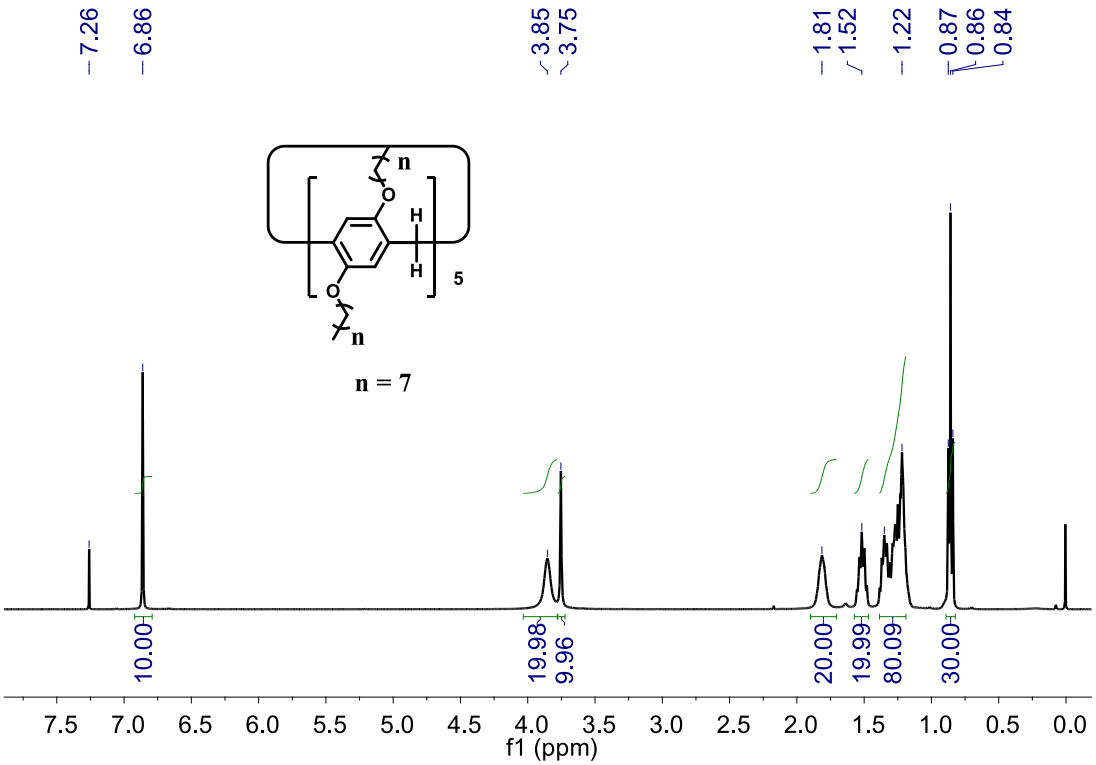

Figure S38. ^{1}H NMR spectrum (400 MHz, chloroform–*d*, room temperature) of **H8**.

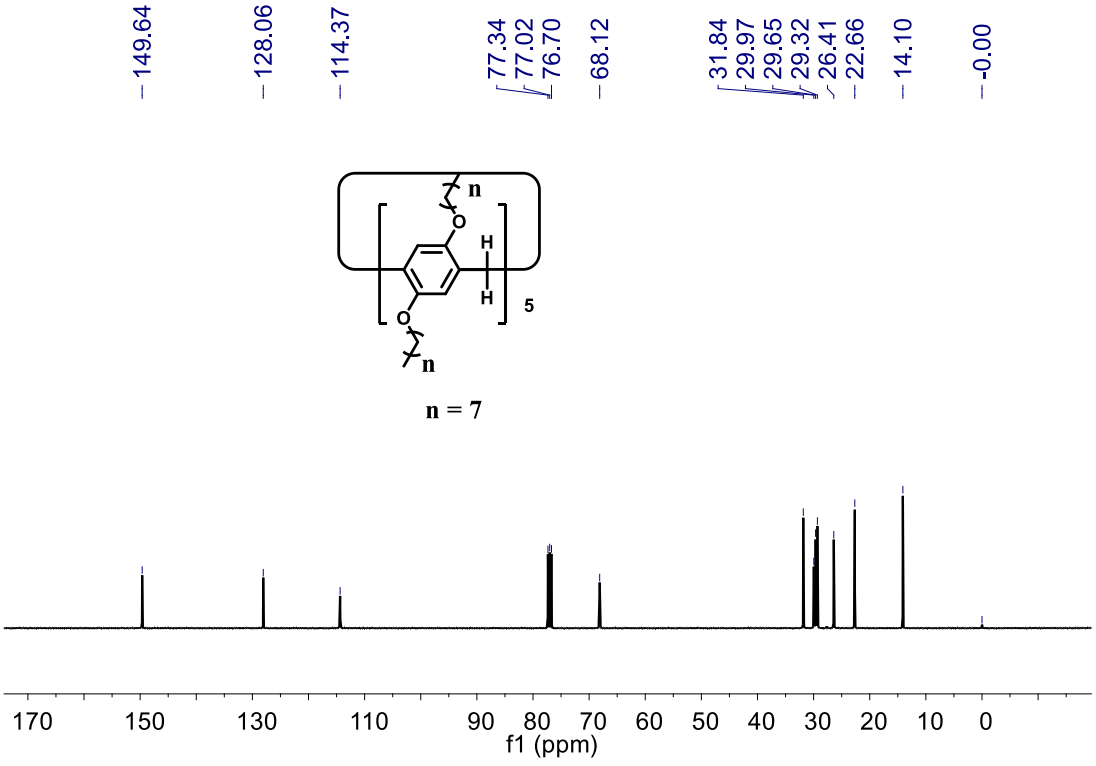

Figure S39. ^{13}C NMR spectrum (101 MHz, chloroform–*d*, room temperature) of **H8**

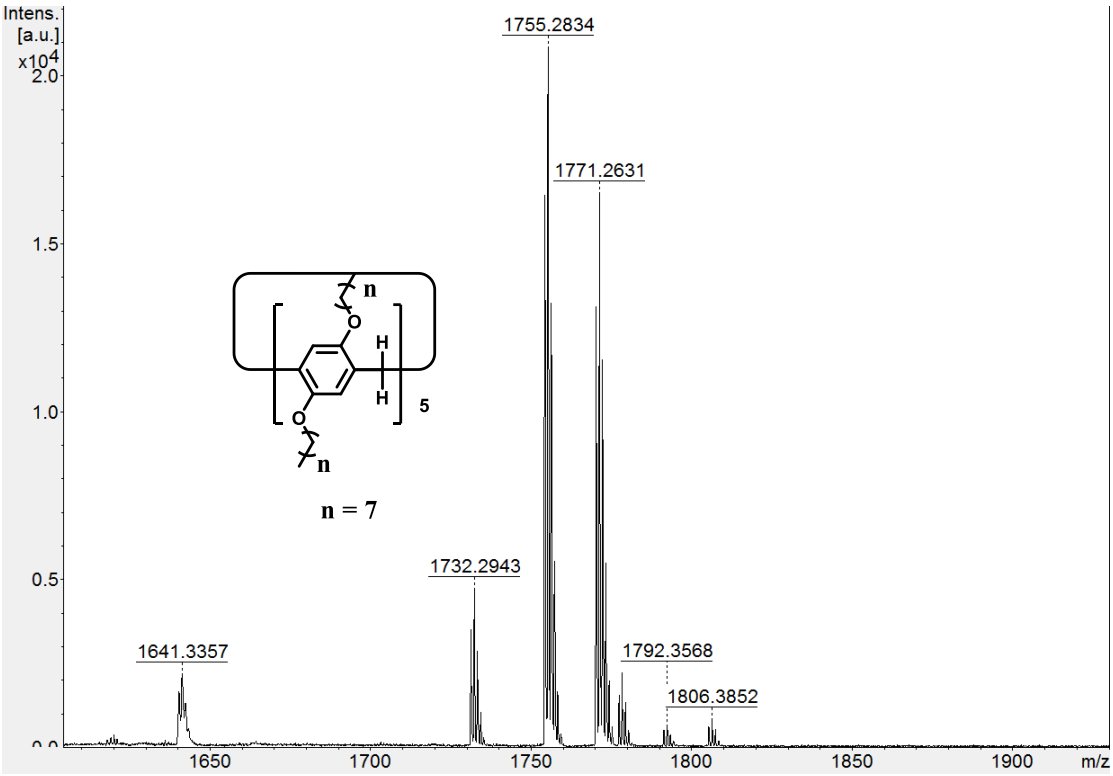

Figure S40. MALDI-HRMS of **H8**.

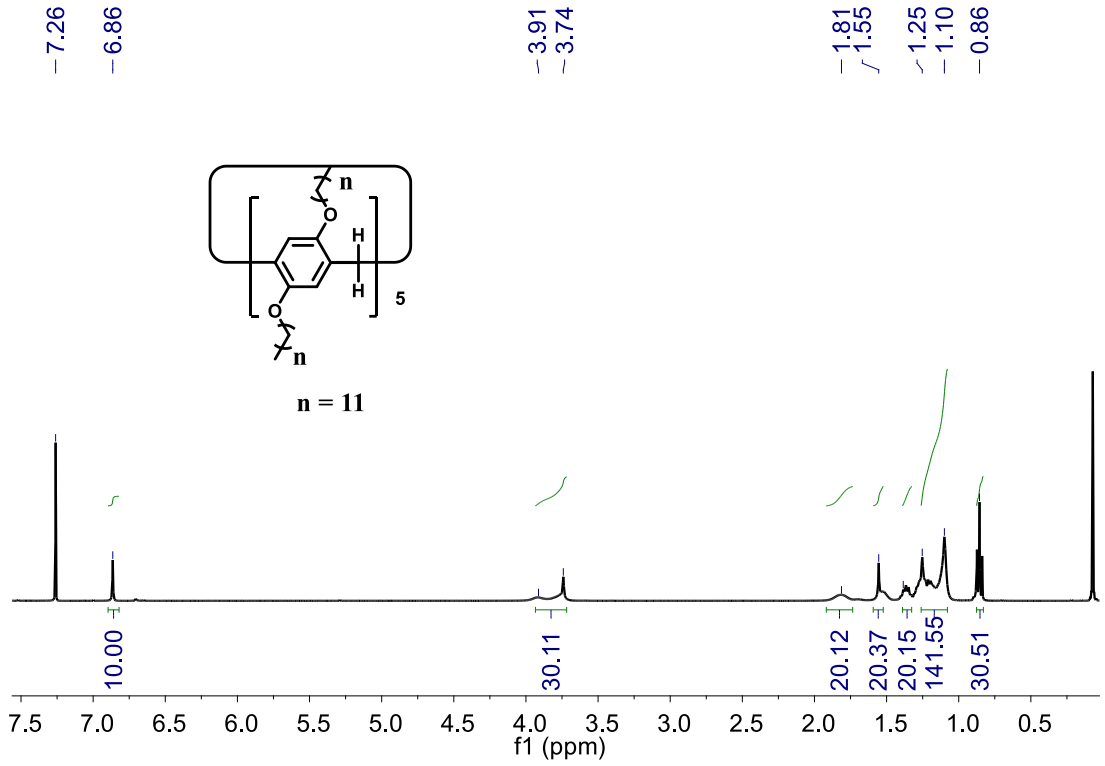

Figure S41. ^{1}H NMR spectrum (400 MHz, chloroform–*d*, room temperature) of **H12**.

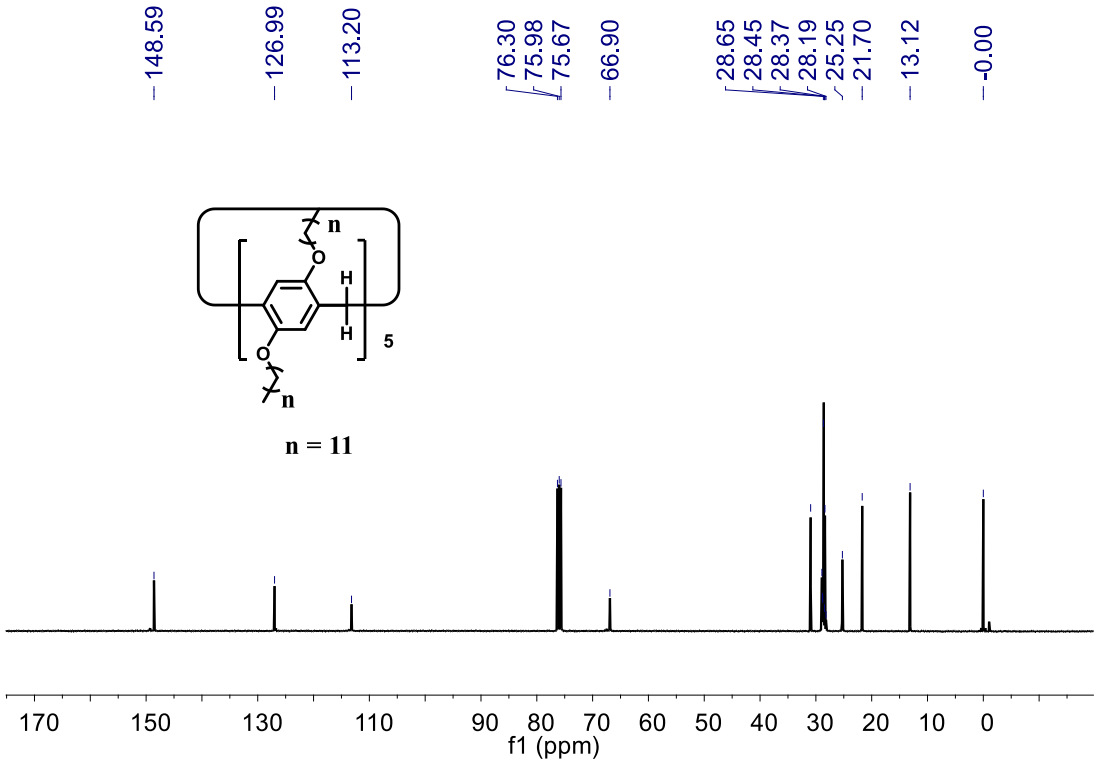

Figure S42. ^{13}C NMR spectrum (101 MHz, chloroform–*d,* room temperature) of **H12**.

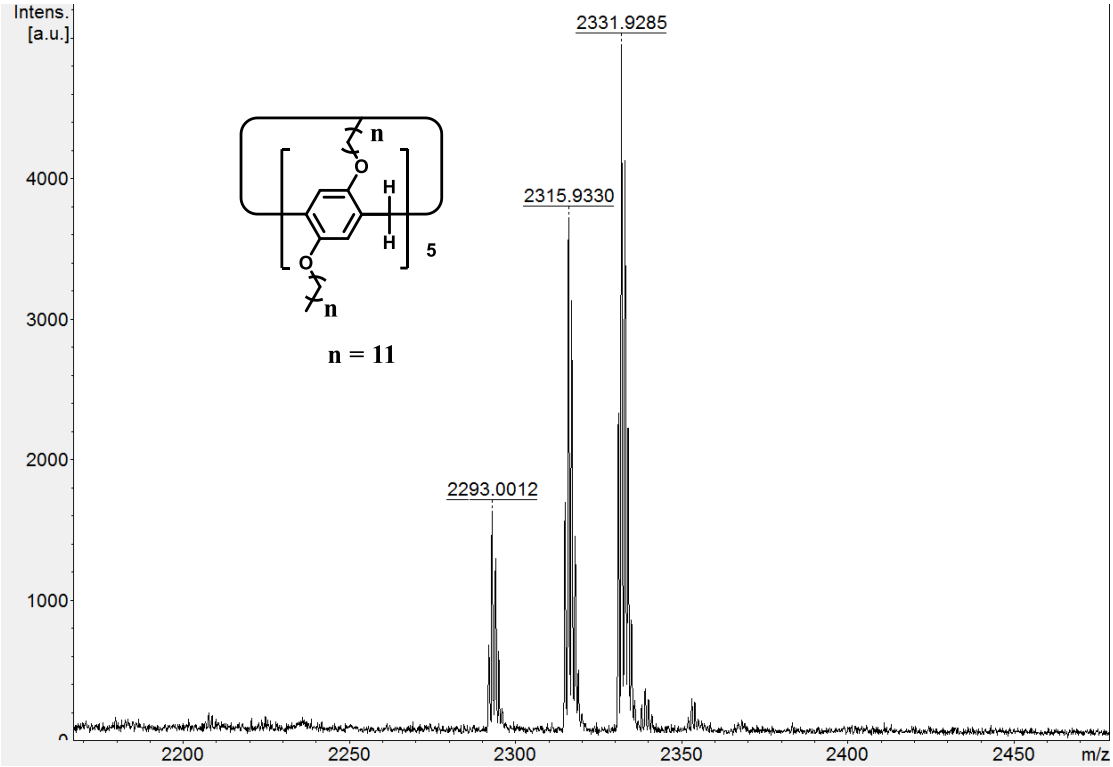

Figure S43. MALDI-HRMS of **H12**.

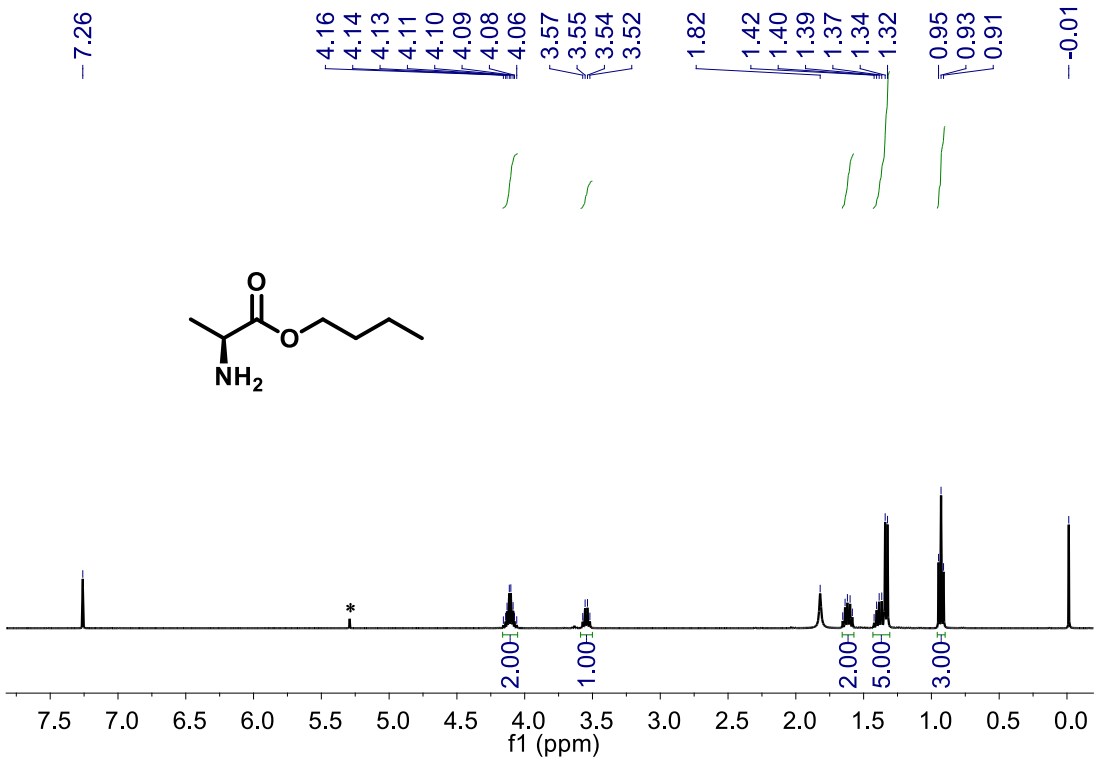

Figure S44. ^{1}H NMR spectrum (400 MHz, chloroform–*d*, room temperature) of **8**. *CH_2Cl_2.

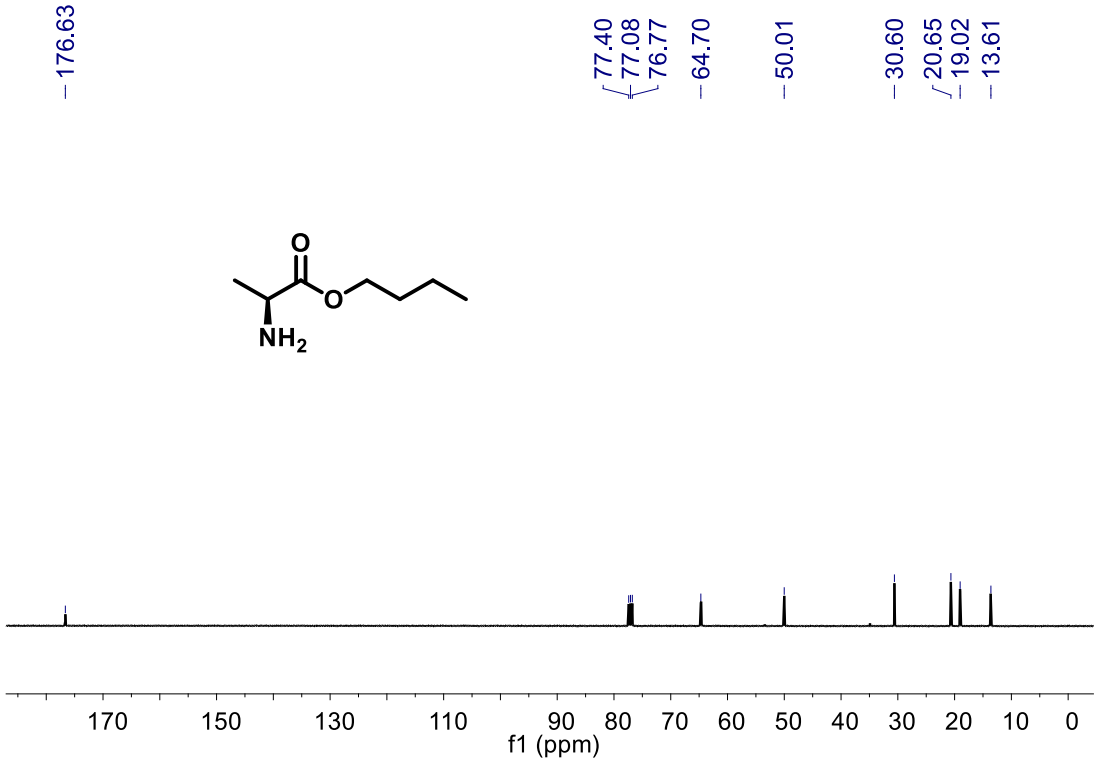

Figure S45. ^{13}C NMR spectrum (101 MHz, chloroform–*d*, room temperature) of **8**.

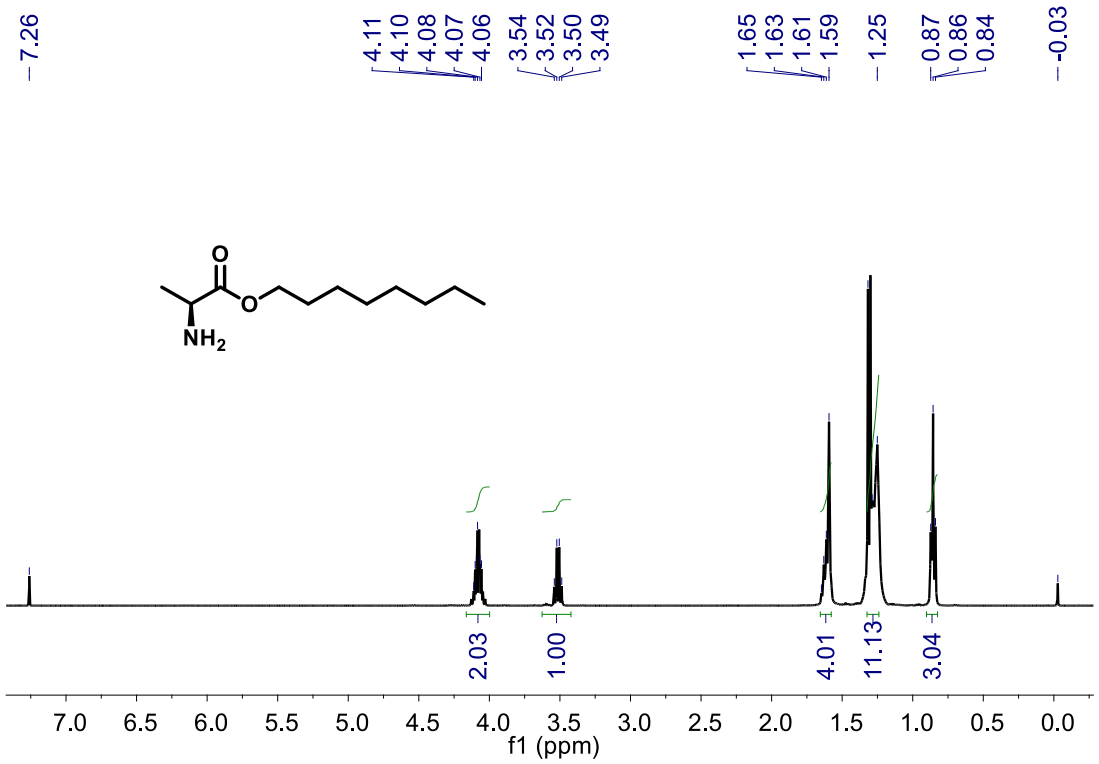

Figure S46. ^{1}H NMR spectrum (400 MHz, chloroform–*d*, room temperature) of **9**.

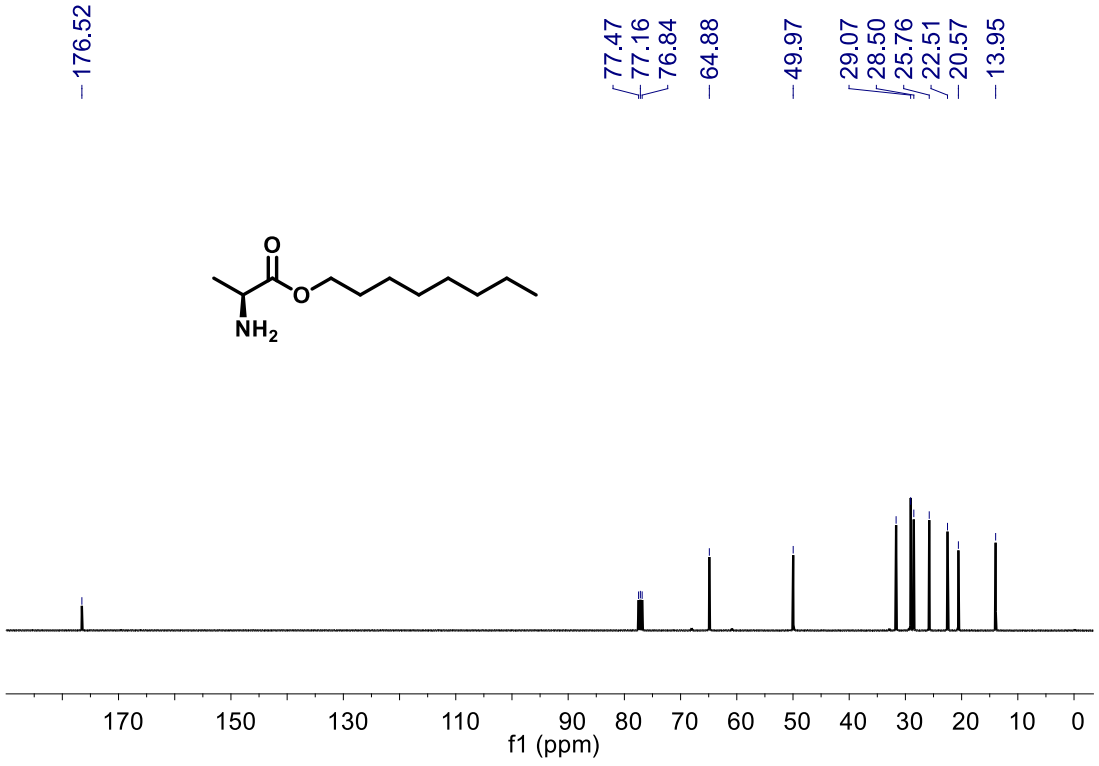

Figure S47. ^{13}C NMR spectrum (101 MHz, chloroform–*d*, room temperature) of **9**.

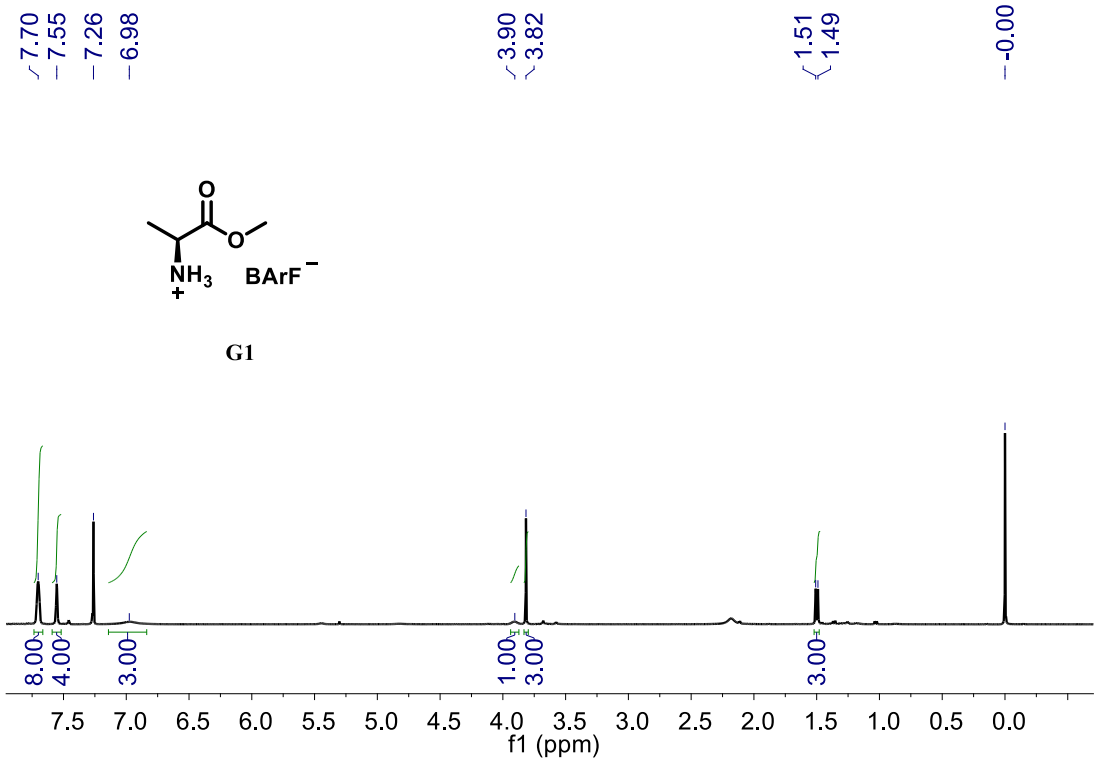

Figure S48. ^{1}H NMR spectrum (400 MHz, chloroform–*d*, room temperature) of **G1**.

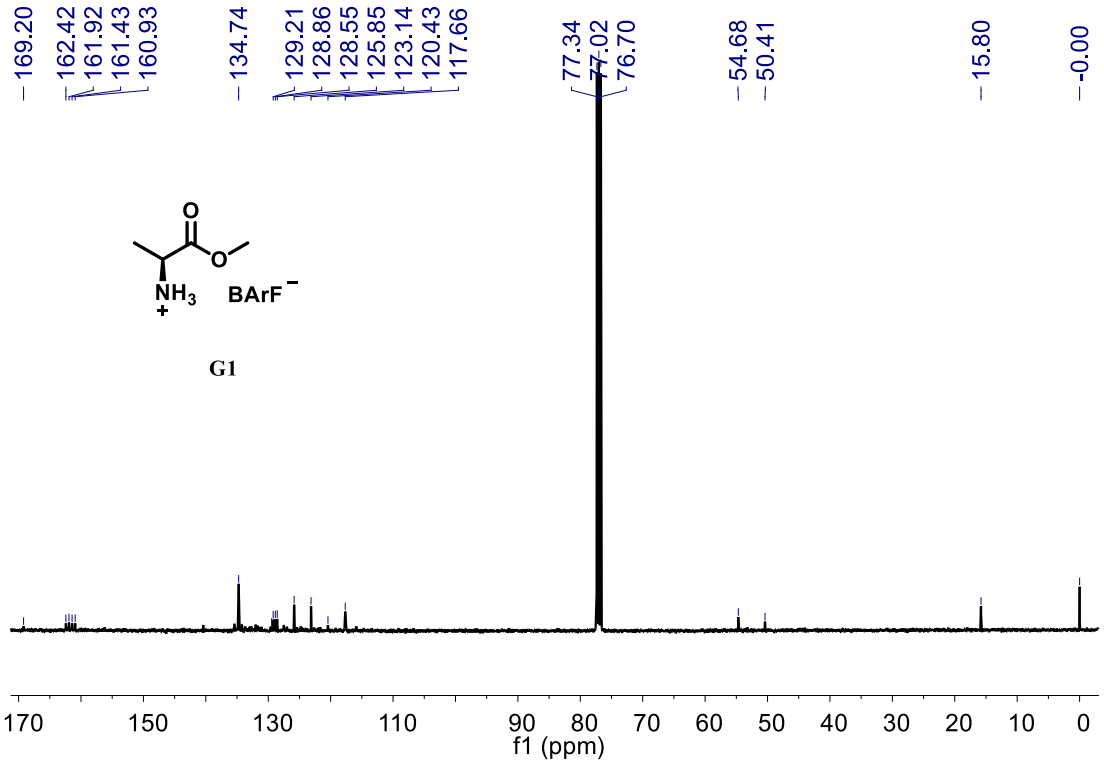

Figure S49. ^{13}C NMR spectrum (101 MHz, chloroform–*d*, room temperature) of **G1**.

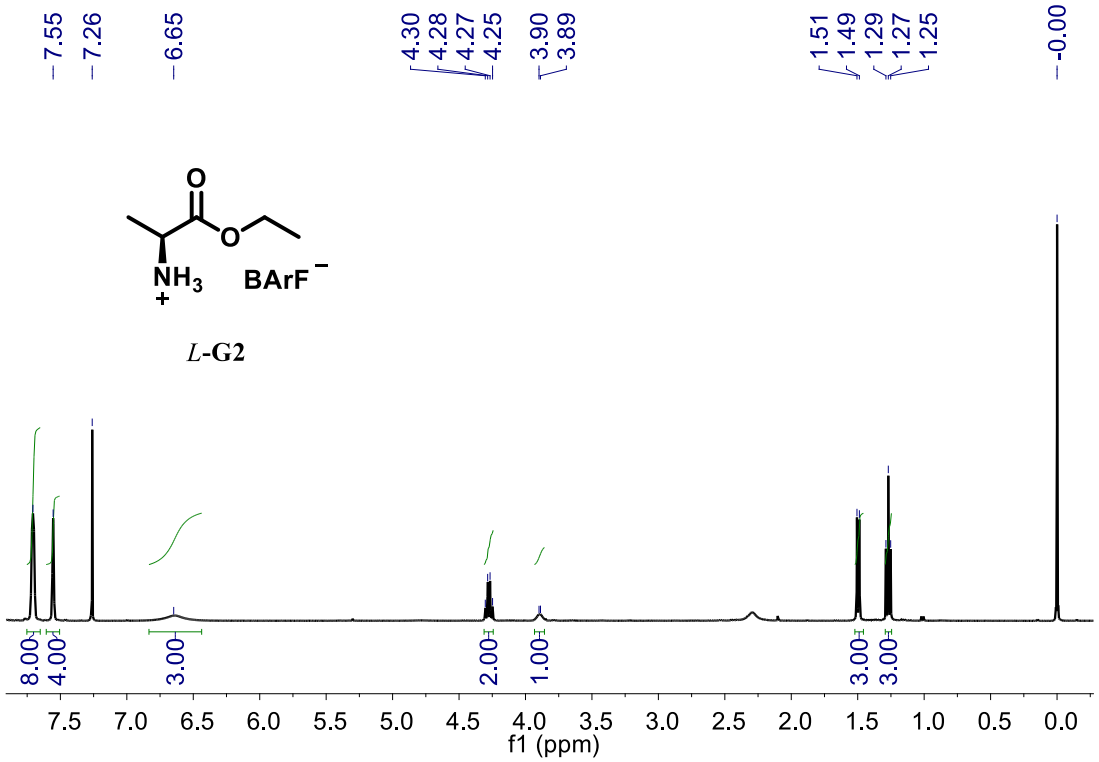

Figure S50. ^{1}H NMR spectrum (400 MHz, chloroform–*d*, room temperature) of *L*-**G2**.

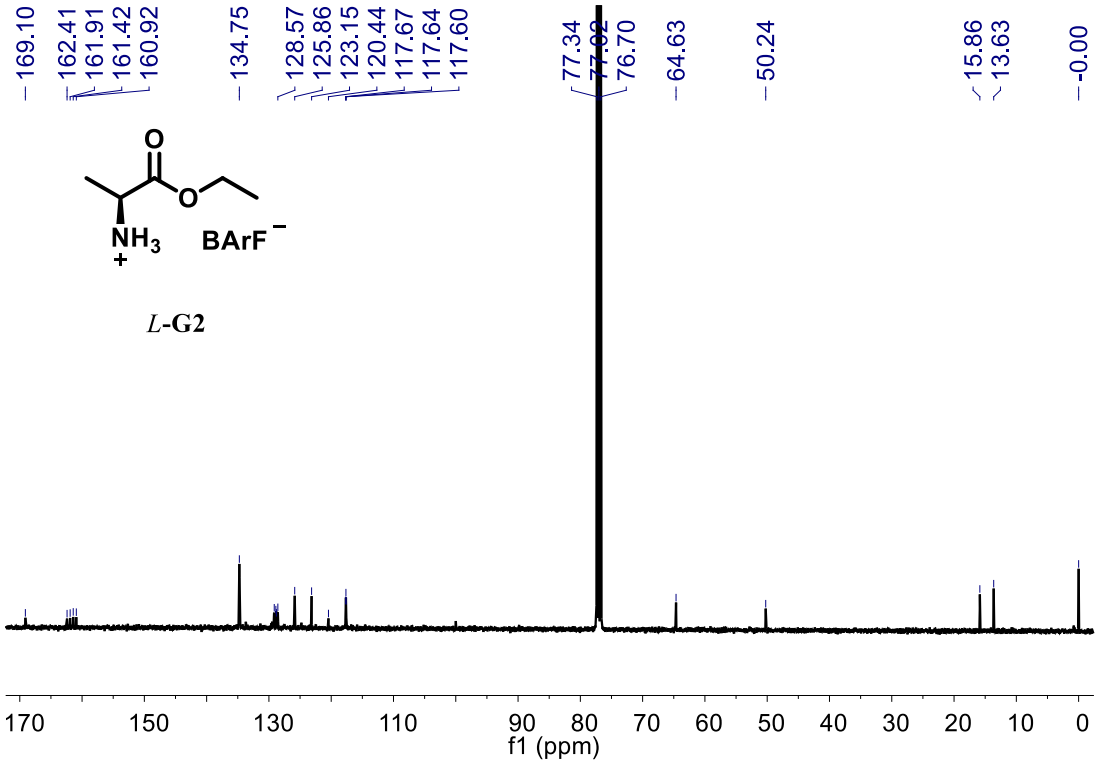

Figure S51. ^{13}C NMR spectrum (101 MHz, chloroform–*d*, room temperature) of *L*-**G2**.

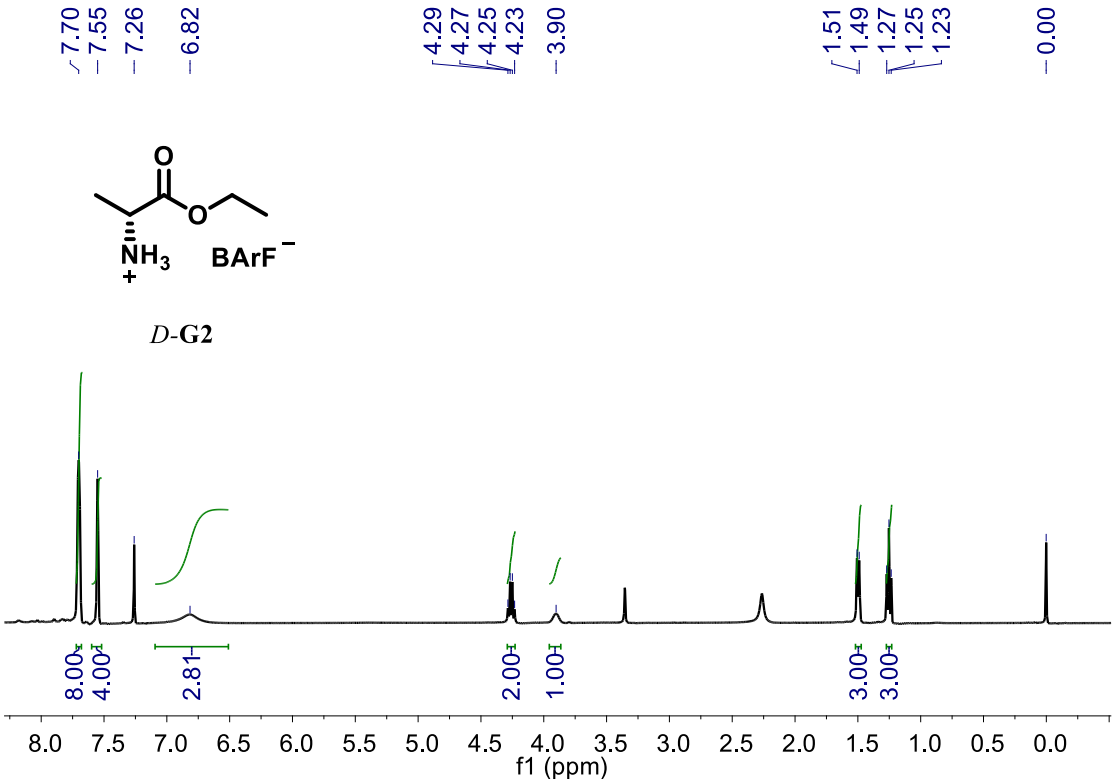

Figure S52. ^{1}H NMR spectrum (400 MHz, chloroform–*d*, room temperature) of *D*-**G2**.

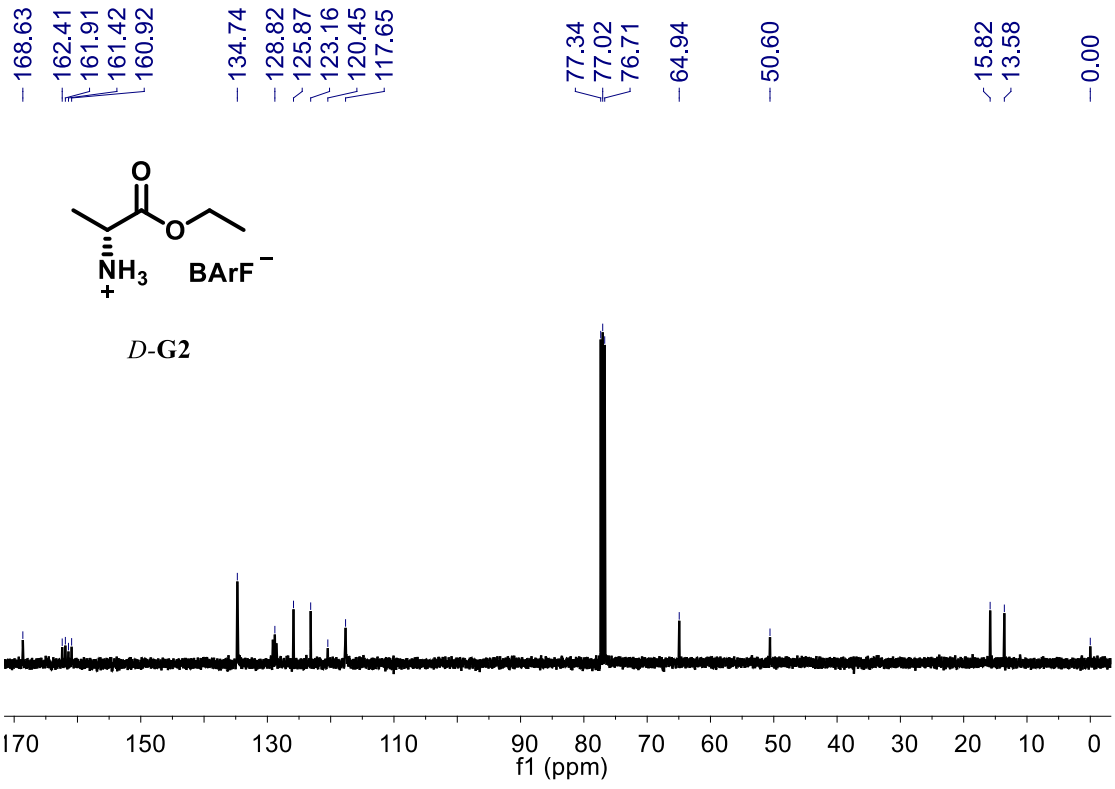

Figure S53. ^{13}C NMR spectrum (101 MHz, chloroform–*d*, room temperature) of *D*-**G2**.

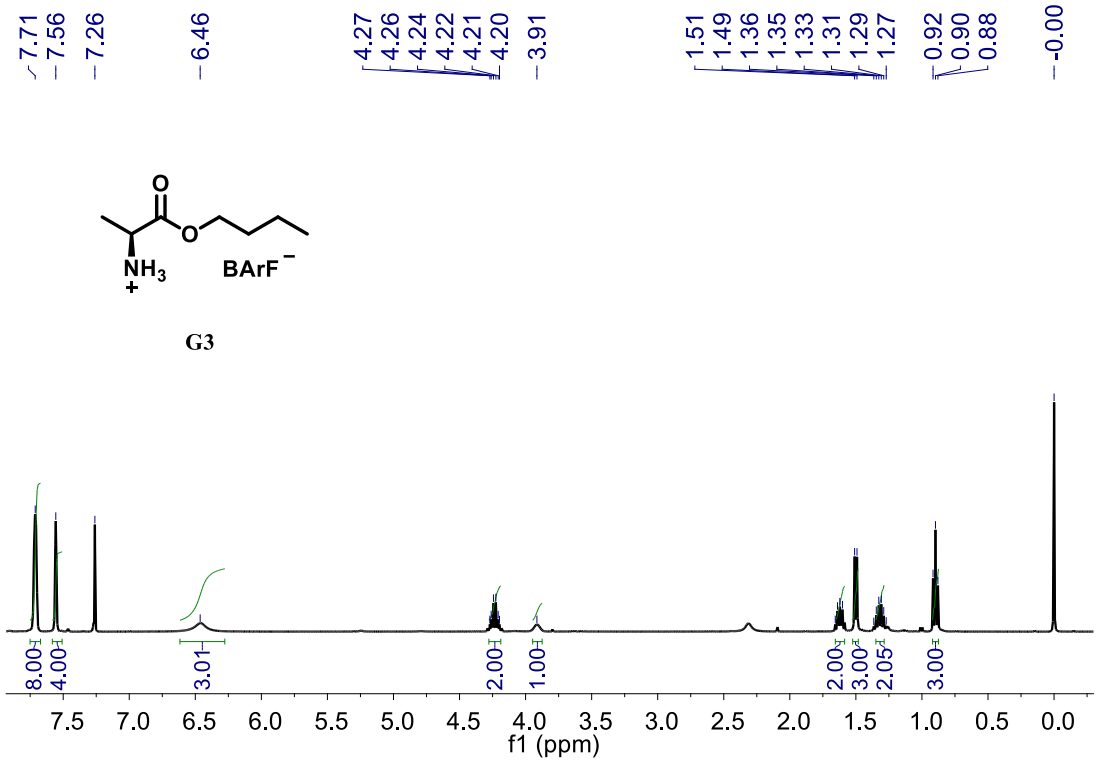

Figure S54. ^{1}H NMR spectrum (400 MHz, chloroform–*d*, room temperature) of **G3**.

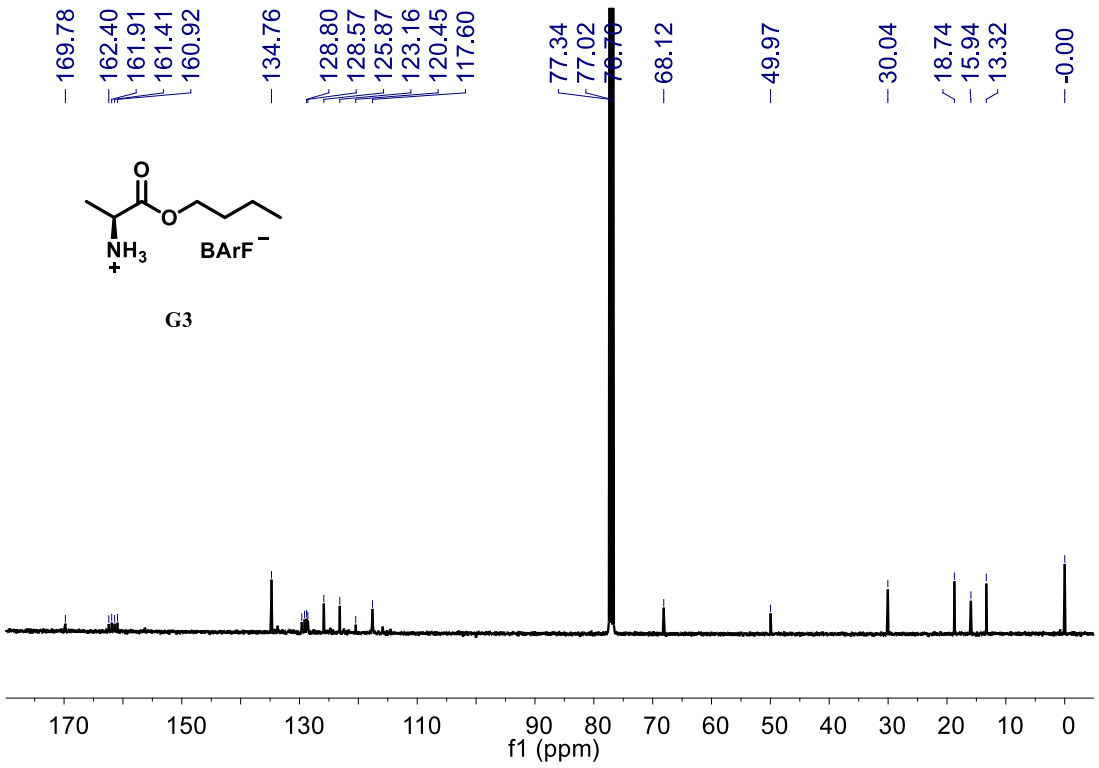

Figure S55. ^{13}C NMR spectrum (101 MHz, chloroform–*d*, room temperature) of **G3**.

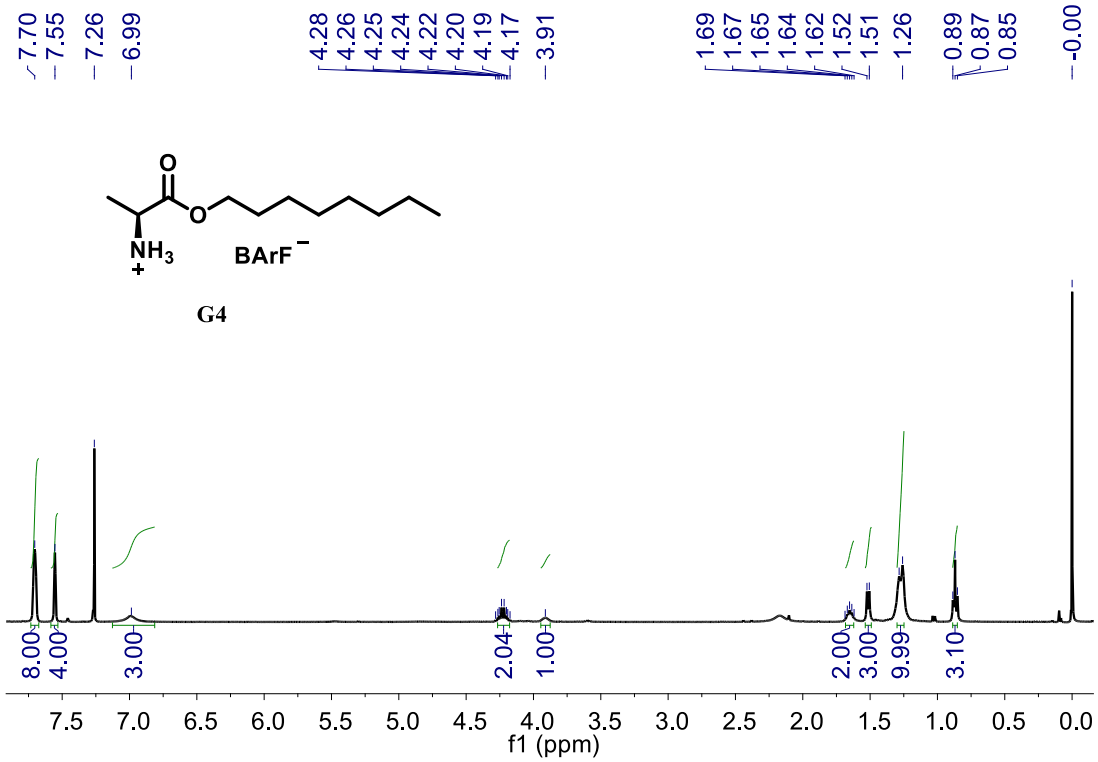

Figure S56. [1]H NMR spectrum (400 MHz, chloroform–*d*, room temperature) of **G4**.

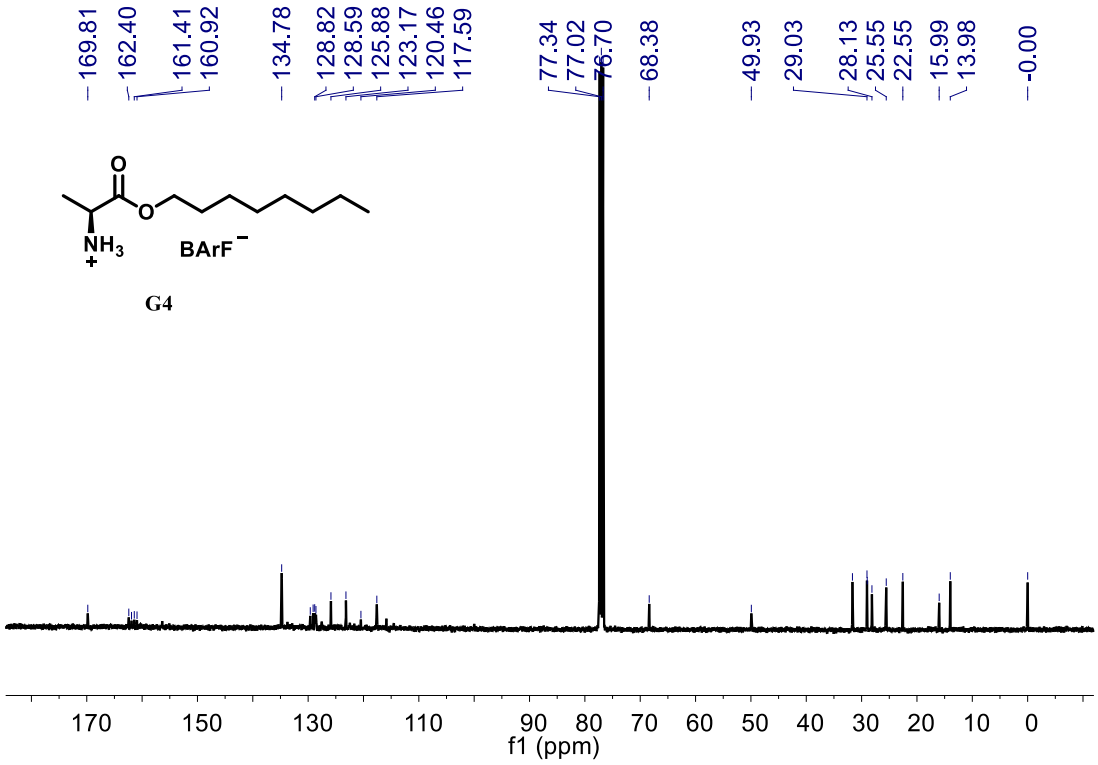

Figure S57. [13]C NMR spectrum (101 MHz, chloroform–*d*, room temperature) of **G4**.

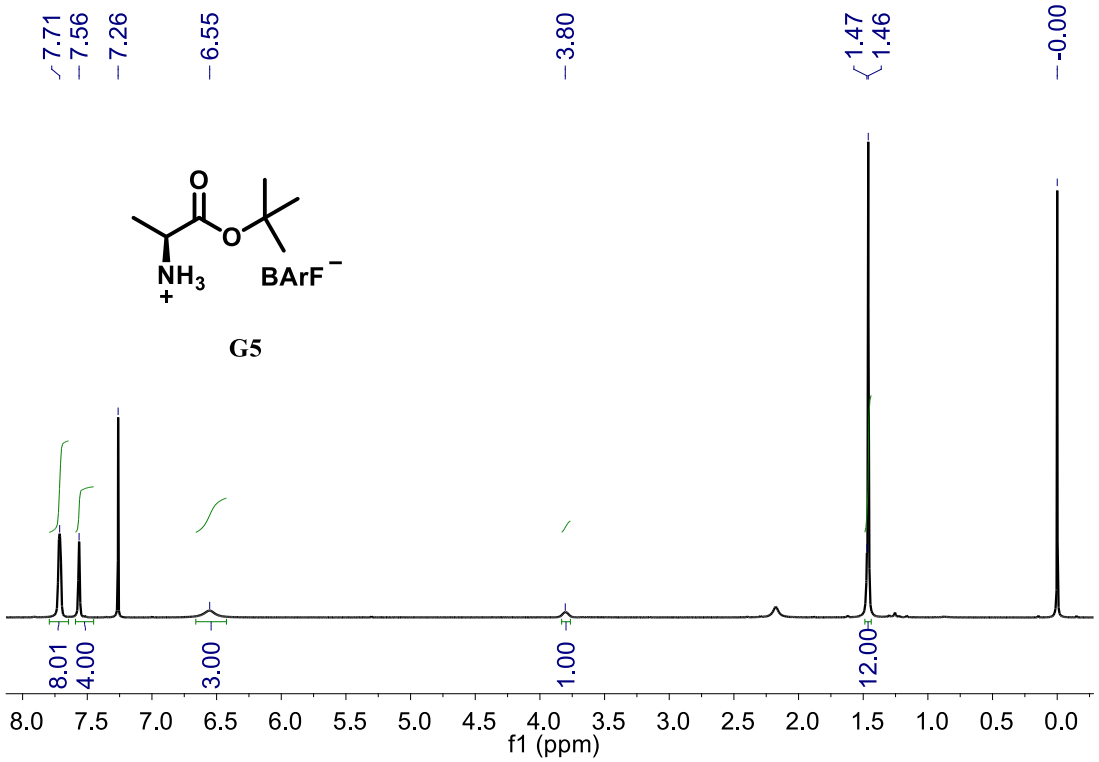

Figure S58. ^{1}H NMR spectrum (400 MHz, chloroform–*d*, room temperature) of **G5**.

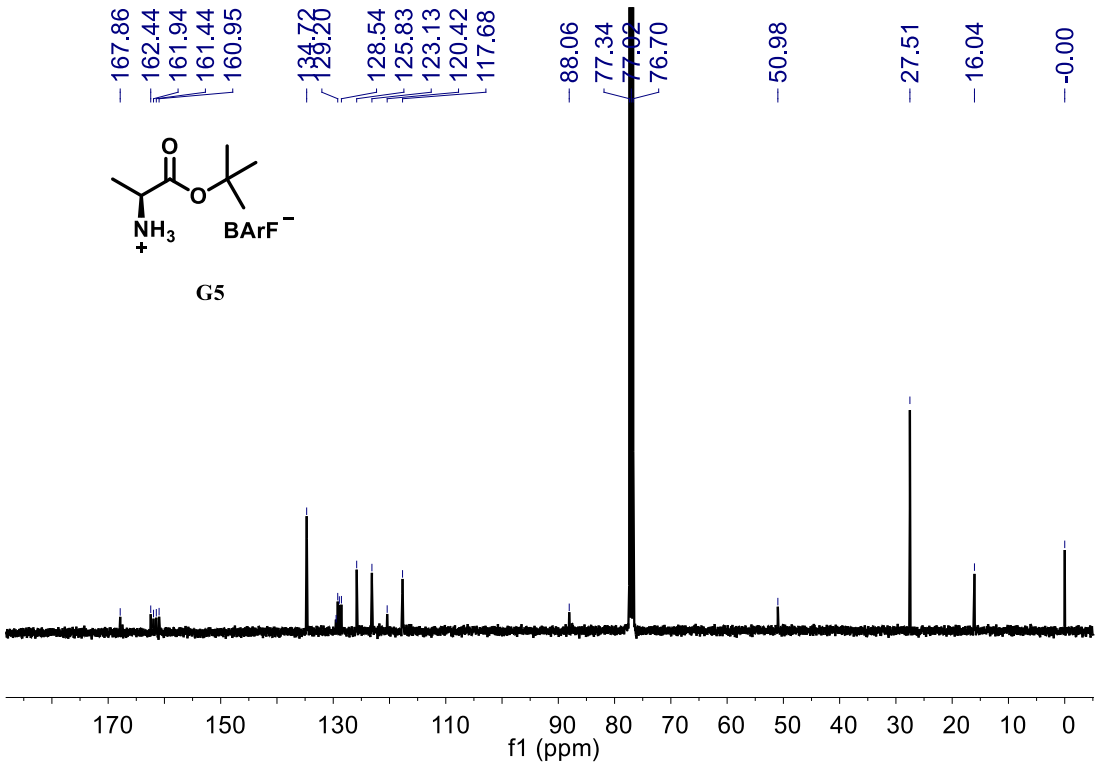

Figure S59. ^{13}C NMR spectrum (101 MHz, chloroform–*d*, room temperature) of **G5**.

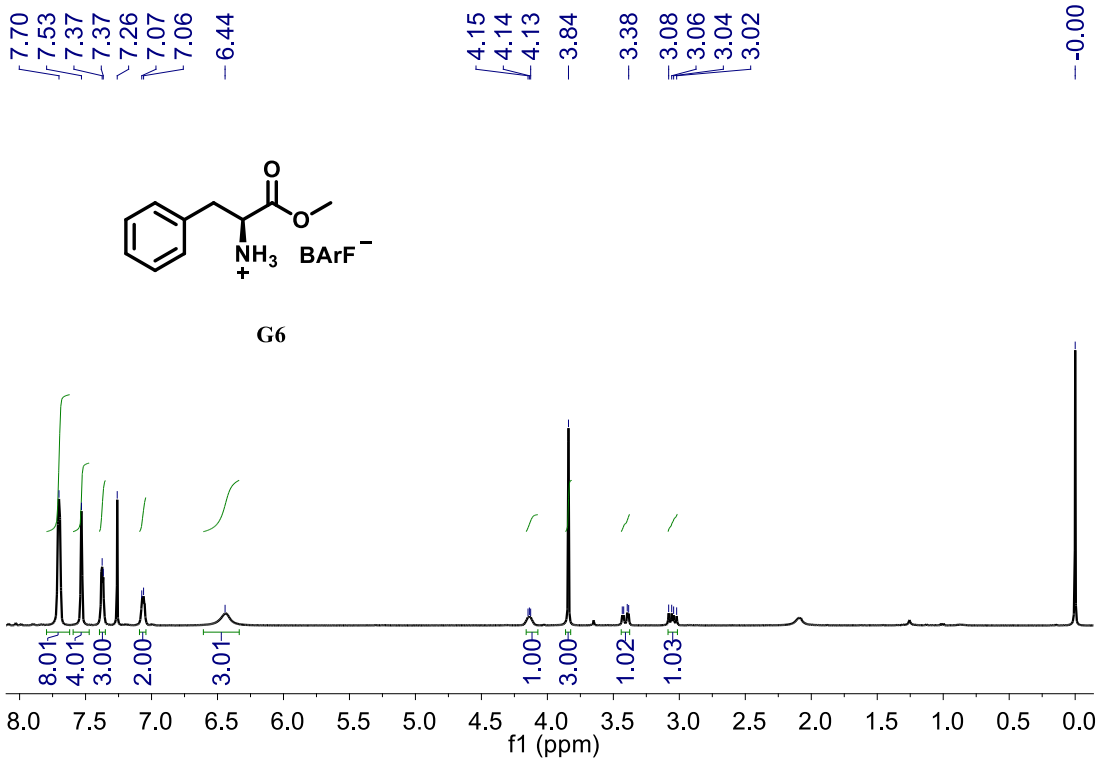

Figure S60. ^{1}H NMR spectrum (400 MHz, chloroform–*d*, room temperature) of **G6**.

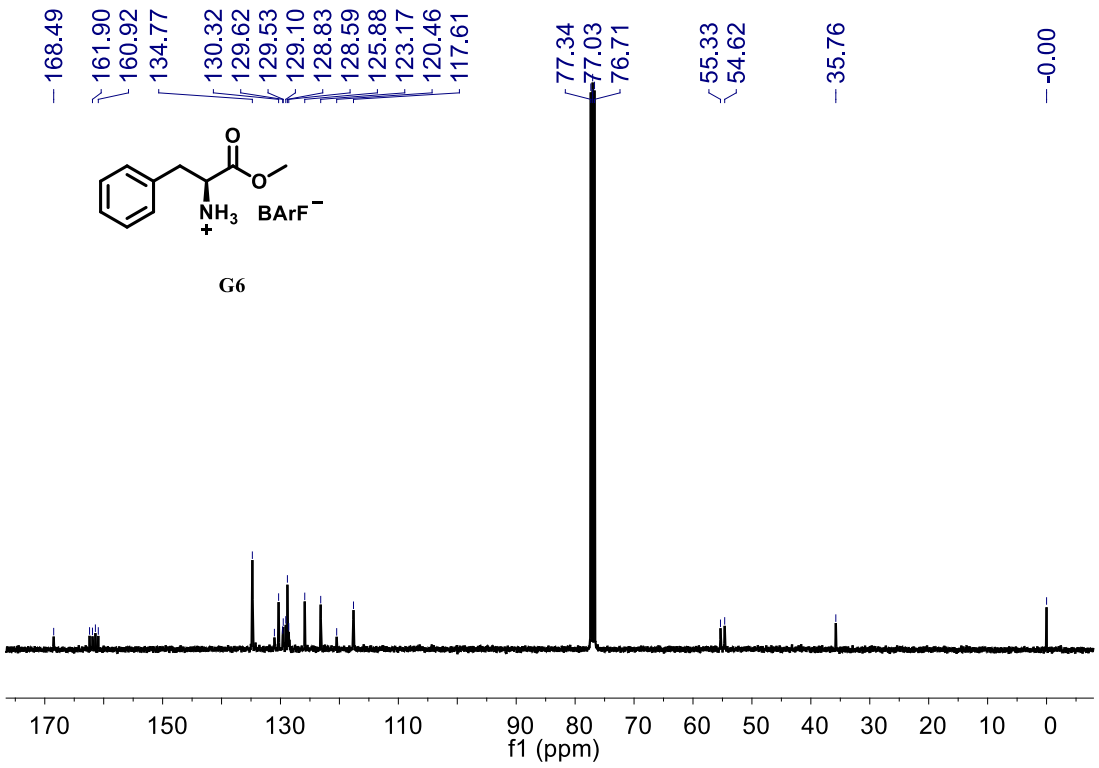

Figure S61. ^{13}C NMR spectrum (101 MHz, chloroform–*d*, room temperature) of **G6**.

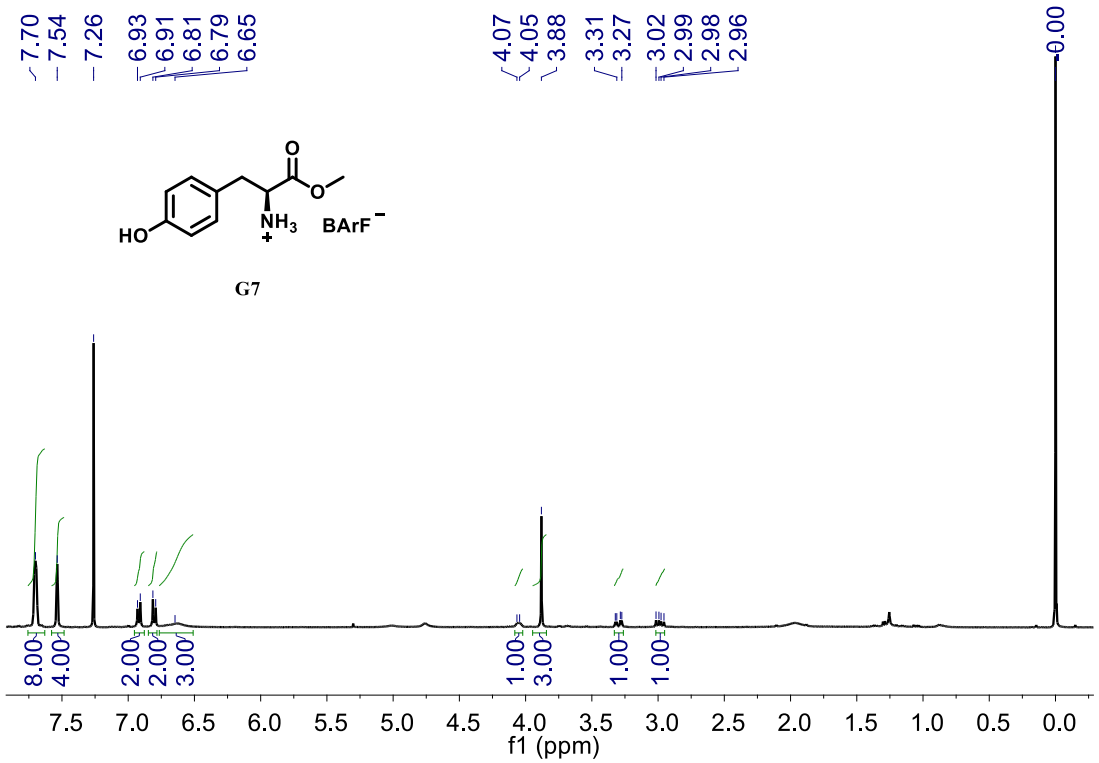

Figure S62. ^{1}H NMR spectrum (400 MHz, chloroform–*d*, room temperature) of **G7**.

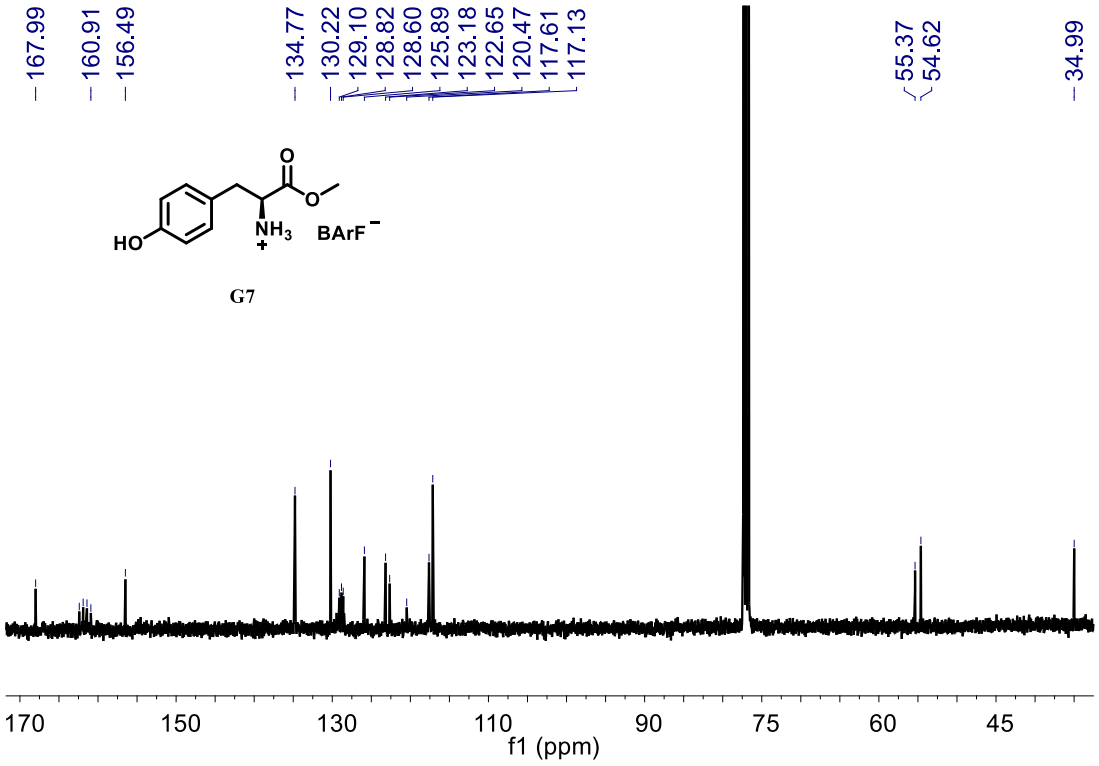

Figure S63. ^{13}C NMR spectrum (101 MHz, chloroform–*d*, room temperature) of **G7**.

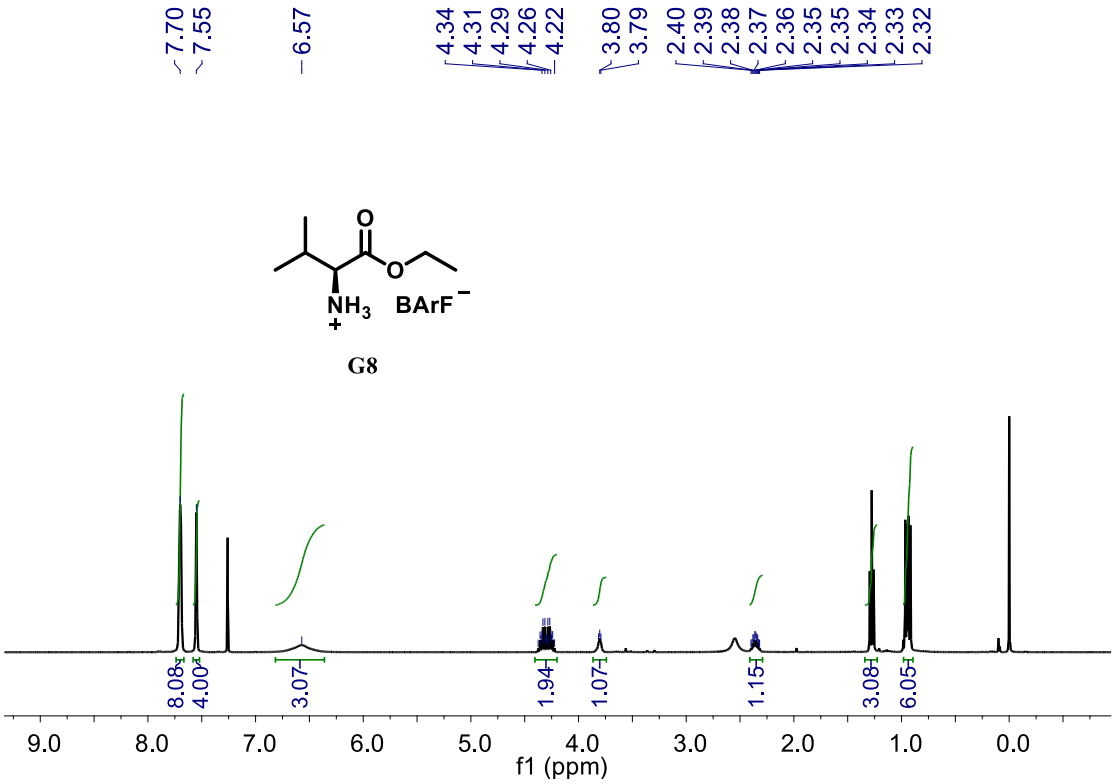

Figure S64. ^{1}H NMR spectrum (400 MHz, chloroform–*d*, room temperature) of **G8**.

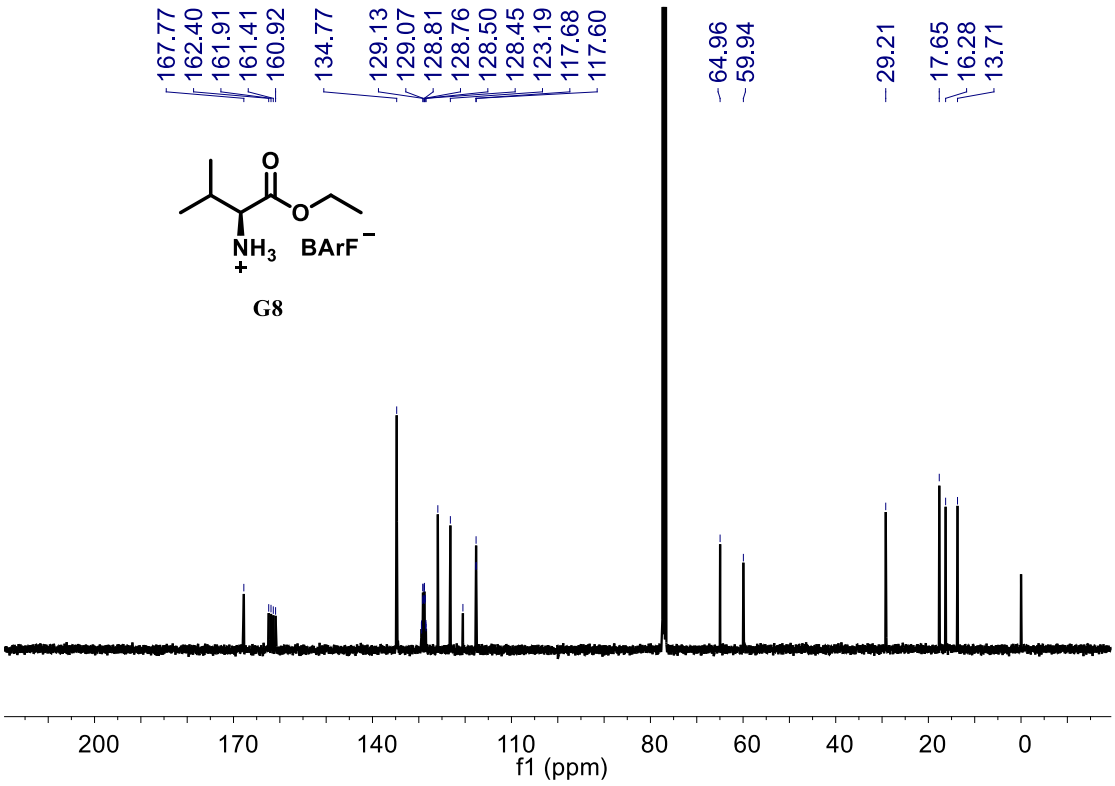

Figure S65. ^{13}C NMR spectrum (101 MHz, chloroform–*d*, room temperature) of **G8**.

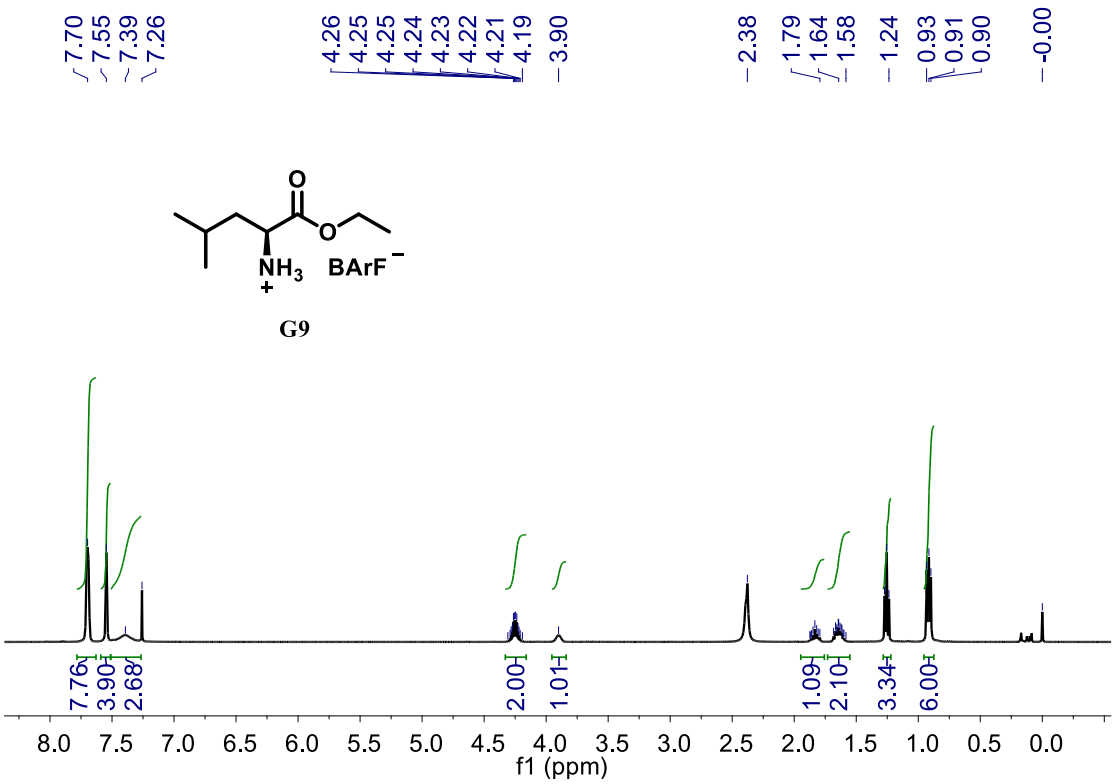

G9

Figure S66. ^{1}H NMR spectrum (400 MHz, chloroform–*d*, room temperature) of **G9**.

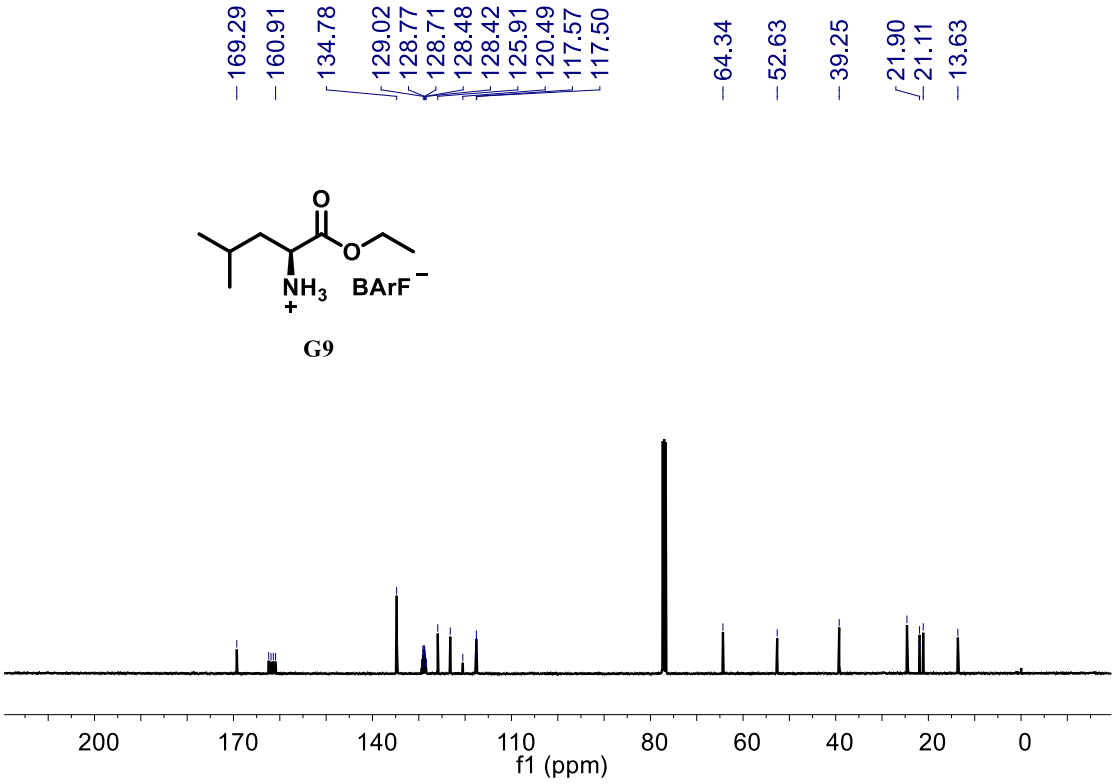

G9

Figure S67. ^{13}C NMR spectrum (101 MHz, chloroform–*d*, room temperature) of **G9**.

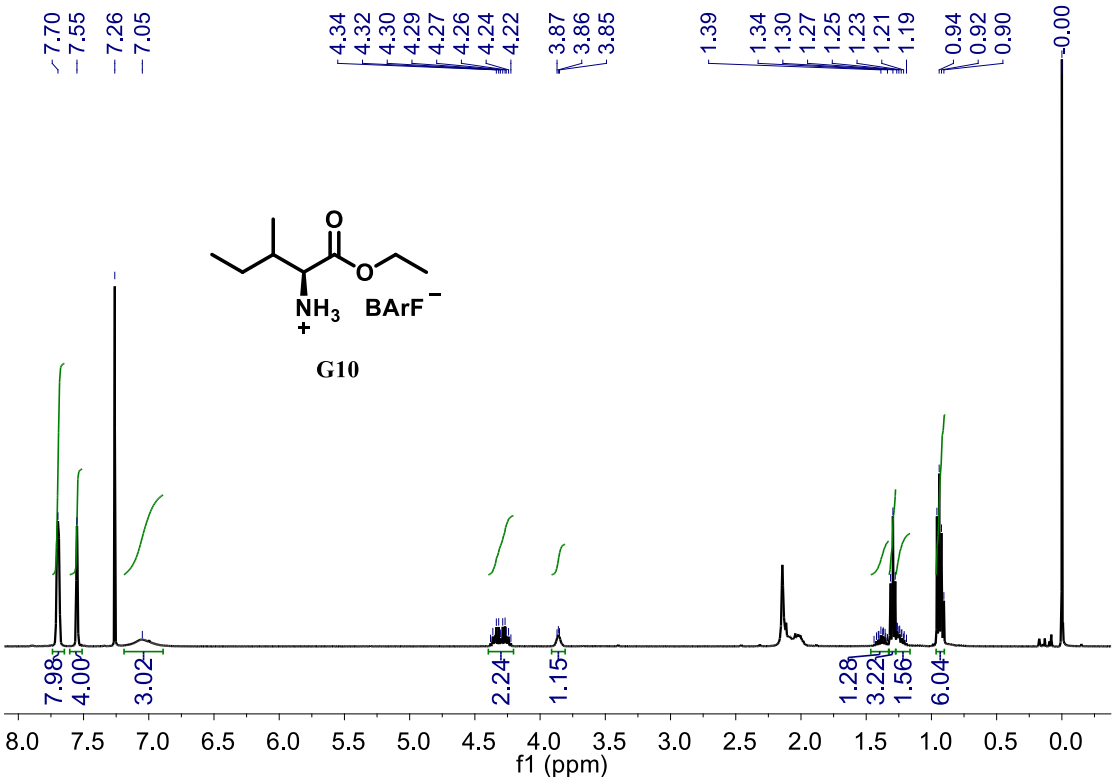

Figure S68. ^{1}H NMR spectrum (400 MHz, chloroform–*d*, room temperature) of **G10**.

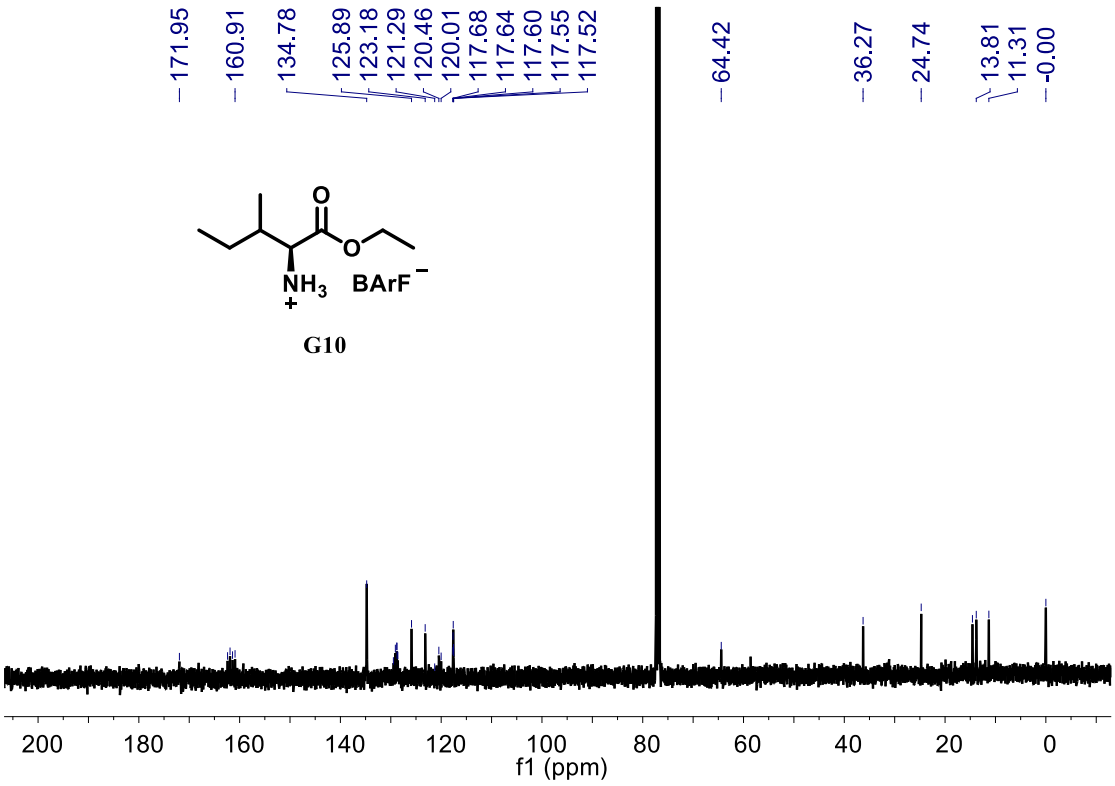

Figure S69. ^{13}C NMR spectrum (101 MHz, chloroform–*d*, room temperature) of **G10**.

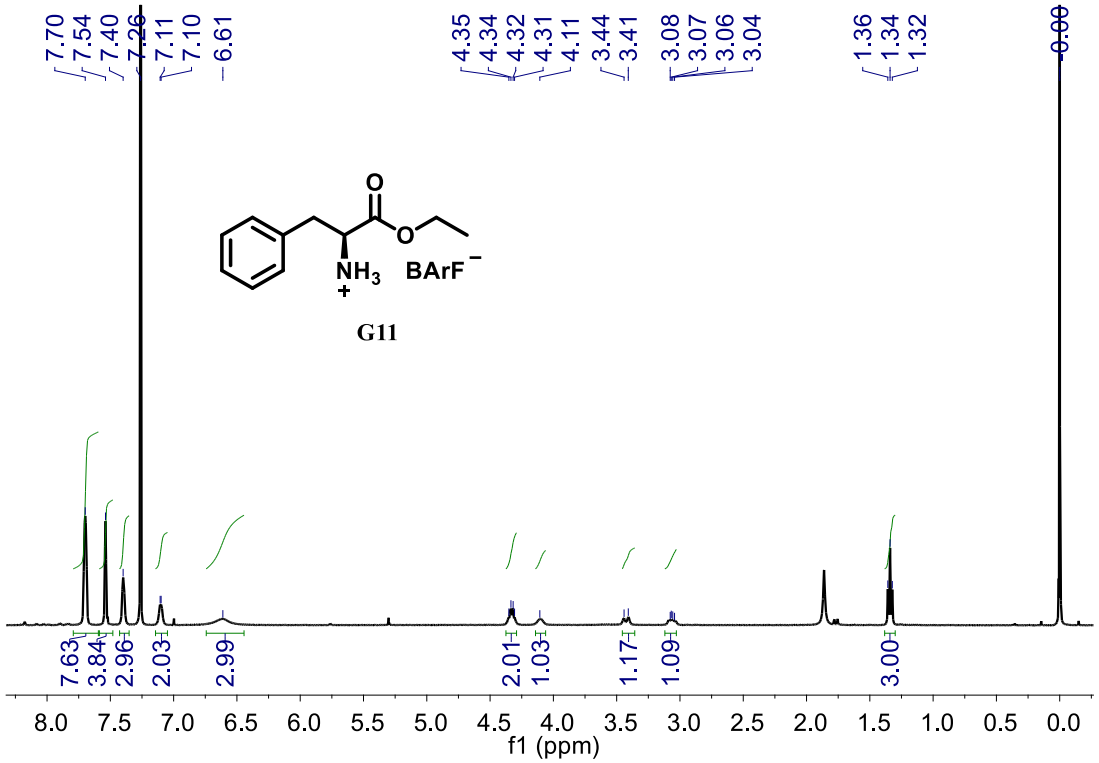

Figure S70. ^{1}H NMR spectrum (400 MHz, chloroform–*d*, room temperature) of **G11**.

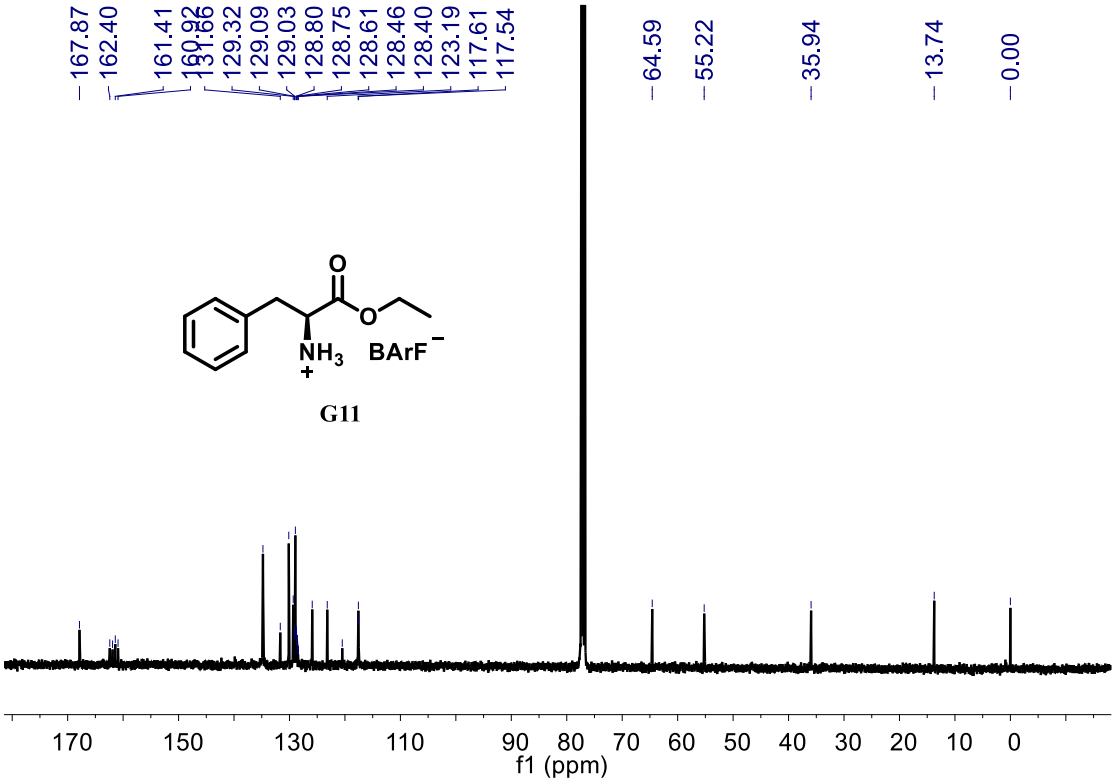

Figure S71. ^{13}C NMR spectrum (101 MHz, chloroform–*d*, room temperature) of **G11**.

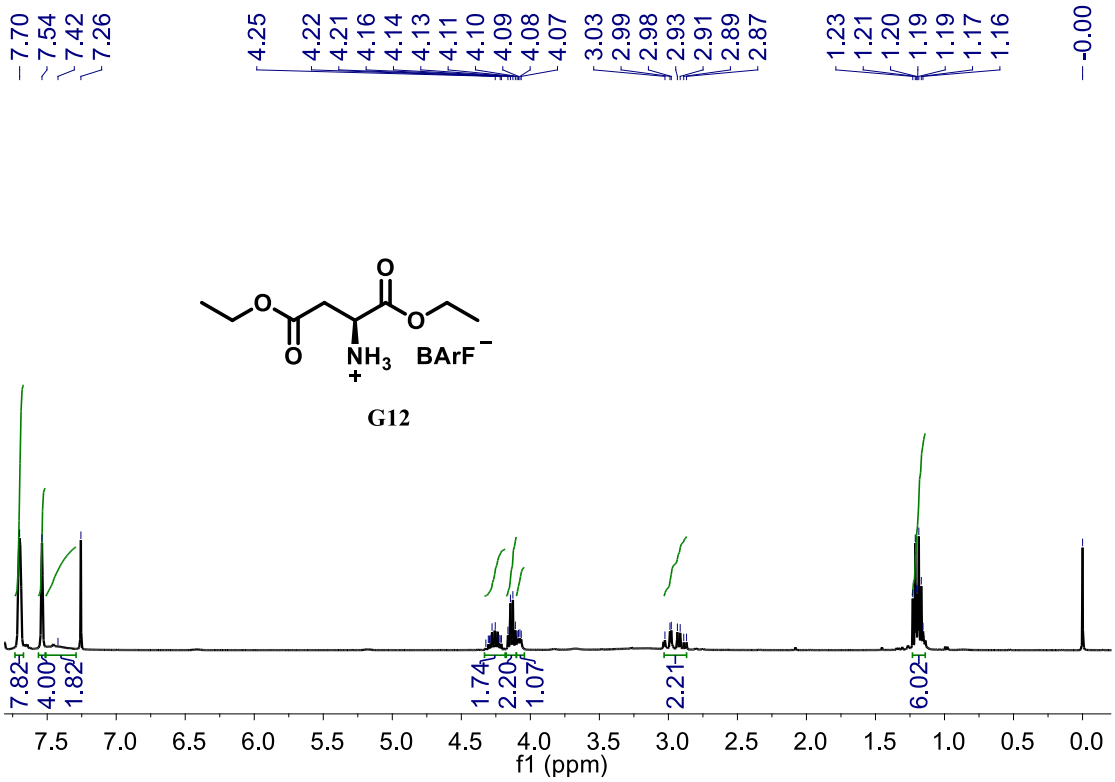

Figure S72. ^{1}H NMR spectrum (400 MHz, chloroform–*d*, room temperature) of **G12**.

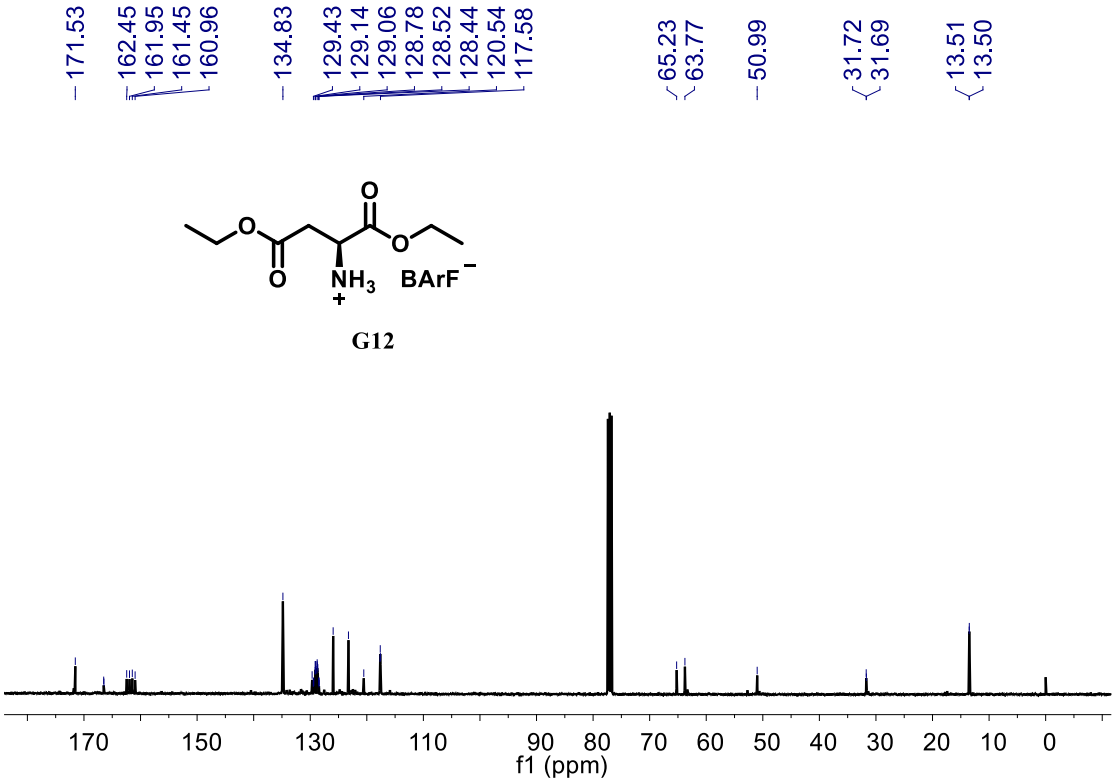

Figure S73. ^{13}C NMR spectrum (101 MHz, chloroform–*d*, room temperature) of **G12**.

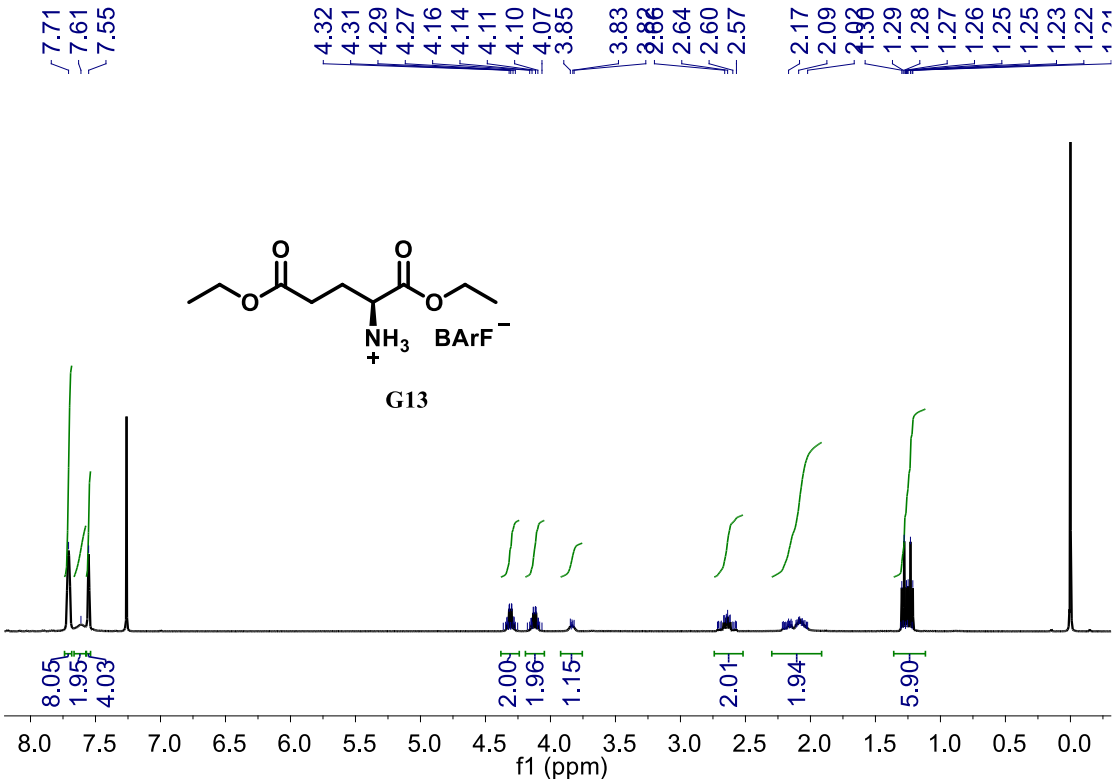

Figure S74. ^{1}H NMR spectrum (400 MHz, chloroform–*d*, room temperature) of **G13**.

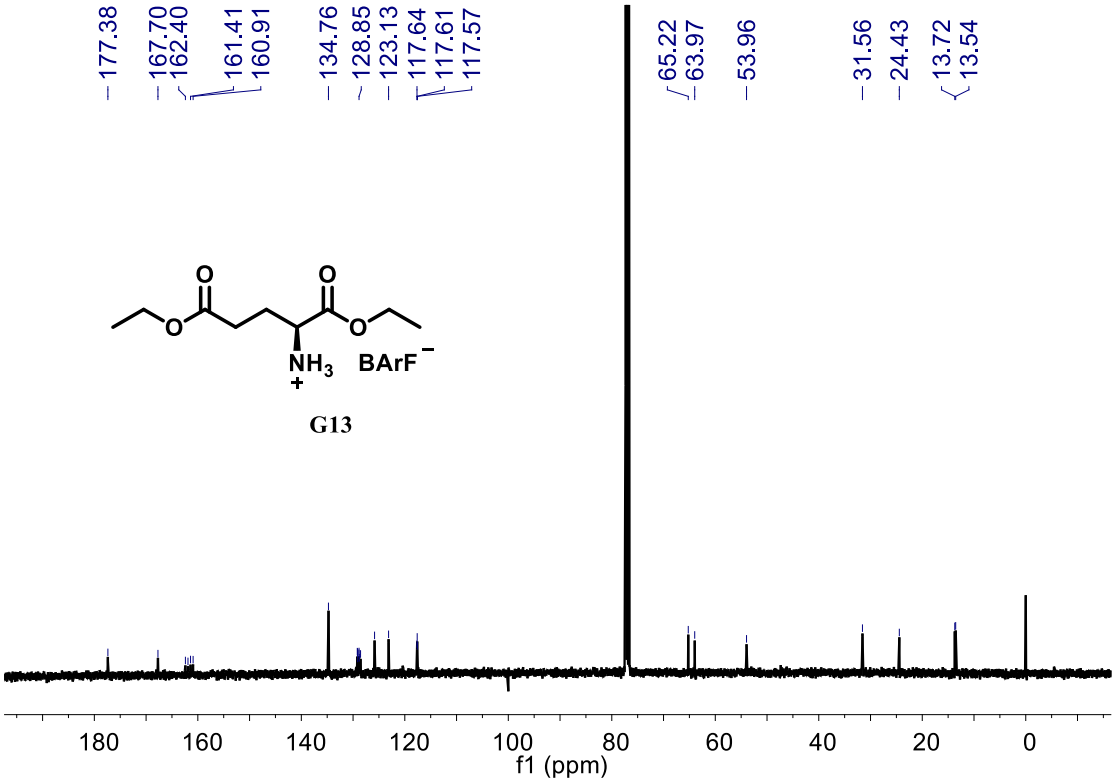

Figure S75. ^{13}C NMR spectrum (101 MHz, chloroform–*d*, room temperature) of **G13**.

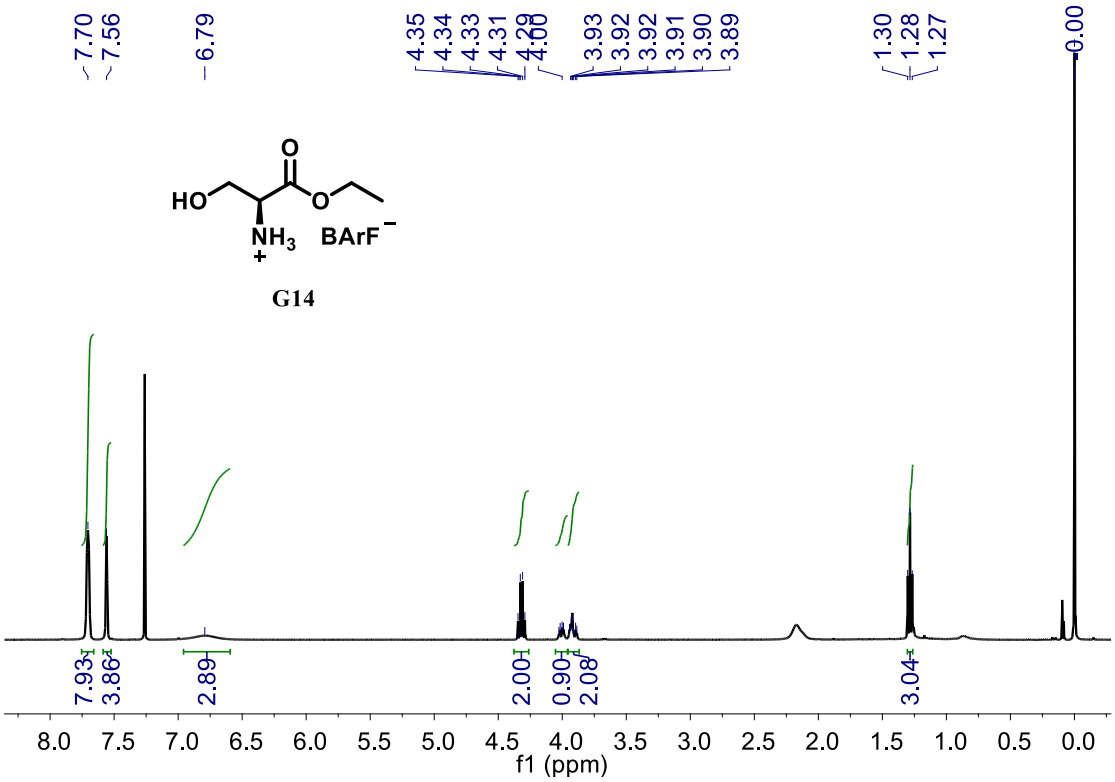

Figure S76. ^{1}H NMR spectrum (400 MHz, chloroform–*d*, room temperature) of **G14**.

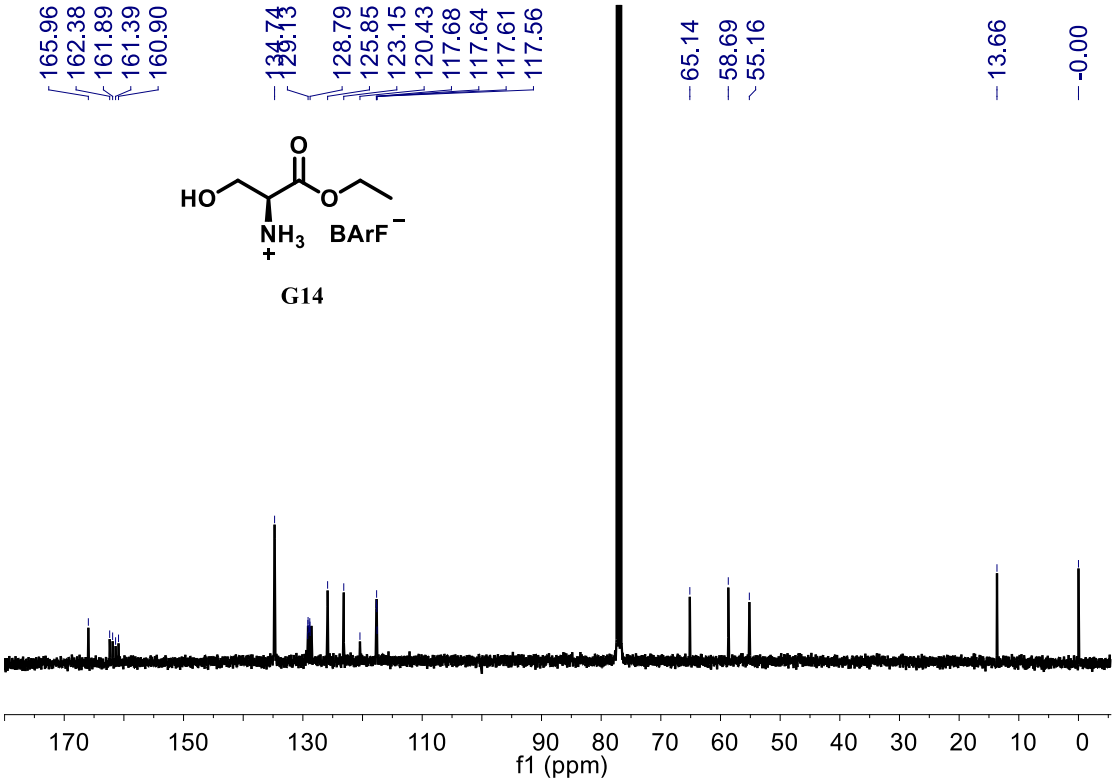

Figure S77. ^{13}C NMR spectrum (101 MHz, chloroform–*d*, room temperature) of **G14**.

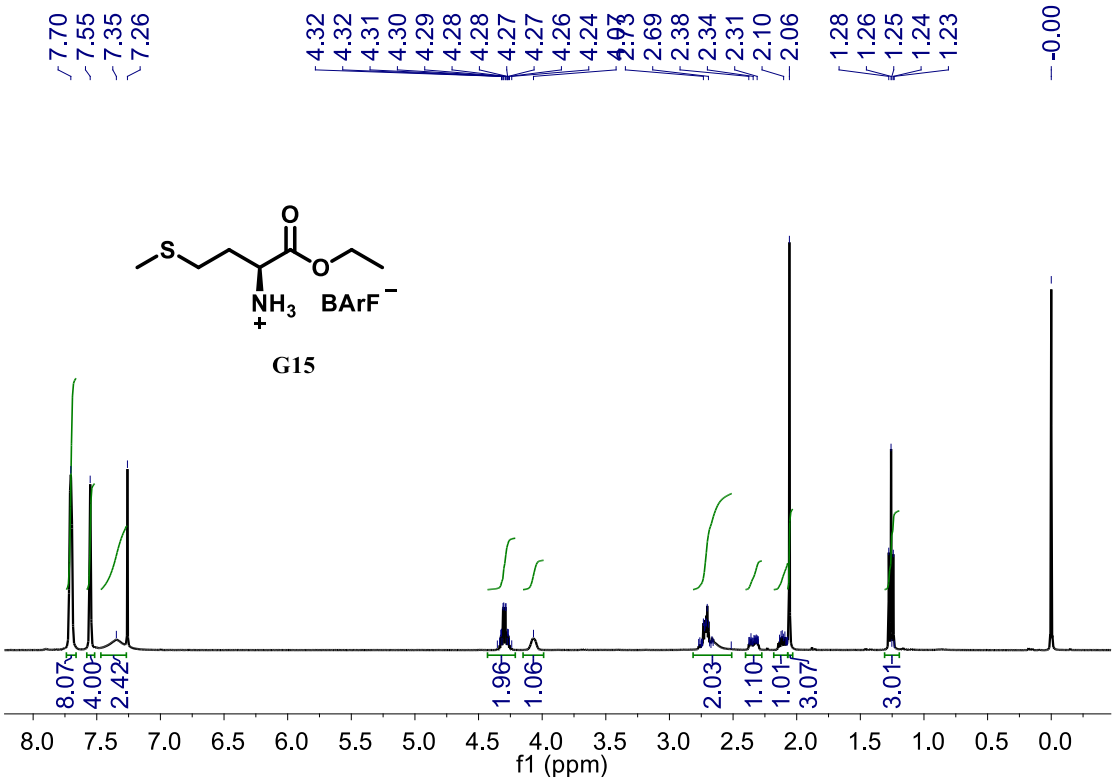

Figure S78. ^{1}H NMR spectrum (400 MHz, chloroform–*d*, room temperature) of **G15**.

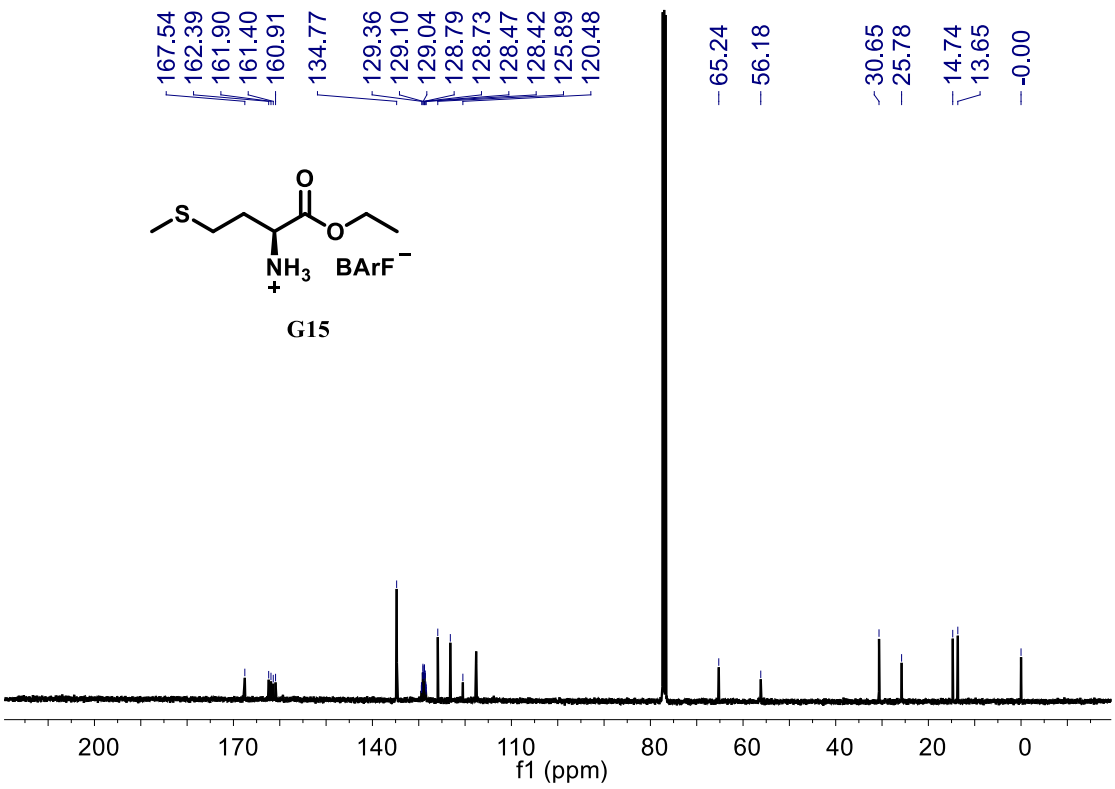

Figure S79. ^{13}C NMR spectrum (101 MHz, chloroform–*d*, room temperature) of **G15**.

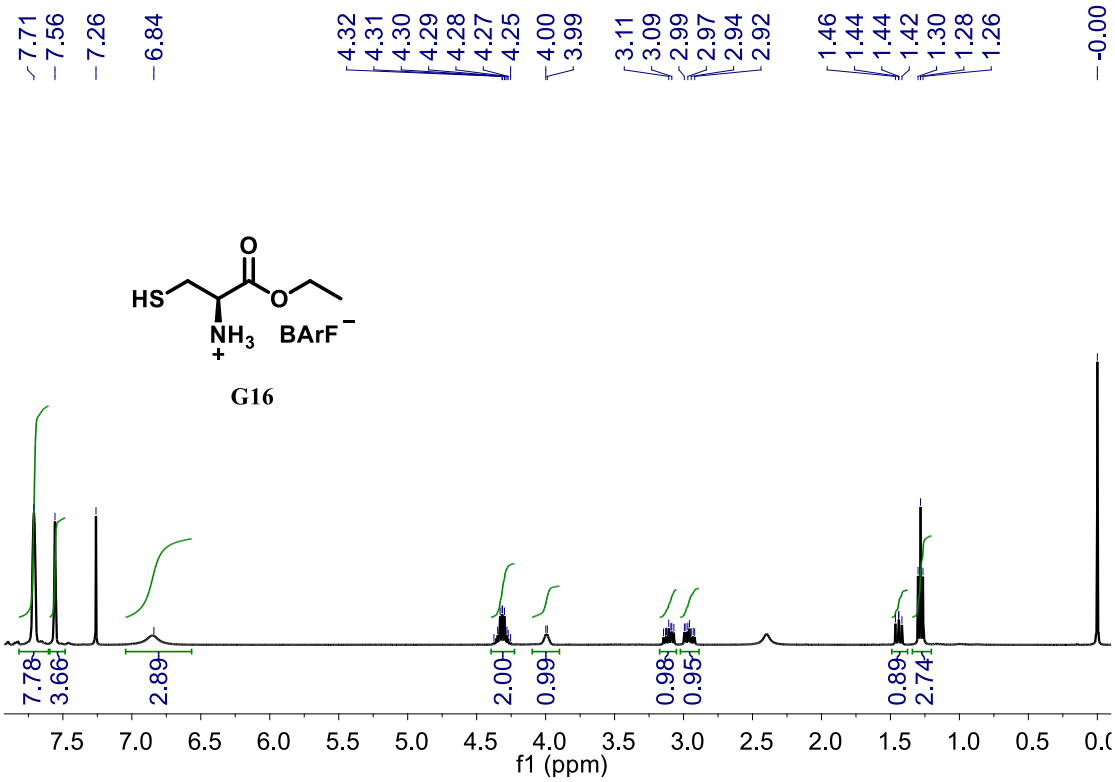

Figure S80. ^{1}H NMR spectrum (400 MHz, chloroform–*d*, room temperature) of **G16**.

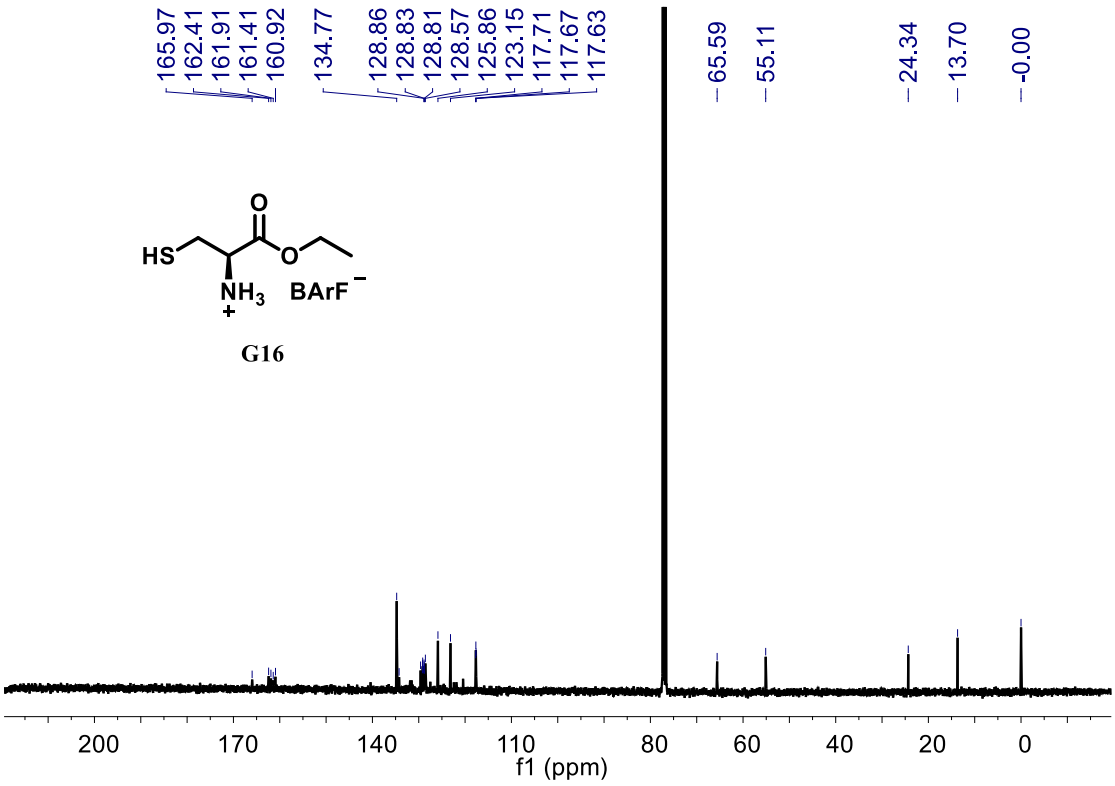

Figure S81. ^{13}C NMR spectrum (101 MHz, chloroform–*d*, room temperature) of **G16**.

4 UV-Vis spectrum of guest.

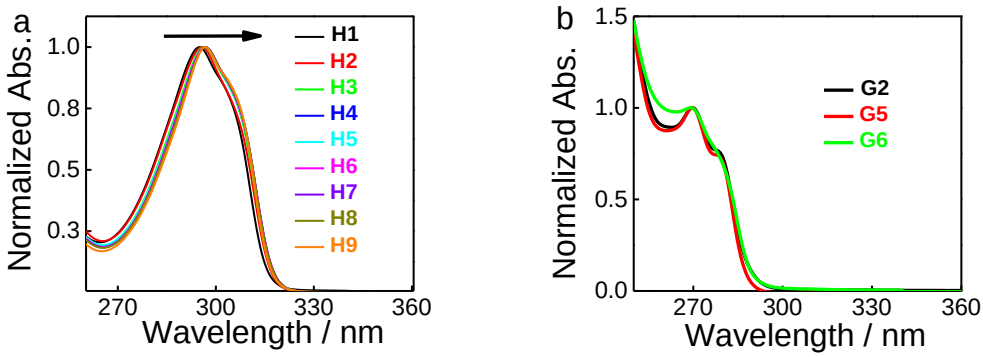

Figure S82. Normalized UV-Vis spectra of **G2**, **G5** and **G6** in $CHCl_3$ at room temperature.

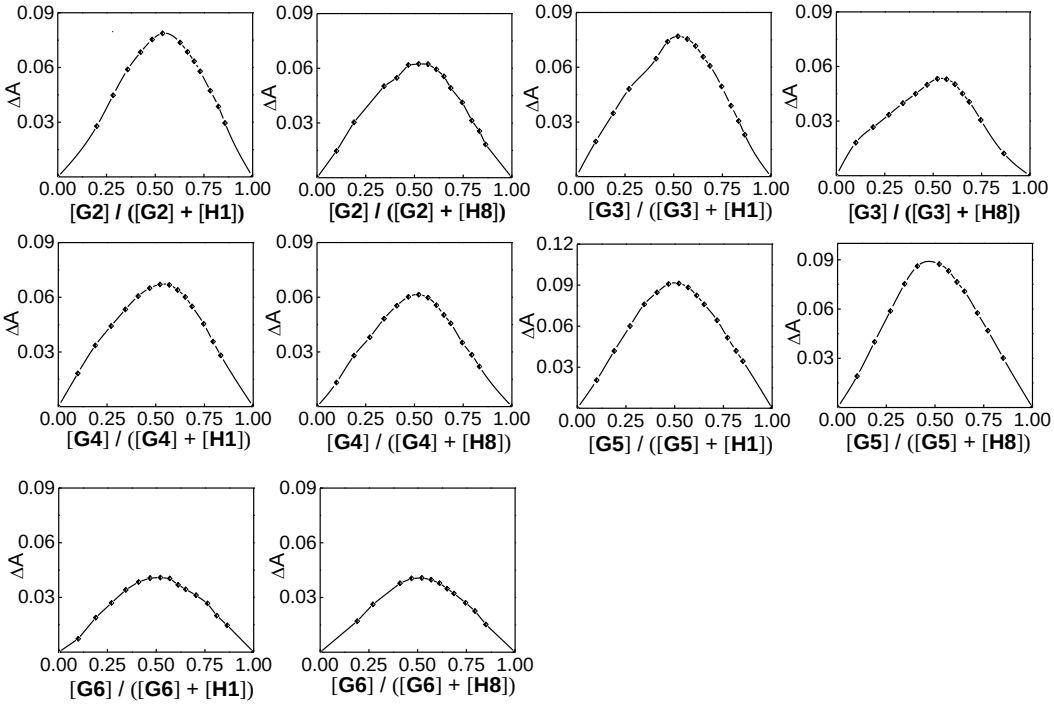

Figure S83. Job's plot of the change in the UV–vis absorption spectrum showing the stoichiometry of the complexation of **G2** to **G6** with **H1** or **H8** in $CHCl_3$ (rt). ΔAbsorbance at 303 nm was used for plot. $C_{[G]+[H]} = 5.0 \times 10^{-5}$ M.

5 Spectroscopic studies and Isothermal Titration Calorimetry (ITC) of host and guest binding complexes

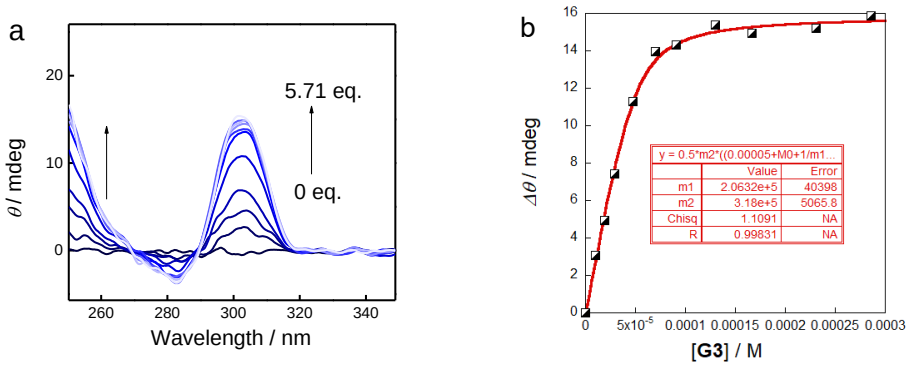

Figure S84. CD spectral changes of **H1** (5.0×10^{-5} M) upon titration with **G3** ($0 - 2.85 \times 10^{-4}$ M) in $CHCl_3$ at 25 °C (left). The non-linear curve-fitting (CD titrations) for the complexation of **G3** (right) with **H1** (302.2 nm) in $CHCl_3$ at 25 °C, the association constants (K_a) for the complexes is 2.06 (± 0.4) × 10^5 M^{-1}.

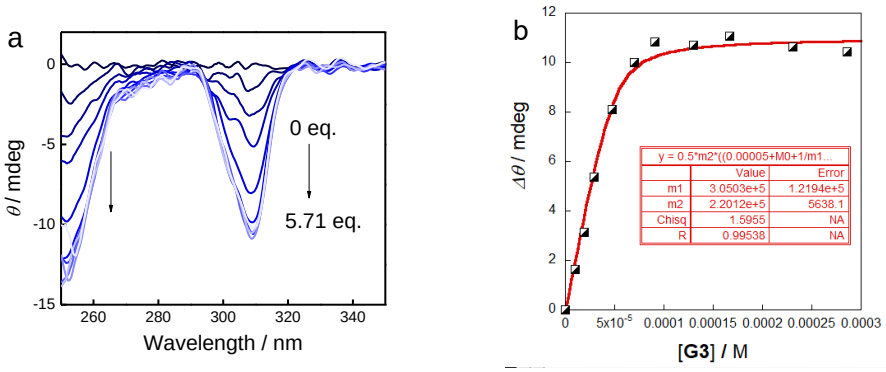

Figure S85. CD spectral changes of **H8** (5.0×10^{-5} M) upon titration with **G3** ($0 - 2.85 \times 10^{-4}$ M) in $CHCl_3$ at 25 °C (left). The non-linear curve-fitting (CD titrations) for the complexation of **G3** (right) with **H8** (309.5 nm) in $CHCl_3$ at 25 °C, the association constants (K_a) for the complexes is 3.05 (± 1.2) × 10^5 .

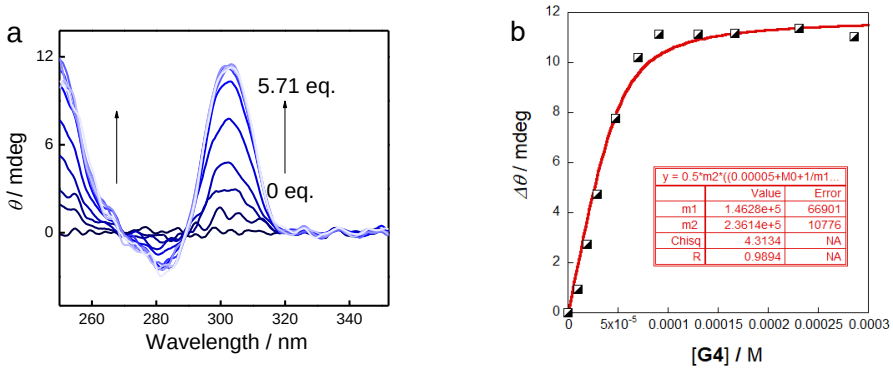

Figure S86. CD spectral changes of **H1** (5.0×10^{-5} M) upon titration with **G4** ($0 - 2.85 \times 10^{-4}$ M) in $CHCl_3$ at 25 °C (left). The non-linear curve-fitting (CD titrations) for the complexation of **G4** (right) with **H1** (302 nm) in $CHCl_3$ at 25 °C, the association constants (K_a) for the complexes is 1.46 (± 0.67) × 10^5 M^{-1}.

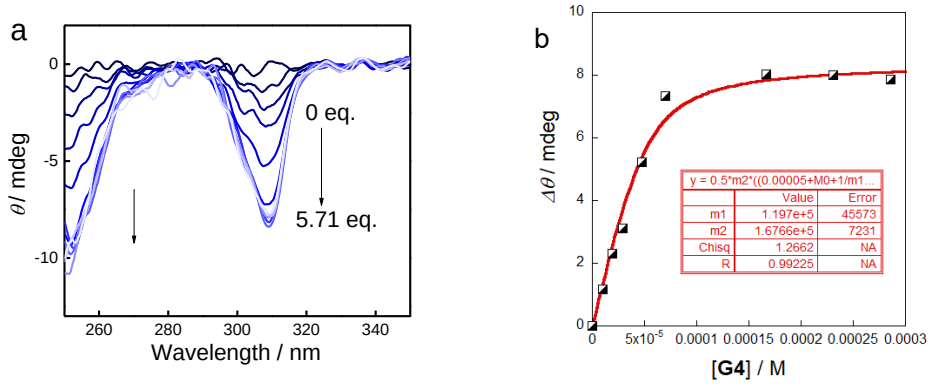

Figure S87. CD spectral changes of **H8** (5.0×10^{-5} M) upon titration with **G4** ($0 – 2.85 \times 10^{-4}$ M) in $CHCl_3$ at 25 °C (left). The non-linear curve-fitting (CD titrations) for the complexation of **G4** (right) with **H8** (309.5 nm) in $CHCl_3$ at 25 °C, the association constants (K_a) for the complexes is 1.20 (± 0.46) × 10^5 M^{-1}.

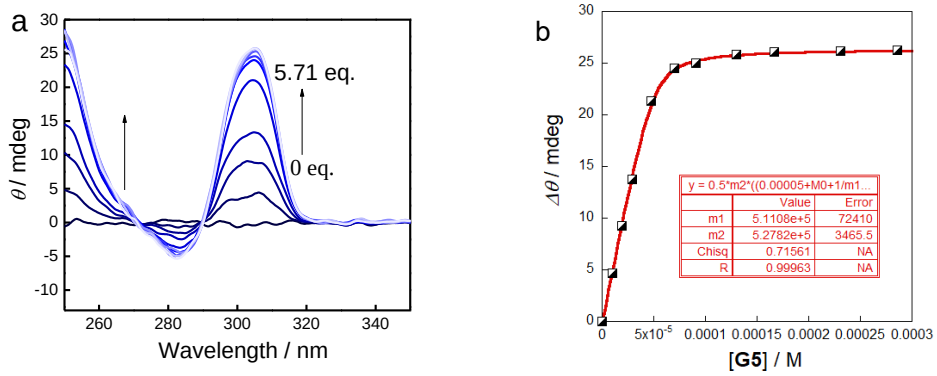

Figure S88. CD spectral changes of **H1** (5.0×10^{-5} M) upon titration with **G5** ($0 – 2.85 \times 10^{-4}$ M) in $CHCl_3$ at 25 °C (left). The non-linear curve-fitting (CD titrations) for the complexation of **G5** (right) with **H1** (305 nm) in $CHCl_3$ at 25 °C, the association constants (K_a) for the complexes is 5.11 (± 0.72) × 10^5 M^{-1}.

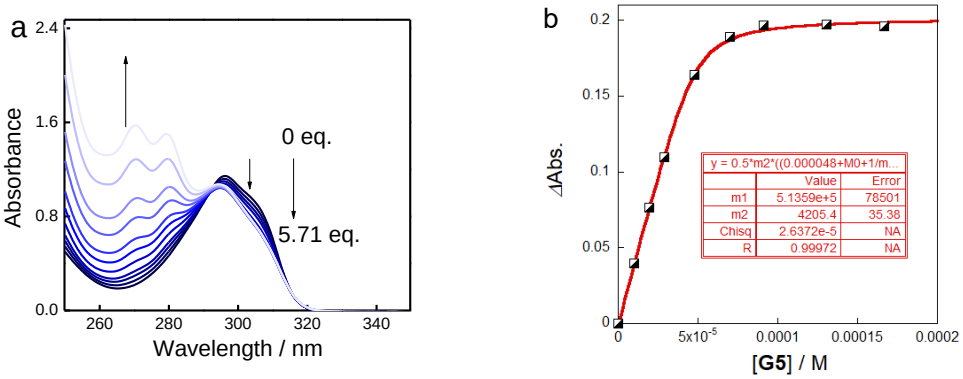

Figure S89. UV spectral changes of **H8** (5.0×10^{-5} M) upon titration with **G5** ($0 – 2.85 \times 10^{-4}$ M) in $CHCl_3$ at 25 °C (left). The non-linear curve-fitting (UV titrations) for the complexation of **G5** (right) with **H8** (304 nm) in $CHCl_3$ at 25 °C, the association constants (K_a) for the complexes is 5.14 (± 0.78) × 10^5 M^{-1}.

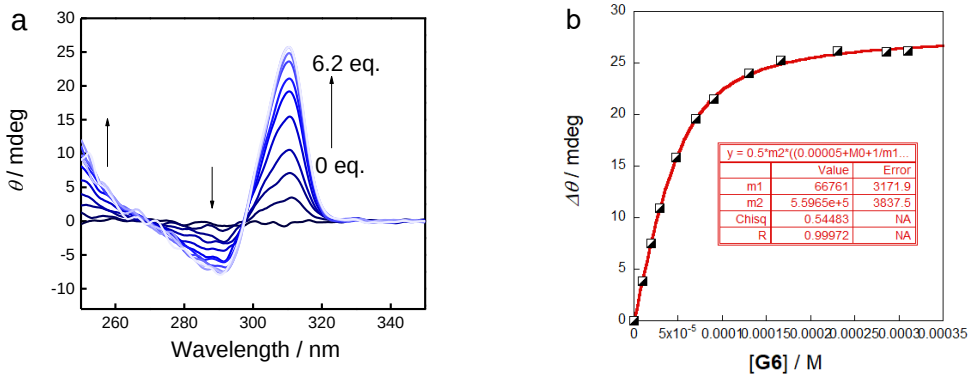

Figure S90. CD spectral changes of **H1** (5.0×10^{-5} M) upon titration with **G6** ($0 – 3.1 \times 10^{-4}$ M) in $CHCl_3$ at 25 °C (left). The non-linear curve-fitting (CD titrations) for the complexation of **G6** (right) with **H1** (310.5 nm) in $CHCl_3$ at 25 °C, the association constants (K_a) for the complexes is 6.68 (± 0.32) × 10^4 M^{-1}.

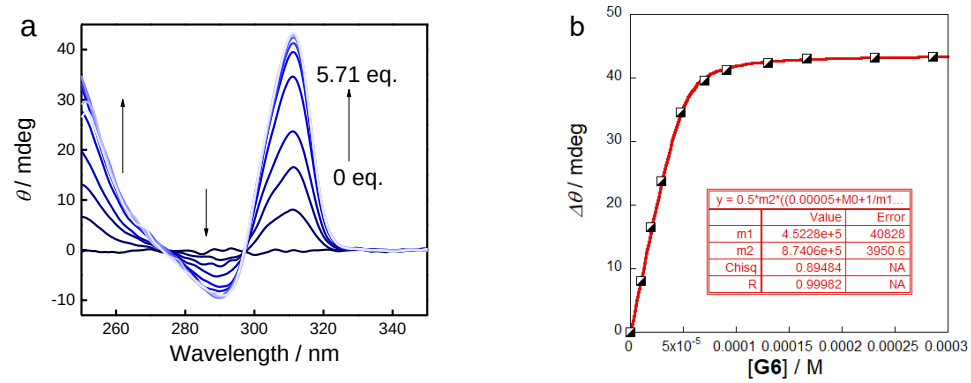

Figure S91. CD spectral changes of **H8** (5.0×10^{-5} M) upon titration with **G6** ($0 – 2.85 \times 10^{-4}$ M) in $CHCl_3$ at 25 °C (left). The non-linear curve-fitting (CD titrations) for the complexation of **G6** (right) with **H8** (311.2 nm) in $CHCl_3$ at 25 °C, the association constants (K_a) for the complexes is 4.52 (± 0.41) × 10^5 M^{-1}.

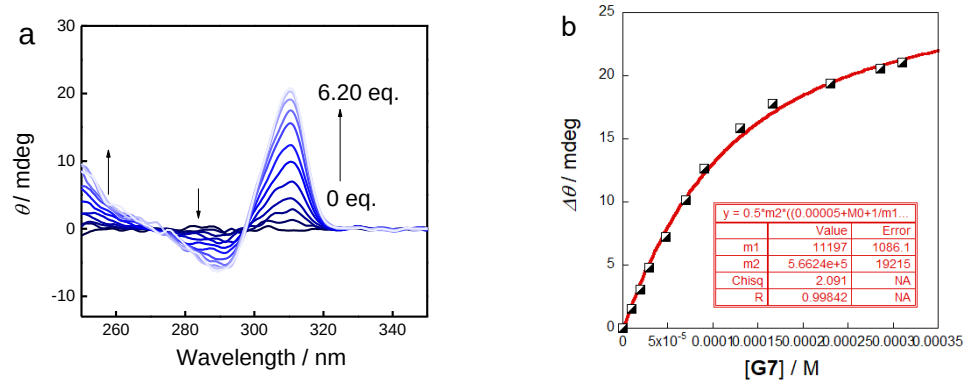

Figure S92. CD spectral changes of **H1** (5.0×10^{-5} M) upon titration with **G7** ($0 – 3.1 \times 10^{-4}$ M) in $CHCl_3$ at 25 °C (left). The non-linear curve-fitting (CD titrations) for the complexation of **G7** (right) with **H1** (310.5 nm) in $CHCl_3$ at 25 °C, the association constants (K_a) for the complexes is 1.12 (± 0.11) × 10^4 M^{-1}.

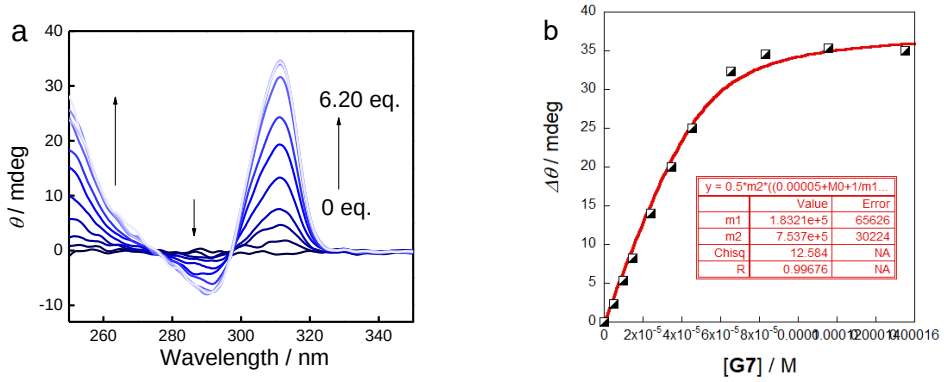

Figure S93. CD spectral changes of **H8** (5.0×10^{-5} M) upon titration with **G7** ($0 - 3.1 \times 10^{-4}$ M) in $CHCl_3$ at 25 °C (left). The non-linear curve-fitting (CD titrations) for the complexation of **G7** (right) with **H8** (311.3 nm) in $CHCl_3$ at 25 °C, the association constants (K_a) for the complexes is 1.83 (± 0.66) × 10^5 M^{-1}.

Table S1. Binding constants of the hosts and guest in $CHCl_3$ at 25 °C.[a]

	G3	G4	G5	G6	G7
H1	2.1E5 ± 4.0E4	1.5E5 ± 6.7E4	5.1E5 ± 7.2E4	6.7E4 ± 3.2E3	1.1E4 ± 1.1E3
H8	3.05E5 ± 1.2E5	1.2E5 ± 4.5E4	5.1E5 ± 7.8E4[b]	4.5E5 ± 4.1E4	1.8E5 ± 4.8E3

[a]CD titrations data of **H1** and **H8** complex with amino acid derivatives, association constant *K* / M^{-1}. [b]UV-Vis titrations data.

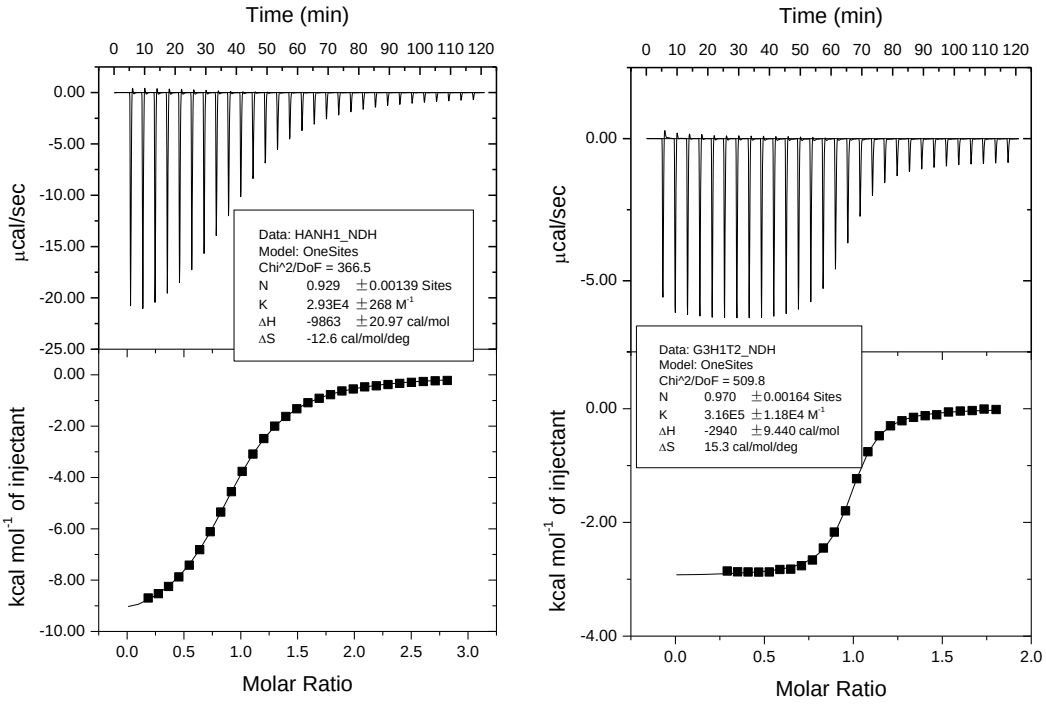

Figure S94. ITC data for **hexanedinitrile** and **H1** in $CHCl_3$ at 25 °C. **hexanedinitrile** was titrated at 5 mM into a 0.4 mM solution of **H1**. At top is the raw data for power versus time. At bottom are integrated enthalpy values versus the molar ratio of **hexanedinitrile**: **H1** =1:1. These data were fit to the "one sites of model" using Origin 7.0 software (left). ITC data for **G2** and **H1** in $CHCl_3$ at 25 °C. **G2** was titrated at 4 mM into a 0.5 mM solution of **H1**. At top is the raw data for power versus time. At bottom are integrated enthalpy values versus the molar ratio of **G2**: **H1** =1:1. These data were fit to the "one sites of model" using Origin 7.0 software (right).

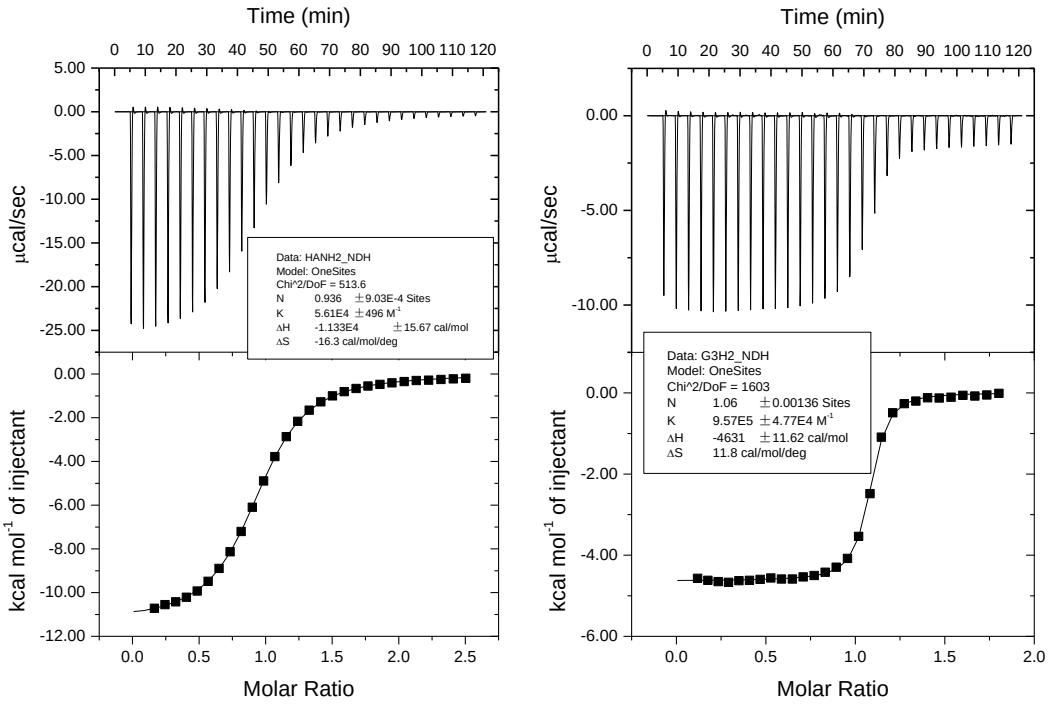

Figure S95. ITC data for **hexanedinitrile** and **H2** in $CHCl_3$ at 25 °C. **hexanedinitrile** was titrated at 5 mM into a 0.45 mM solution of **H2**. At top is the raw data for power versus time. At bottom are integrated enthalpy values versus the molar ratio of **hexanedinitrile**: **H2** =1:1. These data were fit to the "one sites of model" using Origin 7.0 software (left). ITC data for **G2** and **H2** in $CHCl_3$ at 25 °C. **G2** was titrated at 4 mM into a 0.5 mM solution of **H2**. At top is the raw data for power versus time. At bottom are integrated enthalpy values versus the molar ratio of **G2**: **H2** =1:1. These data were fit to the "one sites of model" using Origin 7.0 software (right).

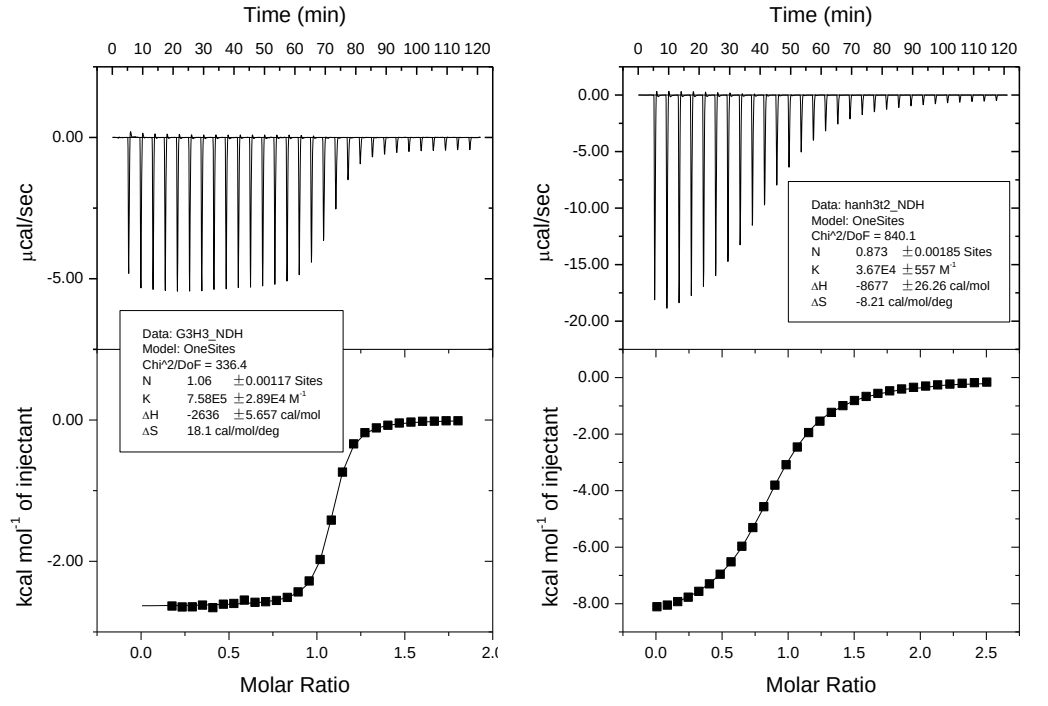

Figure S96. ITC data for **hexanedinitrile** and **H3** in $CHCl_3$ at 25 °C. **hexanedinitrile** was titrated at 5 mM into a 0.45 mM solution of **H3**. At top is the raw data for power versus time. At bottom are integrated enthalpy values versus the molar ratio of **hexanedinitrile**: **H3** =1:1. These data were fit to the "one sites of model" using Origin 7.0 software (left). ITC data for **G2** and **H3** in $CHCl_3$ at 25 °C. **G2** was titrated at 4 mM into a 0.5 mM solution of **H3**. At top is the raw data for power versus time. At bottom are integrated enthalpy values versus the molar ratio of **G2**: **H3** =1:1. These data were fit to the "one sites of model" using Origin 7.0 software (right).

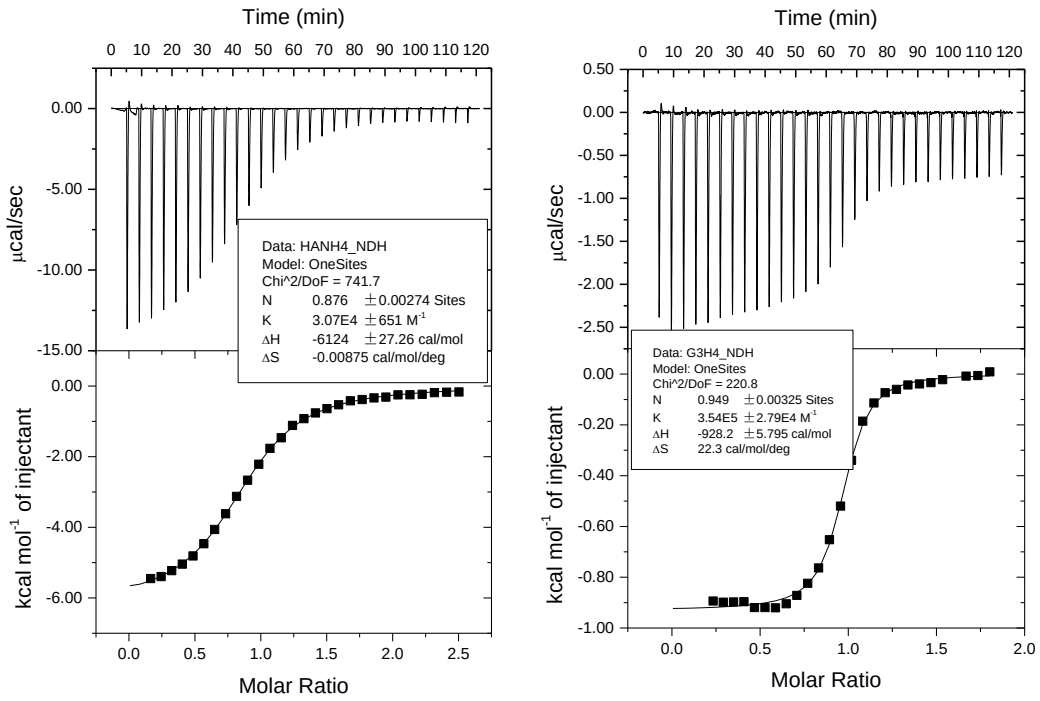

Figure S97. ITC data for **hexanedinitrile** and **H4** in $CHCl_3$ at 25 °C. **hexanedinitrile** was titrated at 5 mM into a 0.45 mM solution of **H4**. At top is the raw data for power versus time. At bottom are integrated enthalpy values versus the molar ratio of **hexanedinitrile**: **H4** =1:1. These data were fit to the "one sites of model" using Origin 7.0 software (left). ITC data for **G2** and **H4** in $CHCl_3$ at 25 °C. **G2** was titrated at 4 mM into a 0.5 mM solution of **H4**. At top is the raw data for power versus time. At bottom are integrated enthalpy values versus the molar ratio of **G2**: **H4** =1:1. These data were fit to the "one sites of model" using Origin 7.0 software (right).

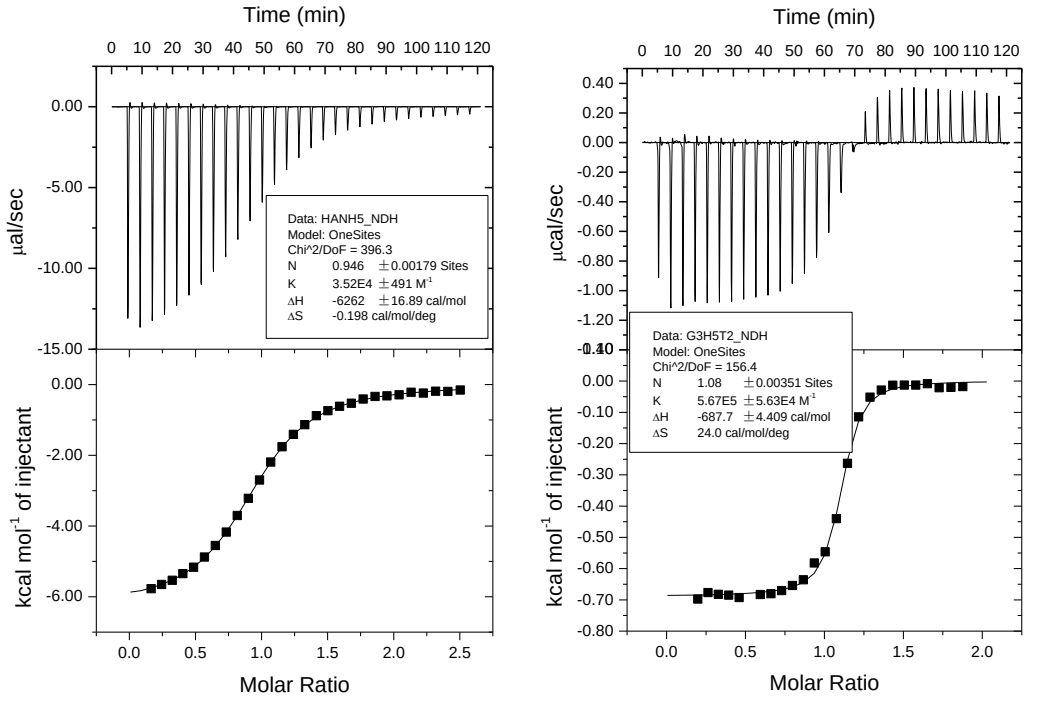

Figure S98. ITC data for **hexanedinitrile** and **H5** in $CHCl_3$ at 25 °C. **hexanedinitrile** was titrated at 5 mM into a 0.45 mM solution of **H5**. At top is the raw data for power versus time. At bottom are integrated enthalpy values versus the molar ratio of **hexanedinitrile**: **H5** =1:1. These data were fit to the "one sites of model" using Origin 7.0 software (left). ITC data for **G2** and **H5** in $CHCl_3$ at 25 °C. **G2** was titrated at 4.5 mM into a 0.5 mM solution of **H5**. At top is the raw data for power versus time. At bottom are integrated enthalpy values versus the molar ratio of **G2**: **H5** =1:1. These data were fit to the "one sites of model" using Origin 7.0 software (right).

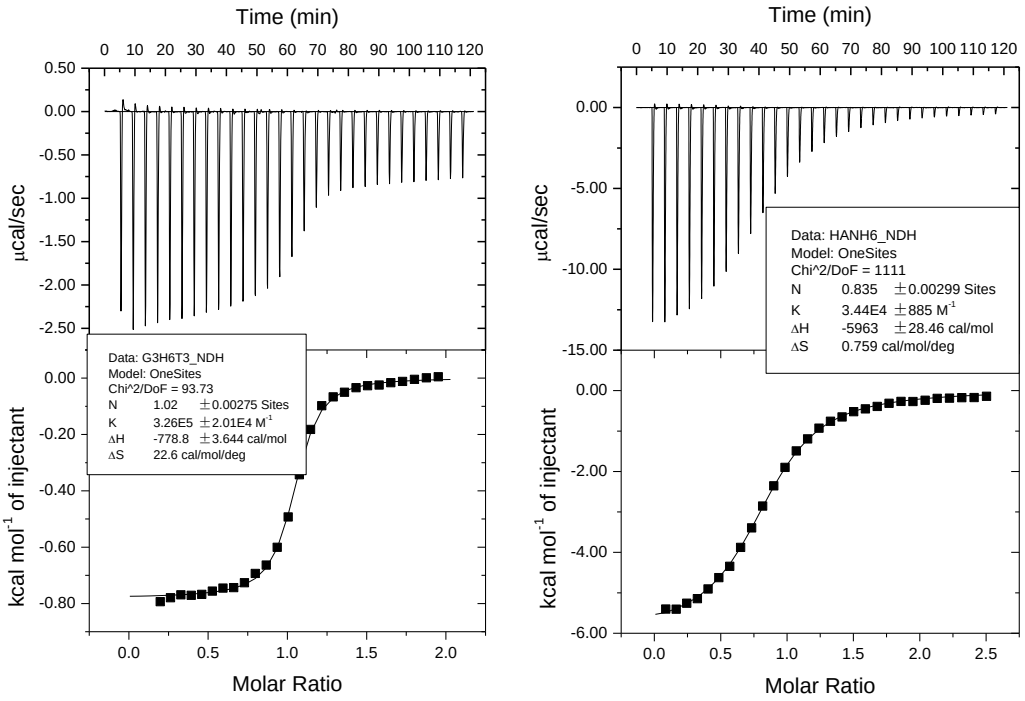

Figure S99. ITC data for **hexanedinitrile** and **H6** in $CHCl_3$ at 25 °C. **hexanedinitrile** was titrated at 5 mM into a 0.45 mM solution of **H6**. At top is the raw data for power versus time. At bottom are integrated enthalpy values versus the molar ratio of **hexanedinitrile**: **H6** =1:1. These data were fit to the "one sites of model" using Origin 7.0 software (left). ITC data for **G2** and **H6** at in $CHCl_3$ at 25 °C. **G2** was titrated at 4.5 mM into a 0.5 mM solution of **H6**. At top is the raw data for power versus time. At bottom are integrated enthalpy values versus the molar ratio of **G2 H6** =1:1. These data were fit to the "one sites of model" using Origin 7.0 software (right).

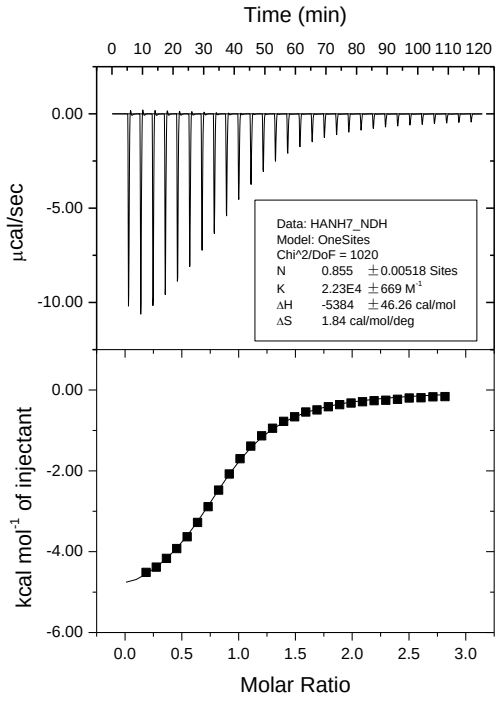

Figure S100. ITC data for **hexanedinitrile** and **H7** in $CHCl_3$ at 25 °C. **hexanedinitrile** was titrated at 5 mM into a 0.4 mM solution of **H7**. At top is the raw data for power versus time. At bottom are integrated enthalpy values versus the molar ratio of **hexanedinitrile**: **H7** =1:1. These data were fit to the "one sites of model" using Origin 7.0 software.

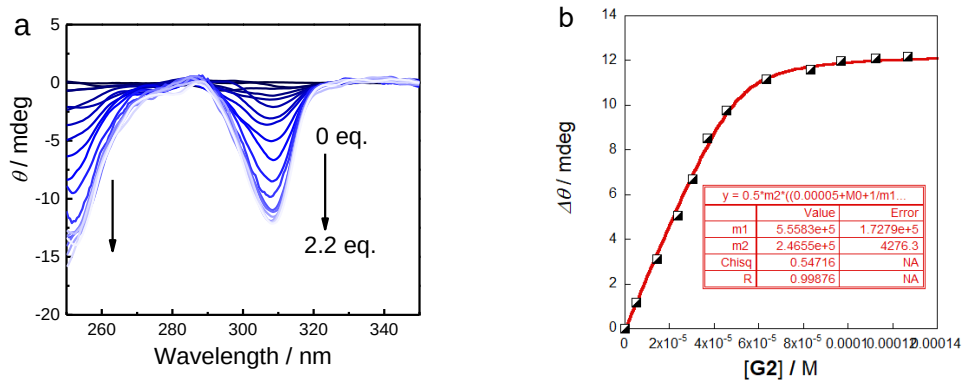

Figure S101. (a) CD spectral changes of **H7** (5.0×10^{-5} M) upon titration with **G2** ($0 – 1.1 \times 10^{-4}$ M) in $CHCl_3$ at 25 °C. (b) The non-linear curve-fitting (CD titrations) for the complexation of **G2** with **H7** (308.5 nm) in $CHCl_3$ at 25 °C, the association constants (K_a) for the complexes is 5.56 (± 1.7) × 10^5 M^{-1}.

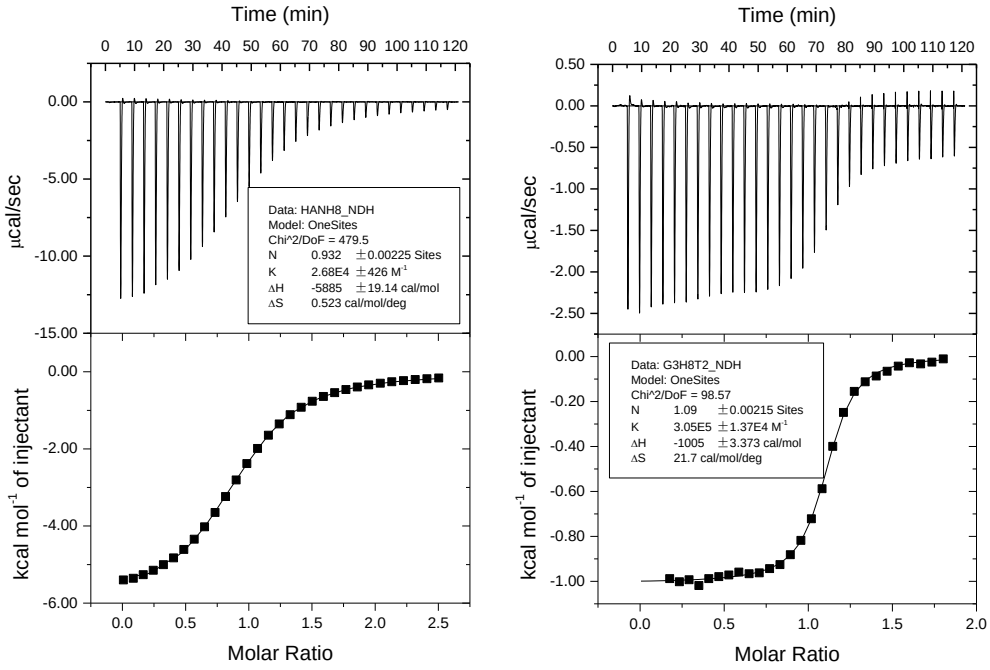

Figure S102. ITC data for **hexanedinitrile** and **H8 in** $CHCl_3$ at 25 °C. **hexanedinitrile** was titrated at 5 mM into a 0.45 mM solution of **H8**. At top is the raw data for power versus time. At bottom are integrated enthalpy values versus the molar ratio of **hexanedinitrile**: **H8** =1:1. These data were fit to the “one sites of model” using Origin 7.0 software (left). ITC data for **G2** and **H8** in $CHCl_3$ at 25 °C. **G2** was titrated at 4 mM into a 0.5 mM solution of **H8**. At top is the raw data for power versus time. At bottom are integrated enthalpy values versus the molar ratio of **G2**: **H8** =1:1. These data were fit to the “one sites of model” using Origin 7.0 software (right).

Table S2. Thermal dynamic parameters for the complexation of P[5]s with hexanedinitrile (HAN) or **G2**.

	G2				HAN			
	ΔG / kJ M^{-1}	K / 10^4 M^{-1}	ΔH / kJ M^{-1}	$\Delta S\,T$ / kJ M^{-1}	ΔG / kJ M^{-1}	K / 10^4 M^{-1}	ΔH / kJ M^{-1}	$\Delta S\,T$ / kJ M^{-1}
H1	-31.4	31.6	-12.3	19.1	-25.6	2.93	-41.3	-15.7
H2	-34.1	95.7	-19.4	14.7	-27.1	5.61	-47.4	-20.3
H3	-33.6	75.8	-11.0	22.6	-13.7	3.67	-36.3	-22.5
H4	-31.7	35.4	-3.9	27.8	-25.6	3.07	-25.6	-0.001
H5	-32.8	56.7	-2.9	29.9	-26.0	3.52	-26.2	-0.2
H6	-31.5	32.6	-3.3	28.2	-27.6	3.44	-26.7	0.8
H7	-32.8	55.6 [a]	-	-	-24.8	2.23	-22.5	2.3
H8	-31.3	30.5	-4.2	27.1	-25.3	2.68	-24.6	0.7

[a]CD data, other binding constants and Thermal dynamic parameters come from ITC data.

6 Fluorescence spectra of host and guest binding complexes

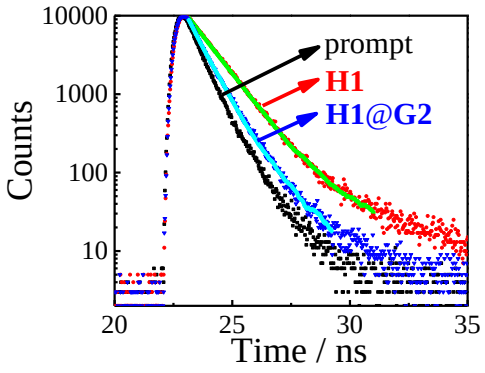

Figure S103. Fluoresence decay of **H1** (0.05 mM) and **H1@G2** ([**G2**] = 2[**H1**] = 0.1 mM, λ_{ex} = 280 nm). All measured in chloroform at 25 °C.

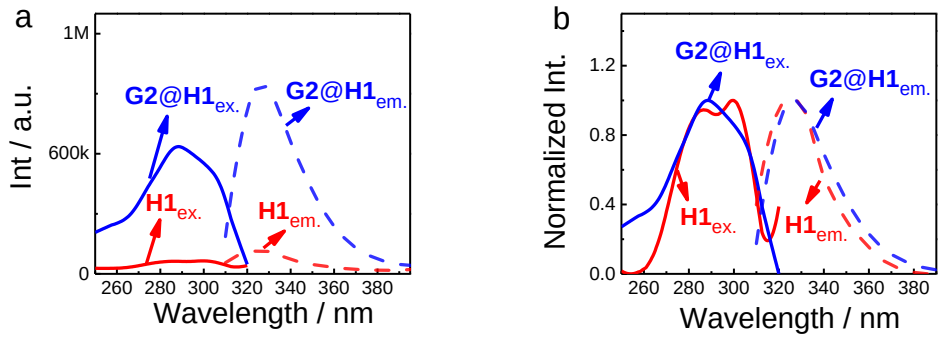

Figure S104. a) Fluorescence excitation (λ_{em} = 330 nm, solid line) and emission (λ_{ex} = 302 nm, dash line) spectra of the complexes **G2@H1** (blue line) and **H1** (red line) in $CHCl_3$ in $CHCl_3$ at 25 °C. b) Normalized Fluorescence excitation (λ_{em} = 330 nm, solid line) and emission (λ_{ex} = 302 nm, dash line) spectra of the complexes **G2@H1** (blue line) and **H1** (red line). ($C_{[H1]}$ = 5.0 × 10^{-5} M, $C_{[G2]}$ = 1.0 × 10^{-4} M)

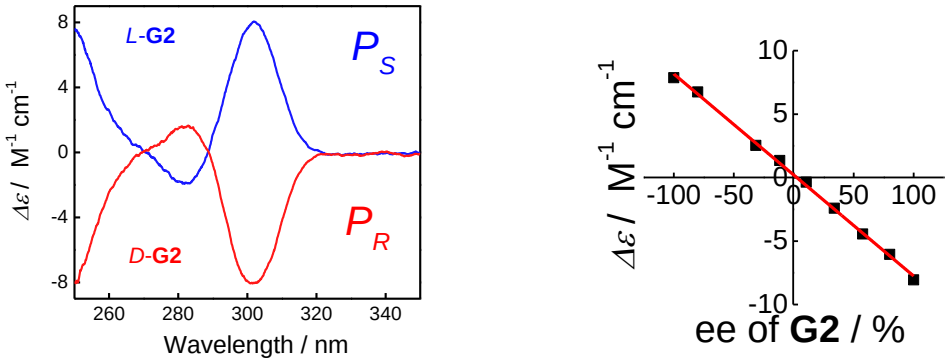

Figure S105. a) CD spectra of **H1** (0.05 mM) in the presence of *L*-**G2** (0.01 mM, blue line) or *D*-**G2** (0.1 mM, red line) in $CHCl_3$ at 25 °C. b) Plot of the ellipticity at 301 nm as a function of %ee, the data are from Fig. 2d in the main text.

Table S3. The ee determination of amines **G2** with **H1** using the calibration line (Fig. 2d).

real ee	$\Delta\varepsilon$ / M^{-1} cm^{-1}	calculated ee	Error /%	Average Error /%
-73.7	-5.5	-71.4	3.1	2.2
-46.7	-3.5	-46.2	1.1	
14.5	1.4	15.1	4.1	
42.1	3.6	42.3	0.5	

7 CD spectra of the complexes

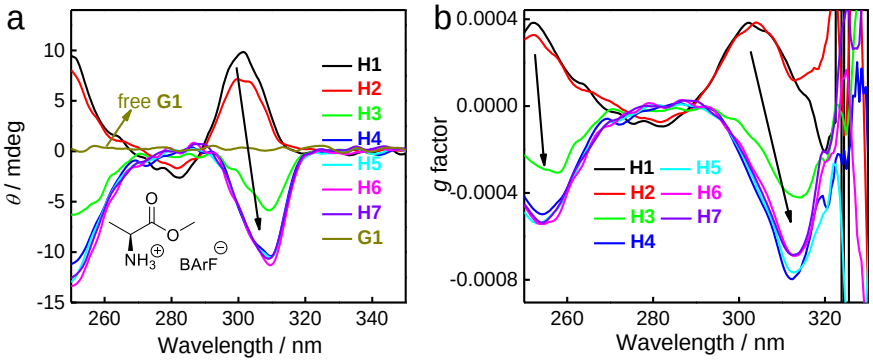

Figure S106. a) CD spectra of different P[5] derivatives (5.0×10^{-5} M) in the presence of compound **G1** (9.1×10^{-5} M) in $CHCl_3$ at 25 °C. b) *g* factor of different P[5] derivatives (5.0×10^{-5} M) in the presence of compound **G1** (9.1×10^{-5} M) in $CHCl_3$ at 25 °C.

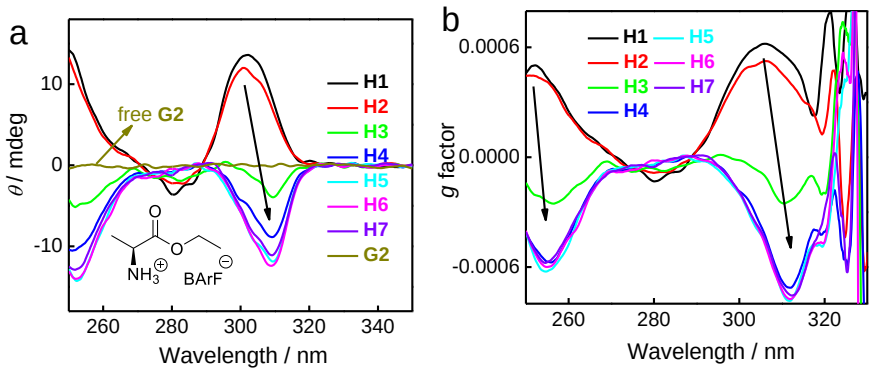

Figure S107. a) CD spectra of different P[5] derivatives (5.0×10^{-5} M) in the presence of compound **G2** (9.1×10^{-5} M) in $CHCl_3$ at 25 °C. b) *g* factor of different P[5] derivatives (5.0×10^{-5} M) in the presence of compound **G2** (9.1×10^{-5} M) in $CHCl_3$ at 25 °C.

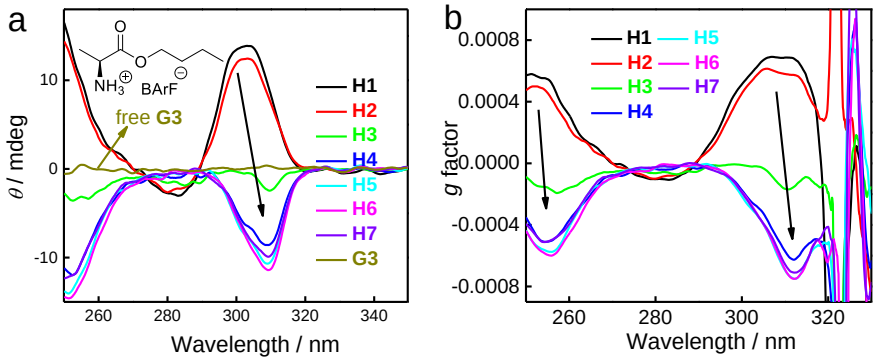

Figure S108. a) CD spectra of different P[5] derivatives (5.0×10^{-5} M) in the presence of compound **G3** (9.1×10^{-5} M) in $CHCl_3$ at 25 °C. b) *g* factor of different P[5] derivatives (5.0×10^{-5} M) in the presence of compound **G3** (9.1×10^{-5} M) in $CHCl_3$ at 25 °C.

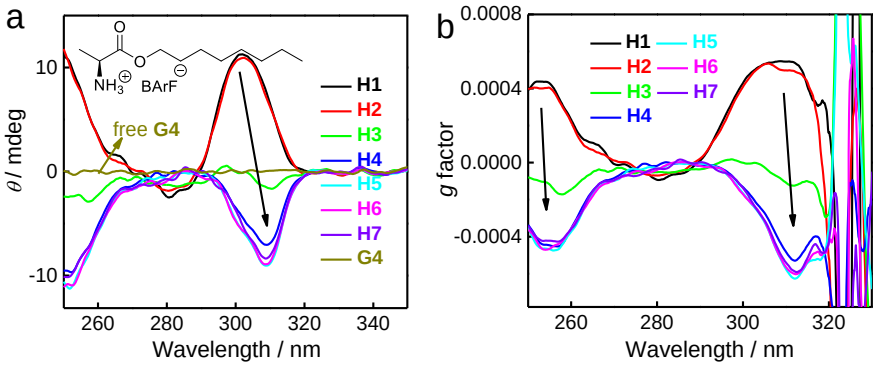

Figure S109. a) CD spectra of different P[5] derivatives (5.0×10^{-5} M) in the presence of compound **G4** (9.1×10^{-5} M) in $CHCl_3$ at 25 °C. b) *g* factor of different P[5] derivatives (5.0×10^{-5} M) in the presence of compound **G4** (9.1×10^{-5} M) in $CHCl_3$ at 25 °C.

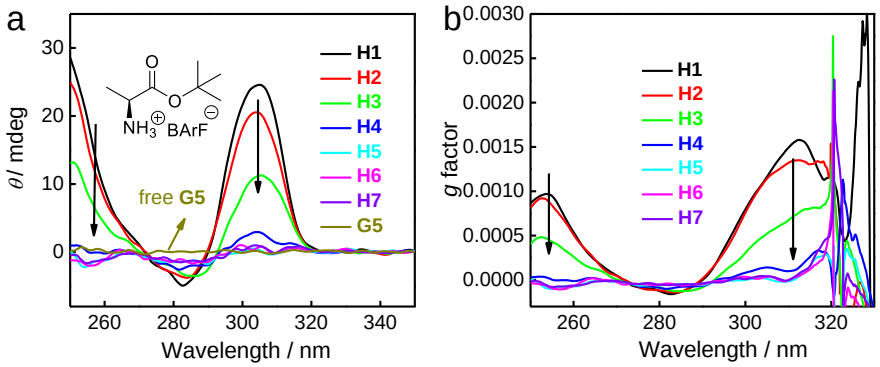

Figure S110. a) CD spectra of different P[5] derivatives (5.0×10^{-5} M) in the presence of compound **G5** (9.1×10^{-5} M) in $CHCl_3$ at 25 °C. b) *g* factor of different P[5] derivatives (5.0×10^{-5} M) in the presence of compound **G5** (9.1×10^{-5} M) in $CHCl_3$ at 25 °C.

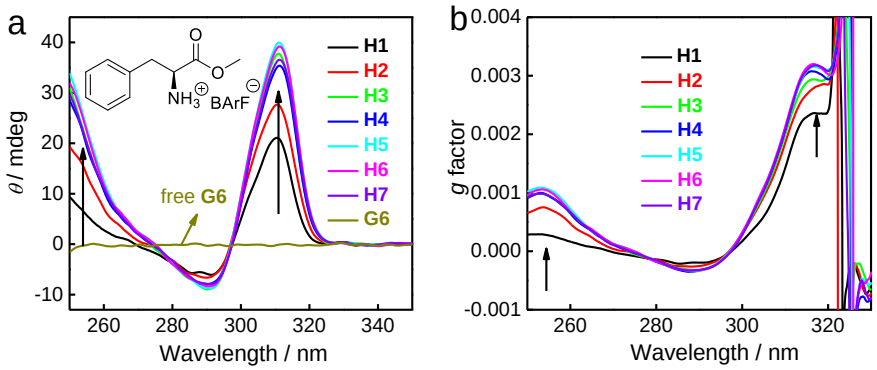

Figure S111. a) CD spectra of different P[5] derivatives (5.0×10^{-5} M) in the presence of compound **G6** (9.1×10^{-5} M) in $CHCl_3$ at 25 °C. b) *g* factor of different P[5] derivatives (5.0×10^{-5} M) in the presence of compound **G6** (9.1×10^{-5} M) in $CHCl_3$ at 25 °C.

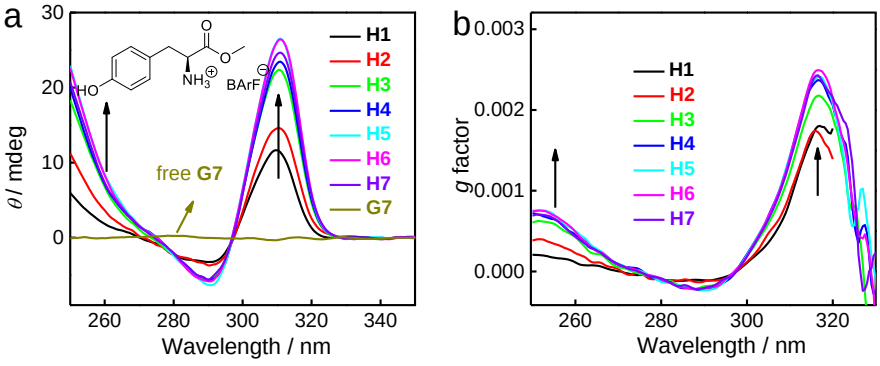

Figure S112. a) CD spectra of different P[5] derivatives (5.0×10^{-5} M) in the presence of compound **G7** (9.1×10^{-5} M) in $CHCl_3$ at 25 °C. b) *g* factor of different P[5] derivatives (5.0×10^{-5} M) in the presence of compound **G7** (9.1×10^{-5} M) in $CHCl_3$ at 25 °C.

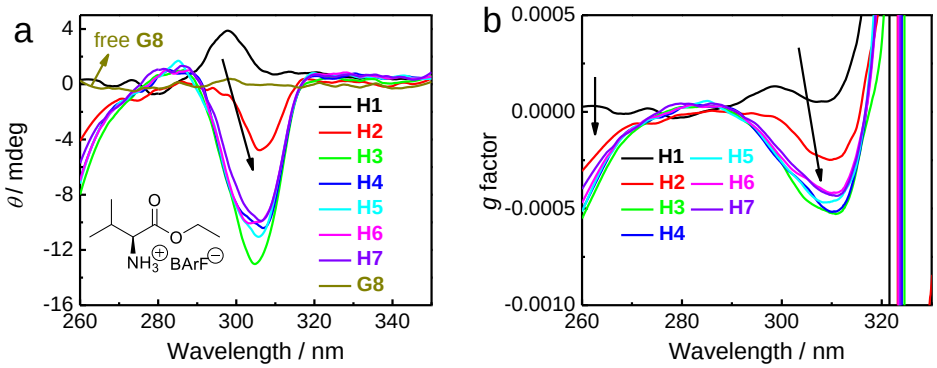

Figure S113. a) CD spectra of different P[5] derivatives (5.0×10^{-5} M) in the presence of compound **G8** (9.1×10^{-5} M) in $CHCl_3$ at 25 °C. b) *g* factor of different P[5] derivatives (5.0×10^{-5} M) in the presence of compound **G8** (9.1×10^{-5} M) in $CHCl_3$ at 25 °C.

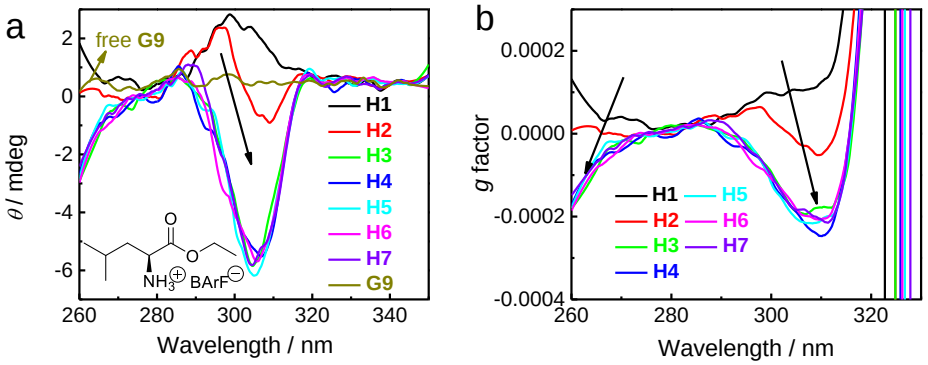

Figure S114. a) CD spectra of different P[5] derivatives (5.0×10^{-5} M) in the presence of compound **G9** (9.1×10^{-5} M) in $CHCl_3$ at 25 °C. b) *g* factor of different P[5] derivatives (5.0×10^{-5} M) in the presence of compound **G9** (9.1×10^{-5} M) in $CHCl_3$ at 25 °C.

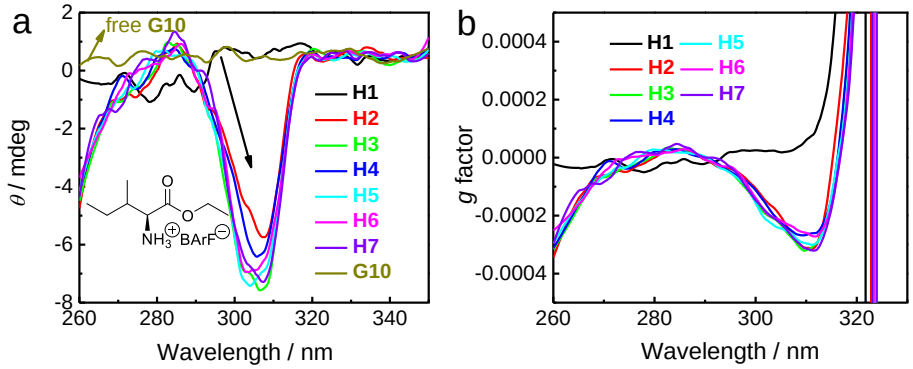

Figure S115. a) CD spectra of different P[5] derivatives (5.0×10^{-5} M) in the presence of compound **G10** (9.1×10^{-5} M) in $CHCl_3$ at 25 °C. b) *g* factor of different P[5] derivatives (5.0×10^{-5} M) in the presence of compound **G10** (9.1×10^{-5} M) in $CHCl_3$ at 25 °C.

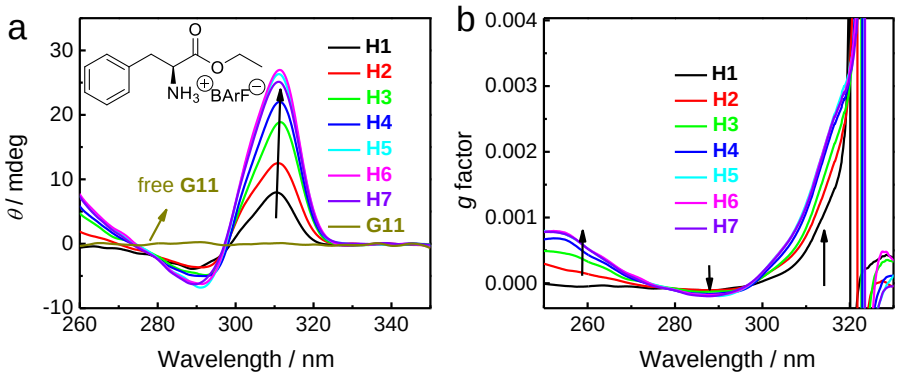

Figure S116. a) CD spectra of different P[5] derivatives (5.0×10^{-5} M) in the presence of compound **G11** (9.1×10^{-5} M) in $CHCl_3$ at 25 °C. b) *g* factor of different P[5] derivatives (5.0×10^{-5} M) in the presence of compound **G11** (9.1×10^{-5} M) in $CHCl_3$ at 25 °C.

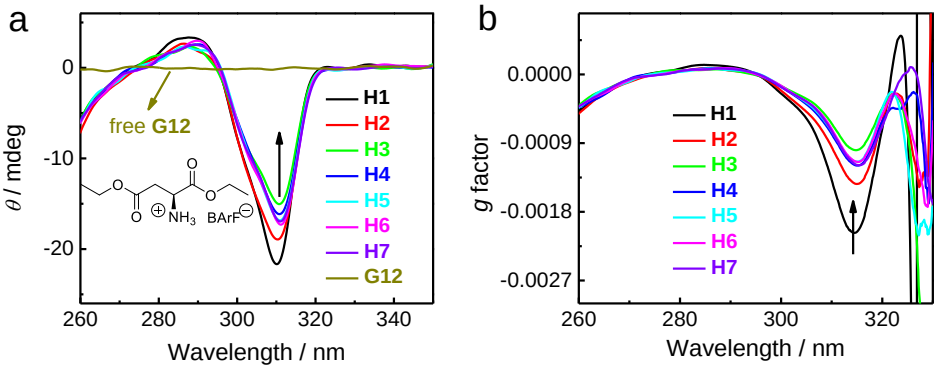

Figure S117. a) CD spectra of different P[5] derivatives (5.0×10^{-5} M) in the presence of compound **G12** (9.1×10^{-5} M) in $CHCl_3$ at 25 °C. b) *g* factor of different P[5] derivatives (5.0×10^{-5} M) in the presence of compound **G12** (9.1×10^{-5} M) in $CHCl_3$ at 25 °C.

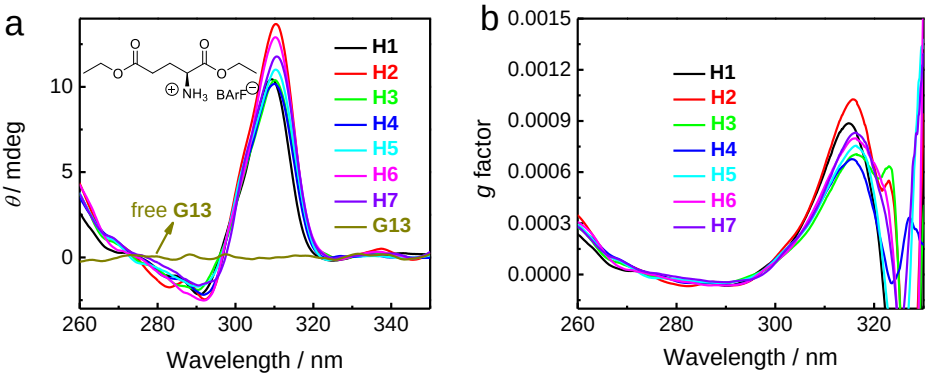

Figure S118. a) CD spectra of different P[5] derivatives (5.0×10^{-5} M) in the presence of compound **G13** (9.1×10^{-5} M) in $CHCl_3$ at 25 °C. b) *g* factor of different P[5] derivatives (5.0×10^{-5} M) in the presence of compound **G13** (9.1×10^{-5} M) in $CHCl_3$ at 25 °C.

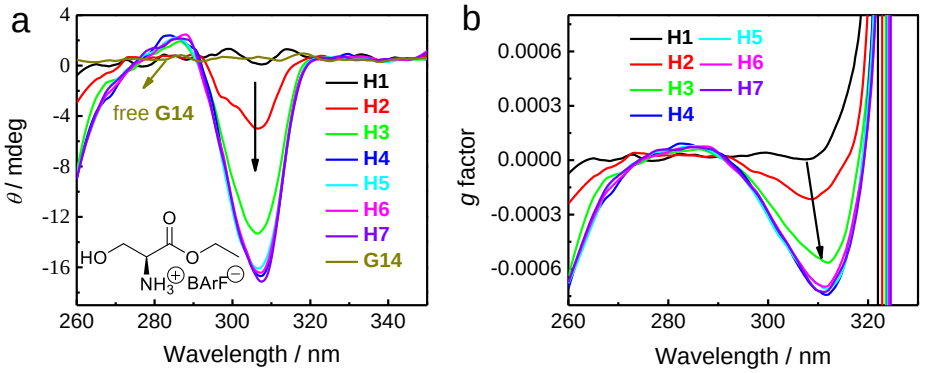

Figure S119. a) CD spectra of different P[5] derivatives (5.0×10^{-5} M) in the presence of compound **G14** (9.1×10^{-5} M) in $CHCl_3$ at 25 °C. b) *g* factor of different P[5] derivatives (5.0×10^{-5} M) in the presence of compound **G14** (9.1×10^{-5} M) in $CHCl_3$ at 25 °C.

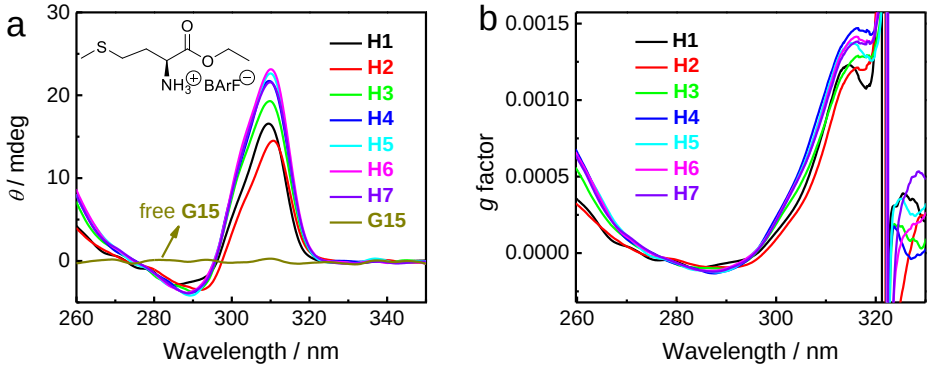

Figure S120. a) CD spectra of different P[5] derivatives (5.0×10^{-5} M) in the presence of compound **G15** (9.1×10^{-5} M) in $CHCl_3$ at 25 °C. b) *g* factor of different P[5] derivatives (5.0×10^{-5} M) in the presence of compound **G15** (9.1×10^{-5} M) in $CHCl_3$ at 25 °C.

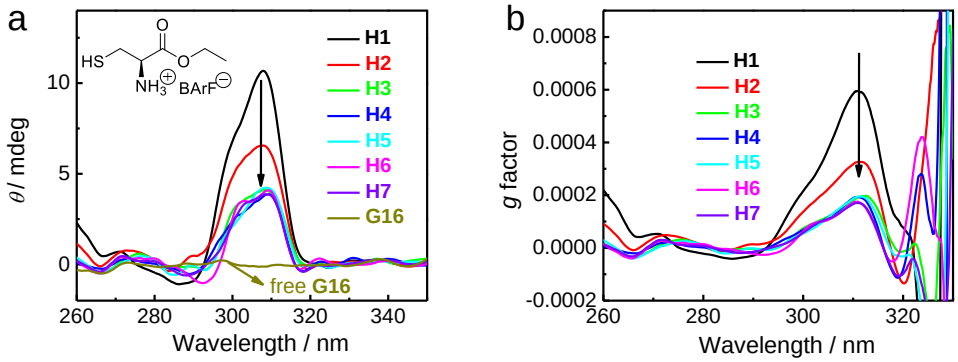

Figure S121. a) CD spectra of different P[5] derivatives (5.0×10^{-5} M) in the presence of compound **G16** (9.1×10^{-5} M) in $CHCl_3$ at 25 °C. b) *g* factor of different P[5] derivatives (5.0×10^{-5} M) in the presence of compound **G16** (9.1×10^{-5} M) in $CHCl_3$ at 25 °C.

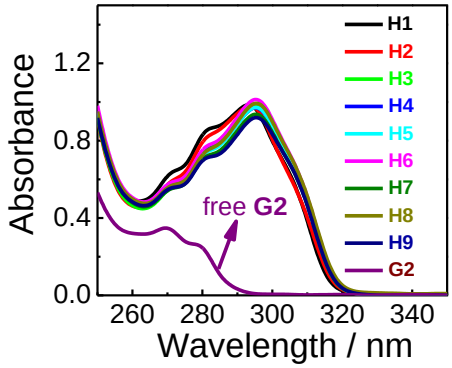

Figure S122. Uv-vis spectra of different P[5] derivatives (5.0×10^{-5} M) in the presence of compound **G2** (9.1×10^{-5} M) in $CHCl_3$ at 25 °C.

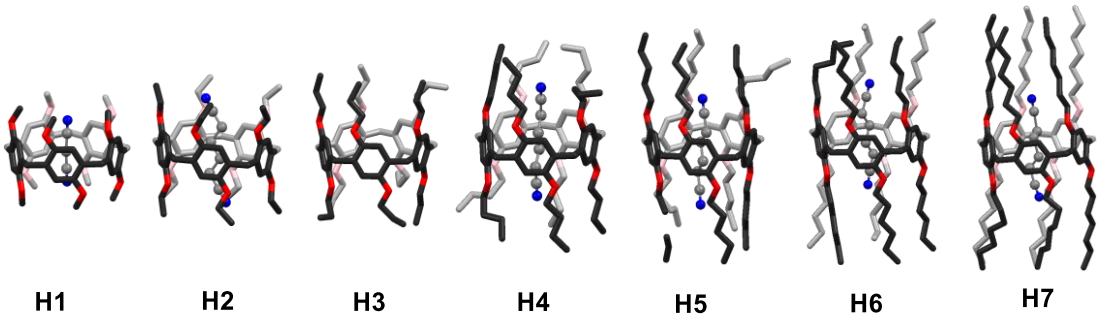

Figure S123. Single crystal X-ray structure of P[5] homologs **H1**–**H7** complexed with HAN. (crystal data of **H1**[2], **H2**[3], **H3**[4] are from previous literatures) C-gray, N-blue, O-red, Hydrogen atoms were hidden for clarity.

8 Study on the model of complexes

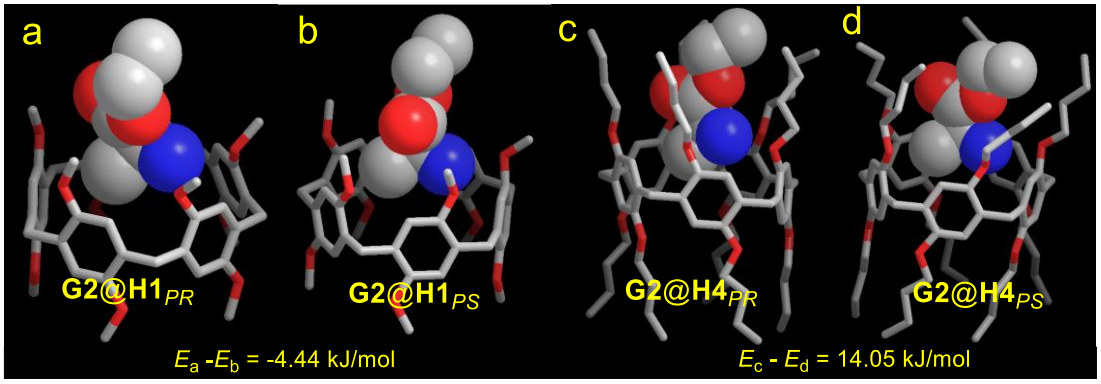

Figure S124. PM6-optimized structures and energies of the four complexes of *L*-**G2** with P5 host **H1 or H4**: (a) **G2@H1**$_{PR}$, (b) **G2@H1**$_{PS}$, (c) **G2@H4**$_{PR}$, (d) **G2@H4**$_{PS}$, Color code: grey for carbon, red for oxygen, blue for nitrogen, and hydrogen atoms were hidden for clarity. Stability order: **G2@H1**$_{PR}$ < **G2@H1**$_{PS}$, **G2@H4**$_{PS}$ < **G2@H4**$_{PR}$.

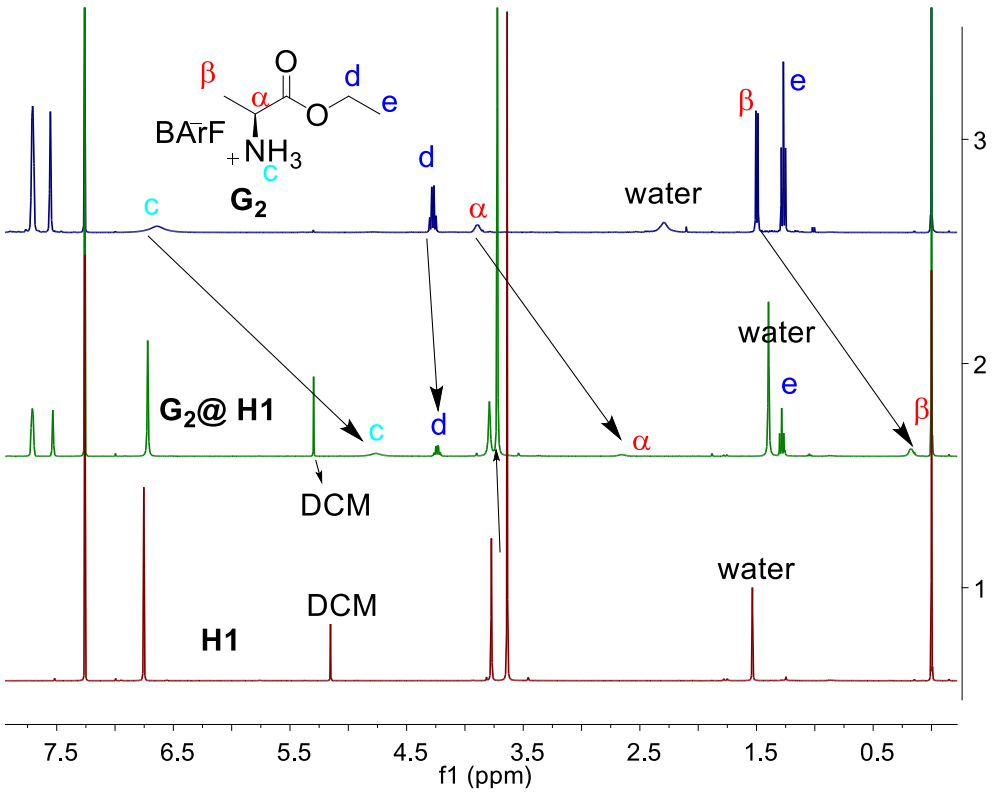

Figure S125. ^{1}H NMR spectra (400 MHz, $CDCl_3$, 25°C) of **H1** (blue spectrum), **G2@H1** (green spectrum) and **G2** (red spectrum).

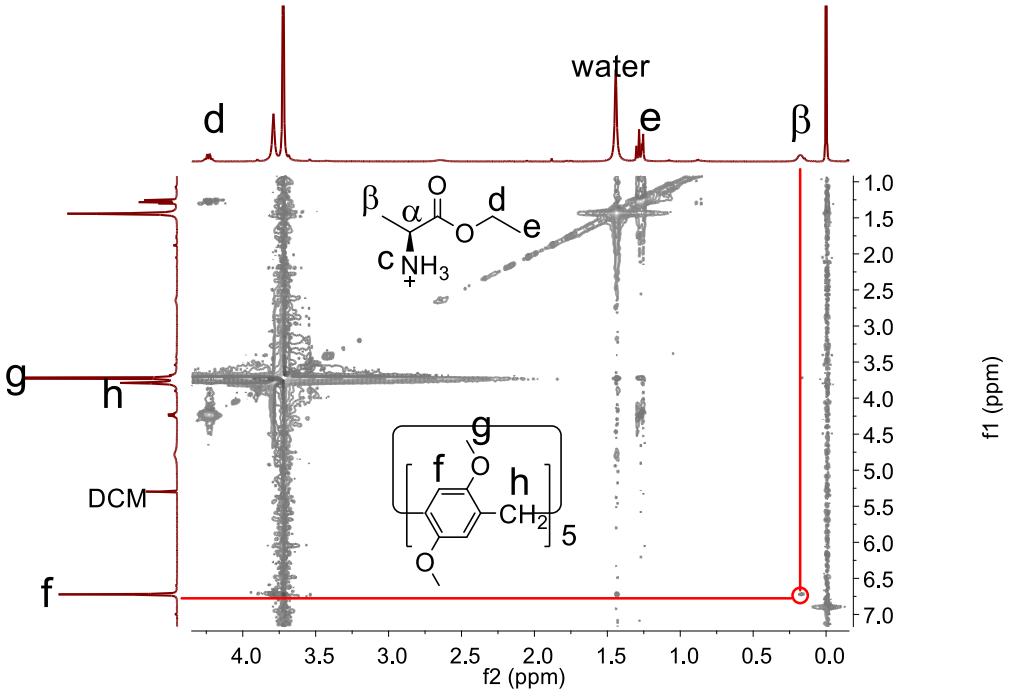

Figure S126. ^{1}H-^{1}H ROESY NMR spectra of complexes ([**G2**] = [**H1**] = 3 mM, 400 MHz, $CDCl_3$).

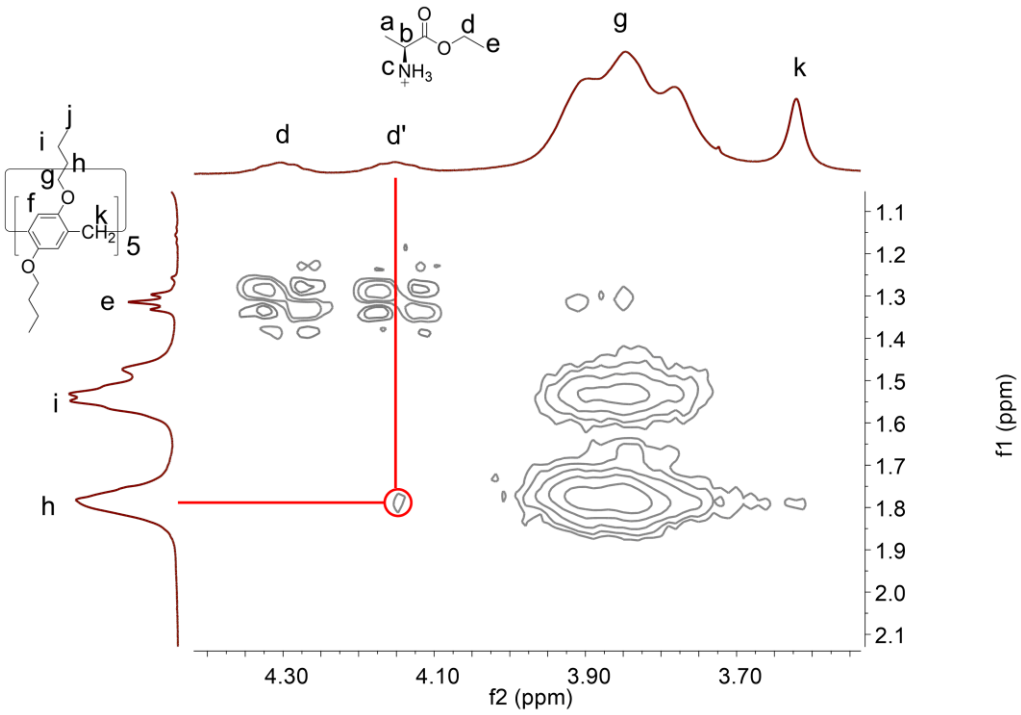

Figure S127. ^{1}H-^{1}H ROESY NMR spectra of complexes ([**G2**] = [**H1**] = 3 mM, 400 MHz, $CDCl_3$).

References

1 (a) T. Ogoshi, S. Kanai, S. Fujinami, T.-a. Yamagishi and Y. Nakamoto, *J. Am. Chem. Soc.*, 2008, **130**, 5022-5023 (For the synthesis of **H1**); (b) T. Ogoshi, K. Kitajima, T. Aoki, S. Fujinami, T.-a. Yamagishi and Y. Nakamoto, *J. Org. Chem.*, 2010, **75**, 3268-3273 (For the synthesis of **H2~H6, H9**); (c) J. Cao, Y. Shang, B. Qi, X. Sun, L. Zhang, H. Liu, H. Zhang and X. Zhou, *RSC Adv.*, 2015, **5**, 9993-9996 (For the synthesis of **H8**).

2 O. Tomoki, K. Suguru, F. Shuhei, Y. Tada-Aki, N. Yoshiaki, *J. Am. Chem. Soc.* 2008, **130**, 5022-5023.

3 S. Xiaoyan, C. Songhui, L. Jian, C. Zhenxia, W. Linhong, J. Xueshun, L. Chunju, *Chem. Commun.* 2012, **48**, 2967-2969.

4 G. Yu, C. Han, Z. Zhang, J. Chen, X. Yan, B. Zheng, S. Liu, F. Huang, *J. Am. Chem. Soc.* 2012, **134**, 8711-8717.